University of Alberta

Use of Dialysis Sampler for Monitored Natural Attenuation Assessment

By

Olumide Iwakun

A thesis submitted to the Faculty of Graduate Studies and Research in partial fulfillment of the requirements for the degree of Master of Science

In

Geoenvironmental Engineering

Department of Civil and Environmental Engineering

Edmonton, Alberta

Spring 2006

Library and
Archives Canada

Published Heritage
Branch

395 Wellington Street
Ottawa ON K1A 0N4
Canada

Bibliothèque et
Archives Canada

Direction du
Patrimoine de l'édition

395, rue Wellington
Ottawa ON K1A 0N4
Canada

Your file Votre référence
ISBN: 0-494-13829-7
Our file Notre référence
ISBN: 0-494-13829-7

NOTICE:
The author has granted a non-exclusive license allowing Library and Archives Canada to reproduce, publish, archive, preserve, conserve, communicate to the public by telecommunication or on the Internet, loan, distribute and sell theses worldwide, for commercial or non-commercial purposes, in microform, paper, electronic and/or any other formats.

The author retains copyright ownership and moral rights in this thesis. Neither the thesis nor substantial extracts from it may be printed or otherwise reproduced without the author's permission.

AVIS:
L'auteur a accordé une licence non exclusive permettant à la Bibliothèque et Archives Canada de reproduire, publier, archiver, sauvegarder, conserver, transmettre au public par télécommunication ou par l'Internet, prêter, distribuer et vendre des thèses partout dans le monde, à des fins commerciales ou autres, sur support microforme, papier, électronique et/ou autres formats.

L'auteur conserve la propriété du droit d'auteur et des droits moraux qui protège cette thèse. Ni la thèse ni des extraits substantiels de celle-ci ne doivent être imprimés ou autrement reproduits sans son autorisation.

In compliance with the Canadian Privacy Act some supporting forms may have been removed from this thesis.

While these forms may be included in the document page count, their removal does not represent any loss of content from the thesis.

Conformément à la loi canadienne sur la protection de la vie privée, quelques formulaires secondaires ont été enlevés de cette thèse.

Bien que ces formulaires aient inclus dans la pagination, il n'y aura aucun contenu manquant.

Canada

University of Alberta

Faculty of Graduate Studies and Research

The undersigned certify that they have read, and recommend to the Faculty of Graduate Studies and Research for acceptance, a thesis entitled Use of Dialysis Sampler for Monitored Natural Attenuation Assessment by Olumide Iwakun in partial fulfillment of the requirements for the degree of Master of Science in Geoenvironmental Engineering.

Dr. Kevin Biggar

Dr. Dave Sego

Dr. Robert Donahue

Dr. Selma Guigard

Dr. Ben Rostron

February 6, 2006

Name of Author: Olumide Iwakun

Title of Thesis: Use of Dialysis Sampler for Monitored Natural Attenuation

Degree: Master of Science

Year this Degree Granted: 2006

Permission is hereby granted to the University of Alberta Library to reproduce single copies of this thesis and to lend or sell such copies for private, scholarly or scientific research purposes only.

The author reserves all other publication and other rights in association with the copyright in the thesis, and except as herein before provided, neither the thesis nor any substantial portion thereof may be printed or otherwise reproduced in any material form whatsoever without the author's prior written permission.

Signature

April 7, 2006

ABSTRACT

Diffusion sampler made from regenerated cellulose dialysis membrane was investigated in this research to resolve issues from previous studies on the need for using deoxygenated infill water in the sampler, its integrity with time and conditions that may limit its use in the field. Theoretical simulation coupled with laboratory and field studies were undertaken to evaluate impacts of using oxygenated infill water and sampler integrity with time. Analytical models using SVFLUX and CHEMFLUX software were also used to evaluate conditions that may limit its use in the field. The theoretical simulation results showed that the impacts of using oxygenated water is not significant for field conditions but dependent on parameters such as sampling interval, diffusion rate into the membrane, presence of ferrous iron, etc. The laboratory results corroborated the theoretical model and showed no significant impacts in using oxygenated infill water at the concentrations tested. The membrane integrity results at two field sites showed no adverse impacts on membrane integrity after 6 months, and the analytical models results showed that diffusion samplers are suitable for sampling wells intercepting thin permeable seam layers, but sampling at discrete intervals within the well is recommended for obtaining representative samples in the formation.

ACKNOWLEDGEMENTS

This study would not have been completed if not for the active support and constructive tutelage of my supervisor Dr. K. Biggar and co-supervisors Dr. R. Donahue and Dr. D. Sego. They tirelessly and enthusiastically provided invaluable guidance towards the completion of this study, which was part of the Consortium for Research on Natural Attenuation (CORONA) project, and funded through the NSERC Collaborative Research and Development (CRD) program, the Canadian Association of Petroleum Producers, Conoco-Phillips Canada Ltd, Devon Canada Ltd, and Environmental Canada. Significant in-kind support was provided by Komex International (James Armstrong) and Maxxam Analytics.

I appreciate the invaluable technical support provided by Mr. Steve Gamble, Ms. Christine Hereygers, Ms. Jela Burkus, and Ms. Lelia Lawson, which greatly aided successful completion of this study. I am also grateful to the administrative staff, Ms. Sally Petaske, Ms. Sandra Humphrey, to mention a few and the entire academic staff of the department for their dedication and commitment to the program. I also appreciate the candid advice and support of my fellow research students in providing environment conducive for learning and their open mindedness.

Nevertheless, I give the outermost thanks to GOD, the grand creator of heaven and earth for keeping me from my mother's womb till this present moment. I thank my parents, Chief and Mrs. Iwakun, for their unwavering support and prayers. I am grateful to my Sisters, "Mosunmola, Dr. Omotebi and Ebunola" with her husband Segun Ogungbesan, for their encouragement, sacrifice and support. My sincere gratitude also goes to my Aunt, Dr. Funmilayo Omotayo with her family for her benevolence, advice and encouragement.

TABLE OF CONTENTS

1 INTRODUCTION 1

1.1 GENERAL BACKGROUND 1

1.2 OBJECTIVES OF THE THESIS 3

1.3 SCOPE OF WORK 3

1.4 ORGANIZATION OF THESIS 3

REFERENCES 4

2 EVALUATION OF A DIFFUSION SAMPLING SYSTEM FOR MNA ASSESSMENT 5

2.1 INTRODUCTION 5

2.1.1 Objectives of Study 7

2.1.2 Scope of Work 8

2.2 THEORETICAL MODEL FORMULATION TO EVALUATE IMPACTS OF THE INFILL WATER 8

2.2.1 Assumptions 8

2.2.2 Diffusion formulation 9

2.2.3 Benzene and Iron Oxidation Calculations 12

2.3 EXPERIMENTAL SET-UP AND DESIGN 17

2.3.1 Laboratory determination of impacts of oxygenated infill water 17

2.3.2 Sampler integrity testing 20

2.4 RESULTS AND DISCUSSION 22

2.4.1 Impacts of dissolved oxygen in the infill water 22

2.4.2 Observations on samples deployed at field sites 27

2.4.3 Sampler integrity testing 28

2.5 CONCLUSIONS AND RECOMMENDATIONS 29

2.5.1 Conclusions *29*

2.5.2 Recommendations for future research *30*

2.6 FIGURES 31

2.7 PLATES 36

REFERENCES 39

3 MODELING OF CONTAMINANT MOVEMENT ACROSS WELL OPEN INTERVAL 42

3.1 INTRODUCTION 42

3.1.1 Objectives of Study *43*

3.1.2 Scope of Work *43*

3.2 GOVERNING EQUATION AND ASSUMPTIONS 43

3.2.1 Seepage Theory *44*

3.2.2 Chemical Transport *45*

3.2.3 Assumptions *49*

3.3 CONCEPTUAL MODEL 49

3.3.1 General domain *49*

3.3.2 Material properties *50*

3.3.3 Boundary Conditions *51*

3.4 RESULTS 52

3.4.1 Results of velocity flow field *52*

3.4.2 Results of contaminant transport *53*

3.5 DISCUSSION 56

3.5.1 Flow field around the well *56*

3.5.2 Contaminant movement within the well 58

3.5.3 Practical Considerations 63

3.6 CONCLUSIONS AND RECOMMENDATIONS 64

3.6.1 Conclusions 64

3.6.2 Recommendations for Future Research 65

3.7 FIGURES 66

3.8 TABLES 80

REFERENCES 82

4 CONCLUSIONS AND RECOMMENDATIONS 83

4.1 CONCLUSIONS 83

4.2 RECOMMENDATIONS 84

APPENDIX A: RESULTS DATA ON THE IMPACTS OF OXYGENATION OF INFILL WATER AND THE INTEGRITY OF THE DIALYSIS SAMPLERS WITH TIME 86

APPENDIX A.1 CONCENTRATION PROFILES BASED ON THE ANALYTICAL EQUATIONS DEVELOPED FOR THE DIALYSIS SAMPLERS 87

APPENDIX A.2 RESULTS OF LABORATORY EXPERIMENTS ON THE IMPACTS OF INFILL WATER OXYGENATION IN THE SAMPLERS 98

APPENDIX A.3 SORPTION BATCH TEST RESULTS FOR DIALYSIS MEMBRANE ANALYZED BASED ON LANGMUIR ADSORPTION ISOTHERM 106

APPENDIX A.4 ANALYSES OF BTEX DATA 110

APPENDIX A.5 METHODS 125

APPENDIX B: DATA FROM THE SVFLUX AND CHEMFLUX MODELS ON THE MOVEMENT OF CONTAMINANT ACROSS THE WELL OPEN INTERVAL 136

APPENDIX B.1 FLOW FIELD AROUND THE WELL BY VARYING SAND PACK PERMEABILITY 137

APPENDIX B.2 CONCENTRATION PROFILES FOR ALL THE CASE MODELS 139

APPENDIX B.3 CONCENTRATION PROFILES WITHIN THE WELL 156

LIST OF TABLES

Table 3.1 Basic Configuration 80

Table 3.2 Properties of materials used for the simulation. 80

Table 3.3 Sectional boundary conditions of the conceptual model 81

LIST OF FIGURES

Figure 2.1 Schematic diagram of Laboratory set-up to determine the impacts of infill deionised water. 31

Figure 2.2 Pressure test schematic set-up for integrity test. 31

Figure 2.3 Simulation results for 1mg/L of benzene in laboratory test apparatus. 32

Figure 2.4 Summary of analytical simulation for benzene for the experimental set-up. 32

Figure 2.5 Simulation results for 0.005mg/L benzene for an open system. 33

Figure 2.6 Summary of analytical simulation for an open system. 33

Figure 2.7 Summary of varying biodegradation rate (λ) for an open system. 34

Figure 2.8 Summary of laboratory experiments for BTEX compounds in spiked deionised water. (Error bars indicate standard error associated with 95% confidence interval). 34

Figure 2.9 Summary of laboratory experiments for BTEX compounds in spiked formation water. (Error bars indicate standard error associated with 95% confidence interval). 35

Figure 2.10 Summary of diffusion samplers burst pressure (BP) results. 35

Figure 2.11 Summary of tensile strength test results. 36

Figure 3.1 Domain used for the definition of the conceptual model (Note: The well and sand pack are located at the middle of the domain, and the scale is X=Y=5Z). 66

Figure 3.2 Sectional drawings of the model used showing the stratigraphy of the soils used for the simulations: (a) Case I (b) Case II (c) Case III (All dimensions in metres). 67

Figure 3.3 Layout of the simulation matrix for the models (Note: The suffix A, B, and C corresponds to the CHEMFLUX boundary condition given in Table 3.3 imposed on the model). 68

Figure 3.4 Illustrations of the concentration boundary conditions. (a) shows the sectional view of the boundaries and (b) is a detail of the surface boundary in (a) [For no boundary condition, the initial concentration is taken as zero]. 69

Figure 3.5 Velocity flow field at the middle of the well open interval under different sand pack permeability ratio with the formation. (a) $Ksp/K_f = 100$; (b) $Ksp/K_f = 10$; (c) $Ksp/K_f = 1$; and (d) $Ksp/K_f = 0.1$. [Ksp = Sand pack permeability; K_f = Formation permeability (10^{-6}m/s); the streamlines are at 0.01m equidistant from the centerline of the well. 70

Figure 3.6 Velocity profiles within the well for hydraulic gradient of 0.003 ($n=Ksl/K_f$). 71

Figure 3.7 Example of concentration profile within the well (Case I-Hn100-CHA). 71

Figure 3.8 Effects of seepage velocity on contaminant movement Case II-CHA (a) Seam layer seepage velocity versus concentration at 100days (b) seam layer velocity versus T_{90} for V_f at 57.3m/year (Note: V_f is the seepage velocity of the sand formation). 72

Figure 3.9 Illustration of points plotted within the domain in Figure 3.10(a) and (b). 73

Figure 3.10 Comparison of concentration ratios at the midpoint of the well (a) Concentration ratio at the end of 30 days vs. seam layer seepage velocity,(b) Concentration ratio at the end of 90 days vs. seam layer seepage velocity at different points shown in (a), upstream and downstream of the well's centerline. 74

Figure 3.11 Zone of Influence at the middle of the well open interval 75

Figure 3.12 Concentration profile within the well for the boundary conditions in which monitoring well is sited in already contaminated soil. (a) CHAS –profile without formation concentration gradient, (b) CHCS – profile with formation concentration boundary. 76

Figure 3.13 Effects of initial concentration distribution on contaminant movement within the well. (a) Simulations with $C_{wsl}=0$ & $C_{sl\text{-}S}=0$: (b) Simulations with $C_{sl\text{-}S}=1$ (CHAS). 77

Figure 3.14 Effects of varying dispersivity coefficients using CHA boundary conditions. (a) Concentration profile at the top of the well screen: (b) Concentration profile at the middle of the well screen 78

Figure3.15 Effects of seam layer thickness on equilibration time at the midpoint of the well for Case II-CHA (i.e. SL = 0.1m, V_{sl} = 473m/y, C_{sl} = 1mg/l, & C_f= 0) 79

Figure 3.16 Diffusion sampler concentrations with time for the concentration profile at the middle of the well for Case I-Hn100-CHA (Figure 3.7). 79

LIST OF PLATES

Plate 1 (a) Field sampler (b) Laboratory sampler 36

Plate 2 Field dialysis sampler showing dark substances when retrieved after two months 37

Plate 3 Field dialysis sampler showing some free phase petroleum hydrocarbon (PHC) when retrieved after two months from site 38

LIST OF ABBREVIATIONS AND SYMBOLS

BTEX	Benzene, Toluene, Ethylbenzene, Xylene
CORONA	Consortium for Research on Natural Attenuation
D_eO_x	Deoxygenated infill water
DO	Dissolved oxygen
Fe^{2+}	Ferrous ion
FW	Formation water from site
GCFID	Gas Chromatography with Flame Ionization Detector
ICS	Ion Chromatography System
LDPE	Light Density Polyethylene
LW	Laboratory distilled deionized water
MNA	Monitored Natural Attenuation
O_2	Oxygen
O_x	Oxygenated infill water
PHC	Petroleum Hydrocarbon
VOC	Volatile Organic Compounds

1 Introduction

1.1 General Background

Groundwater contamination arising from the release of petroleum hydrocarbons (PHCs) due to human activities has become a major issue of concerns in recent times. This awareness was born as a result of the observed consequential effects of groundwater contamination. To this effect, various remediation techniques have been developed to achieve site-specific sustainable clean up goals. Of all these techniques, the one that is based solely on the capacity of the environment to degrade, disperse and assimilate PHCs contamination is termed Monitored Natural Attenuation (MNA). According to USEPA (1999), MNA refers to the reliance on natural attenuation processes (within the context of carefully controlled monitored site clean-up approach) to achieve site-specific remedial objectives within a time frame that is reasonable compared to that offered by other more active methods. The attenuation processes include physical, chemical, physiochemical, or biological processes that reduce the mass, toxicity, mobility, volume or concentration of contaminants in soil or groundwater, without human intervention under favorable conditions. These in situ processes include biodegradation, dispersion, dilution, sorption, volatilization, and chemical or physical stabilization, transformation or destruction of contaminants.

For successful implementation of MNA, three activities are involved, namely site characterization, reactive flow and transport modeling, and continuous long term monitoring. Key to these activities is obtaining representative samples from the contaminated groundwater. The University of Alberta includes numerous studies to improve understanding and implementation of MNA in Alberta as part of "Consortium for Research on Natural Attenuation (CORONA)" for upstream oil and gas sites. Different studies have been initiated to determine the impacts of alternative sampling techniques in obtaining representative groundwater samples, one of which is the use of diffusion samplers made from regenerated cellulose.

From previous studies, some issues have been raised on the potential for oxidation of oxidizeable contaminants (or compounds of interest) if oxygenated infill water is used in the sampler and the sampler's integrity of over time. To resolve these issues, analytical modeling coupled with laboratory and field experiments were initiated to determine the impacts of deoxygenated and oxygenated infill water and the structural integrity of the membrane over time. Factors that may limit the use of these samplers in the field are inadequate exchange between the well and the formation; the relative position of the contaminated groundwater flow to the well screen open intervals; the hydraulic properties of the formation adjacent to the well open interval and the stratification of contaminants in the formation. To evaluate the effects of these factors on the use of diffusion samplers and gain understanding into conditions that may limit its use in the field, modeling of movement of contaminants through the well screen due to hydrodynamic flow for various stratigraphic and well conditions were simulated using SVFLUX and CHEMFLUX[1] software. This gave insight on the impacts of groundwater flow parameters, contaminant concentration profile and stratigraphy of the soil adjacent to the well screen open interval, in order to develop guidelines on the use of the dialysis samplers in different well configurations and soil conditions.

---

[1] SVFLUX and CHEMFLUX are developed by SoilVision Systems Ltd. The SVFLUX and CHEMFLUX versions used are 3.19.0002 and 3.02.0001 respectively. The solver used by these programs is FLEXPDE version 3.10a professional from PDE Solutions Inc.

1.2 Objectives of the thesis

The objectives of this thesis are:

- Determination of the impacts of the use of oxygenated deionized and deoxygenated deionized infill water on sample chemical concentration;
- Evaluation of the impacts of time on sampler integrity under field conditions; and
- Evaluation of conditions that may limit the use of the dialysis samplers in different soil stratigraphy and groundwater flow conditions.

1.3 Scope of work

To understand the impacts of infill water oxygenation on chemical equilibration and concentration, an analytical model was developed based on diffusion through a thin membrane to evaluate the impacts on the concentration of BTEX compounds and inorganic ferrous ion. This was followed by laboratory and field experiments to determine the infill water oxygenation effects and the integrity of the dialysis samplers over time. A grab tensile strength test and burst pressure test were used to evaluate the integrity of the dialysis membrane samplers deployed in the field over a six month period. Three-dimensional models with different stratigraphic and flow conditions using SVFLUX and CHEMFLUX were used to evaluate conditions that may limit the use of the dialysis membrane by varying the permeability of the formation adjacent to the well open interval under different concentration gradients.

1.4 Organization of thesis

This thesis is written in paper format and divided into four chapters. Chapter 1 gives the general background to the study and outlines the structure of the work done. Chapter 2 contains a literature review on regenerated cellulose diffusion samplers, formulation of the theoretical model on the impacts of the type of infill water, a description of the experimental set up and design, presentation of the results, discussions, conclusions on major findings on the impacts of infill water in the sampler, and the integrity of the membrane with time.

Chapter 3 details modeling of contaminant movement across the well open interval, brief background to the need of the study and the software used. The model set-up with the basic assumptions of the formulas used, results, discussions, and conclusion on major findings were presented in the chapter as well.

The last chapter, Chapter 4, concludes and summarizes the results of this study, and recommends future work to be undertaken that may improve knowledge on the use of dialysis samplers.

References

U.S. Environmental Protection Agency (USEPA), 1999. Use of Monitored Natural Attenuation at Superfund, RCRA Corrective Action, and Underground Storage Tank Sites, Office of Solid Waste and Emergency Response (OSWER) directive 9200.4-17P. pp3. http://www.epa.gov/swerust1/directiv/d9200417.pdf.

2 Evaluation of a Diffusion Sampling System for MNA assessment

2.1 Introduction

The importance of obtaining representative groundwater samples cannot be over emphasized to properly delineate contaminated groundwater plumes. It is crucial to site characterization and assessment, monitoring, and determination of the type and effectiveness of remedial measures to be implemented. Ideally, a sampler should not alter the chemistry or quality of the sample, be easy to use and relatively inexpensive (Parker and Clark, 2003). The conventional techniques involving the use of bailers and pumping systems may interfere with the quality of samples obtained due to changes in physical conditions of the water during sampling and problems associated with random spacing i.e. variable hydraulic conductivity and variable contaminant concentration of the contributing formation in the well's open interval (Parker, 1994). Due to the shortcomings of these methods in monitoring dissolved hydrocarbons, California EPA (1997) has issued a guidance document on the use of no purge systems for sampling groundwater in monitoring wells. More so, various studies have been conducted on alternative sampling techniques, one of which is the use of diffusion samplers to sample contaminant concentrations in groundwater.

Diffusion samplers are made of plastic or polymeric membranes filled with deionized water that work on the principle of diffusion associated with concentration gradients. The mechanisms involved may include partitioning of the solutes to the membrane and subsequent desorption into the in-filled deionized water (Vroblesky and Hyde, 1997). Various types of membranes including synthetic and natural membranes have been investigated and used to sample organic and inorganic solutes in groundwater. Passive diffusion samplers made from low density polyethylene (LDPE) have been shown to effectively sample low concentrations of volatile organic compounds (VOCs) but were not suitable for inorganic compounds, hydrophilic compounds and larger organic molecules in groundwater (Ehlke et al, 2002). To sample both organic and inorganic constituents of groundwater, different types of membranes such as polysulfone, cellulose acetate, regenerated cellulose, etc, have been used (Margaritz et al, 1989; Tunks et al, 2000; Diog and Liber, 2000; Vroblesky et al, 2000). Of all the dialysis membranes, diffusion samplers made from regenerated cellulose dialysis membrane tubing are better suited for most environmental monitoring applications (Ehlke et al, 2002). They can be used to effectively sample both inorganic and organic compounds including VOCs. They have good chemical compatibility; exclude particulates and most colloids except truly dissolved species due to its ultra small pore size. More so, they are easily constructed and disposable, relatively inexpensive, and do not leach-sampled contaminants (Vroblesky and Pravecek, 2002; Ehlke et al, 2002).

In recent study by Bopp (2004), diffusion samplers were coupled in the development of passive sampling device for combined chemical and toxicological long-term monitoring of groundwater using adherent-dependent permanent vertebrate cell cultures as reporter system in a solvent-free solid phase bioassay (Biosilon). This will enable the assessment of effects elicited by complex mixtures in the environmental sample but this is outside the scope of this study.

Regenerated cellulose requires strict handling, cleaning and storage prior to usage, and the time required for equilibration implies two trips to the monitoring site. Apart from these requirements, concerns have been raised on the potential for chemical or biological degradation of the membrane if deployed in the field for extended period of time, and the potential for the oxidation of highly oxidizeable dissolved constituents of the water being sampled if the infill water contains dissolved oxygen. Other concerns raised include the effects of ionic strength and valence of dissolved ions because according to Vroblesky and Pravecek (2002), regenerated cellulose may have a slight negative surface charge in waters with pH > 3, which may result in sampling bias with respect to cations. There may also be loss of water from the dialysis sampler in highly saline water. In a recent study conducted by Morin (2004) using monovalent and divalent dissolved salts, the ionic charge had no apparent effect on the equilibration of the ions at neutral pH, and the ionic strength had minor effects on water loss. The study also showed the potential for significant water loss if a portion of the sampler is exposed above the groundwater level. In evaluating degradation of the membrane, Imbrigiotta and Ehlke (2002) reported visual degradation of the membrane after approximately one month in a single well. However, no quantitative analysis was presented to ascertain the loss of integrity of the membrane, which may be site specific.

Therefore, in this study, theoretical modeling and laboratory experiments were undertaken to determine the impacts of the use of oxygenated (Ox) and deoxygenated (D_eO_x) deionized infill water in the dialysis sampler, and evaluation of the integrity of the sampler over time in the field.

2.1.1 Objectives of Study

The research objectives of this study are:

- The determination of the impacts of the use of oxygenated deionized and deoxygenated deionized infill water on regenerated cellulose dialysis membrane sampler used to monitor BTEX and inorganic ions, and
- Evaluation of the impacts of time on integrity of the sampler.

2.1.2 *Scope of Work*

The scope of work includes the development of analytical solutions coupled with laboratory experiments to improve understandings of the impacts of the use of oxygenated infill water. Pressure and tensile strength tests were also used to determine the integrity of samplers deployed in the field over a six month period, and the results were compared with new samplers to resolve issues related to sampler integrity over time.

2.2 Theoretical model formulation to evaluate impacts of the infill water

To understand the impacts of the degree of oxygenation of the in-filled water on sample integrity, simulations were made for benzene only, and benzene with iron based on the theoretical knowledge of the diffusion process through the dialysis membrane and reactions with dissolved oxygen (DO) in the sampler.

2.2.1 *Assumptions*

- There are enough microbes in-situ to facilitate the degradation of the benzene;
- The oxidation takes place at the membrane interface as the benzene and iron diffuse through the dialysis membrane;
- The degradation of benzene is limited by the amount of dissolved oxygen (O_2) present;
- The model couples diffusion and first order biodegradation of benzene, and instantaneous oxidation of iron, governed by the rate of diffusion through the membrane and the dissolved oxygen in the sampler;
- The formation fluid has no dissolved oxygen;
- Diffusive flux will continue till the system reaches equilibrium.

2.2.2 *Diffusion formulation*

The geometry of the modelled system is based on laboratory experimental layout described in Section 3. Diffusive flux equation through a thin membrane was developed based on the principle of mass conservation as given below:

For conservation of mass,

$$\frac{\partial M}{\partial t} = JA \qquad [1]$$

$$J = D_m \frac{\partial C}{\partial x} \cong D_m \frac{\Delta C}{\Delta x} \qquad [2]$$

Where M is the mass in the sampler [M],

J is the diffusive mass flux through the membrane [$ML^{-2}T^{-1}$],

A is the surface area of the sampler [L^2],

C is the solute concentration [ML^{-3}], and *t* is the time [T].

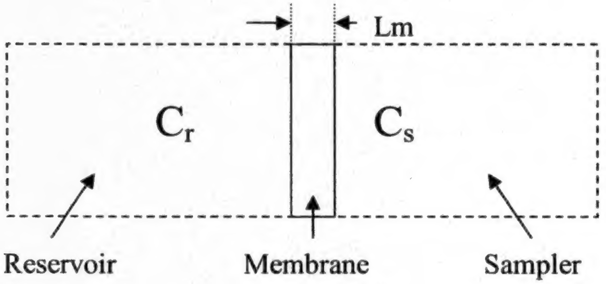

For a given sampler/reservoir system shown above,

$$J = -D_m \frac{(C_s - C_r)}{L_m} \qquad [3]$$

$$M = C_s V_s \qquad [4]$$

$$\frac{\partial M}{\partial t} = \frac{\partial (C_s V_s)}{\partial t} = V_s \frac{\partial C_s}{\partial t} = JA$$

$$V_s \frac{\partial C_s}{\partial t} = -D_m \frac{(C_s - C_r)}{L_m} \times A = \frac{-AD_m}{L_m}(C_s - C_r)$$

$$\frac{\partial C}{\partial t} = \frac{-AD_m}{V_s L_m}(C_s - C_r) \qquad [5]$$

$$\therefore C_s(t) = C_r\left[1 - \exp\left(\frac{-D_m At}{V_S L_m}\right)\right] \qquad [6]$$

Where D_m is the membrane effective diffusion coefficient for the solute [L^2T^{-1}],

C_s is the sampler solute concentration [ML^{-3}],

C_r is the reservoir fluid solute concentration [ML^{-3}],

L_m is the thickness of the sampler, and

V_s is the volume of the sampler.

Equation [6] above has been used by Sanford et al. (1996) to model gas diffusion through a thin membrane by replacing the C_r term with HC_r, where the H is the dimensionless Henry's constant. Divine and McCray (2004) also used the equation above to model solute diffusion through a polyethylene diffusion sampler.

The equation [6] is true when C_r is constant. However, to solve for the condition of temporal variation in C_r, the equation above is invalid thereby requiring a numerical approximate solution as derived below:

$$\frac{\partial C_s}{\partial t} \approx \frac{\Delta C_s}{\Delta t} \qquad [7]$$

Where

$$\Delta C_s = C_s^{i+1} - C_s^i \qquad [8]$$

$$\Delta t = t^{i+1} - t^i \qquad [9]$$

The superscripts "*i*" and "*i*+1" indicate values at the respective time intervals. From the equations above, equation (6) can be re-written using numerical approximation technique as given below:

$$\frac{\Delta C_s}{\Delta t} = \frac{-D_m A}{V_S L_m}\left(C_s^i - C_r^i\right) \qquad [10]$$

Substituting equations (8) and (9) gives:

$$\frac{C_s^{i+1} - C_s^i}{t^{i+1} - t^i} = \frac{-D_m A}{V_S L_m}\left(C_s^i - C_r^i\right) \qquad [11]$$

Rearranging the equation above making C_s^{i+1} as the subject of formula and re-substituting $\Delta t = t^{i+1} - t^i$ yield:

$$C_s^{i+1} = C_s^i + \Delta t\left[\frac{-D_m A}{V_S L_m}\left(C_s^i - C_r^i\right)\right] \qquad [12]$$

Equation [12] above has been used to model diffusion into a polyethylene diffusion sampler (Divine and McCray, 2004) and works well. However, in using the numerical equation above Δt has to be optimized to reduce the round off error. From analysis of equation [12], Δt can be approximated using

$$\Delta t = \frac{1}{2p\left[\frac{D_m A}{V_s L_m}\right]} \le 0.05, \qquad [13]$$

With $p \cong \{2,3,\ldots\}$

It should however be noted that the lower the Δt chosen, the better the approximation. To minimize unusually long iteration, Δt in the range of 0.02 to 0.04 days gives good approximation with very low round off error (less than 0.01%).

2.2.3 Benzene and Iron Oxidation Calculations

2.2.3.1 Benzene stoichiometry

From the stoichiometry of reactions for benzene compounds assuming other thermodynamic conditions are satisfied, a parameter termed the utilization factor (U_F) defined as the mass of electron acceptor consumed or by product produced divided by the mass of electron donor utilized, can be used to quantify oxygen consumption coupled with degradation. For example, in the overall oxidation reaction of benzene given below, the utilization factor for dissolved O_2 is 3.08.

$$C_6H_6 + 7.5O_2 \rightarrow 6CO_2 + 3H_2O \qquad [14]$$

This implies that 1mg of benzene will utilize 3.08 mg of O_2 for complete biodegradation.

2.2.3.2 Iron stoichiometry

The aqueous oxidation of iron in natural systems can be represented by the equation given below (Langmuir, 1997):

$$Fe^{2+} + \tfrac{1}{4}O_2 + \tfrac{5}{2}H_2O \rightarrow Fe(OH)_3 + 2H^+ \qquad [15]$$

From this equation, 56mg of Fe^{2+} requires 8mg of O_2 for complete oxidation. Based on this stoichiometry, the utilization factor "U_{Ffe}" for dissolved oxygen (DO) consumed is 0.142mg for Fe^{2+} oxidation.

2.2.3.3 Models for simulation

2.2.3.3.1 Benzene diffusion and biodegradation

The model assumes a first order biodegradation formulation for benzene expressed as:

$$\frac{\partial C}{\partial t} = -\lambda C \longrightarrow C(t) = C_0 e^{-\lambda t} \qquad [16]$$

Where λ =first order biodegradation rate.

A numerical first order decay model of equation [14] given below was used to simulate residual concentration after the ith interval.

$$Cl_i = Ca_i \left[\frac{1}{2}\right]^{\frac{\Delta t_i}{t_{1/2}}} \qquad [17]$$

Where Cl_i = sampler concentration remaining after degradation at ith interval,

Ca_i = sampler concentration due to diffusion including prior degradation at ith interval,

Δt_i = ith time interval, and

$t_{1/2}$ = degradation half-life of the substance ($t_{1/2}$ of 2.31 days was used for benzene (Rifai and Newell, 2002; USEPA, 2005)).

Re-writing equation [10] to simulate the temporal variation of benzene concentration in the sampler gives:

$$Ca_{i+1} = Cl_i + \Delta t_i \left[\frac{-D_{mb} A}{V_s L_m} \left(Cl_i - Cbr_i\right)\right] \qquad [18]$$

Where, D_{mb} = membrane effective diffusion coefficient for benzene (1.5×10^{-11} m²/s); and

Cbr_i = benzene reservoir concentration at ith interval, representing the temporal variation in the reservoir concentration over time.

To incorporate biodegradation and diffusion into the dialysis sampler, it is necessary to define another concentration term to account for mass loss in the sampler. The term is defined as "Cd_i", which is the degraded concentration at ith interval given by:

$$Cd_i = \Delta C_i = Ca_i - Cl_i \qquad [19]$$

For deoxygenated water inside the sampler, the degraded concentration becomes zero (i.e. $Cl_i = Ca_i$) because the degradation of benzene is limited by the availability of dissolved oxygen.

2.2.3.3.2 *Iron oxidation*

Using the same approximate solution for diffusion through a dialysis membrane and redefining the diffusion equation for iron as given below with different notation to distinguish it from that of benzene diffusion.

$$Cg_{i+1} = Ch_i + \Delta t\left[\frac{-D_{mf}A}{V_s L_m}\left(Ch_i - Cfr_i\right)\right] \qquad [20]$$

$$Ch_i = Cg_i - Cfo_i \qquad [21]$$

Where, Cg_i = diffused Fe^{2+} concentration at ith interval;

Cfo_i = oxidized Fe^{3+} concentration at ith interval;

Ch_i = Fe^{2+} sampler concentration after oxidation at ith interval; and

Cfr_i = reservoir Fe^{2+} concentration at ith interval

D_{mf} = membrane effective diffusion coefficient for Fe^{2+} (2×10^{-11} m^2/s)

For deoxygenated water, the oxidized concentration is zero (i.e. Ch_i = Cg_i) because the oxidized Fe^{2+} concentration is limited by the amount of dissolved oxygen in solution as discussed later in this section. All the diffused Fe^{2+} concentration will be oxidized until all the dissolved oxygen is consumed, Fe^{2+} used-up, or a state of equilibrium is reached if the pH is reduced which will inhibit further oxidation to Fe^{3+}. However, the latter is not accounted for in this model.

2.2.3.3.3 *Coupled Model for benzene and iron oxidation*

To account for concentration of dissolved oxygen used in oxidation, it is necessary to couple the formulated equations with appropriate boundary conditions considering iron and benzene oxidation. Therefore, let Y_i = total concentration of dissolved oxygen in the sampler at ith interval;

Y_{di} = total concentration of dissolved oxygen consumed at ith interval;

Y_{dfi} = dissolved oxygen concentration used up for iron oxidation at ith interval; and

Y_{dbi} = dissolved oxygen used up for benzene degradation at ith interval.

$$\therefore \qquad Y_{di} = Y_{dfi} + Y_{dbi} \qquad [22]$$

$$Y_{i+1} = Y_i - Y_{di} \qquad [23]$$

The boundary conditions used for solving this numerical problem are outlined below:

Cbr_0 = initial benzene concentration in the reservoir at the start of experiment.

Cfr_0 = initial iron concentration in the reservoir at the start of the experiment (5mg/L was assumed for the simulation).

$Cl_0 = 0$ = benzene concentration in the sampler at the start of the experiment.

$Ch_0 = 0$ = iron concentration in the sampler at zero time interval

$Cfo_0 = 0$= oxidized Fe3+ concentration in the sampler at zero time interval

Y_0 = initial dissolved oxygen concentration in the sampler which is assumed to be 6mg/L for the oxygenated water and zero for the deoxygenated water.

Assuming instantaneous iron oxidation, the DO used for iron oxidation at each time step is:

$$Y_{dfi} = U_{Ffe} Cfg_i \qquad [24]$$

When $Y_{dfi} < Y_{i-1}$, $Cfg_i = Cfo_i$ [25]

When $Y_{dfi} \geq Y_{i-1}$, $Y_{dfi} = Y_{i-1}$ [26]

$$\therefore Cfo_i = \frac{Y_{i-1}}{U_{Ffe}} \qquad [27]$$

(Note: U_{Ffe} is the utilization factor for Fe^{2+} oxidation= 0.286)

To avoid negative dissolved oxygen concentration and limit degradation to the available concentration of oxygen a new term "Cc_i" was defined to represent the limiting degradable benzene concentration:

$$Cc_i = \frac{Y_{i-1} - Y_{dfi}}{U_{Fb}} \qquad [28]$$

Where U_{Fb} is the utilization factor for benzene oxidation = 3.08.

Thus, when $Cd_i \leq Cc_i$, $Y_{dbi} = U_{Fb} Cd_i$ [29]

Whenever $Cd_i > Cc_i$, Set $Cd_i = Cc_i$ [30]

$$\therefore Cl_i = Ca_i - Cd_i \qquad [31]$$

The temporal residual concentration of the reservoir for benzene and aqueous iron are calculated as follows:

$$Cbr_{i+1} = Cbr_i - \left[\frac{(Ca_{i+1} - Cl_i) \times nV_s}{V_r} \right] \qquad [32]$$

$$Cfr_{i+1} = Cfr_i - \left[\frac{(Cg_{i+1} - Ch_i) \times nV_s}{V_r} \right] \qquad [33]$$

Where, V_r is the volume of the reservoir (fluid) and n is the number of samplers in each reservoir. For the closed system simulation, n = 3, V_r = 1.513L and $V_s = 0.15L$. For the open system, $V_r >> nV_s$, therefore, the reservoir concentration is constant. A summary of the solution to this numerical formulation is shown in section 4

2.3 Experimental Set-up and Design

To examine the impacts of oxygenated (O_x) and deoxygenated (D_eO_x) water, and sampler integrity with time, the following experimental set-up and design were used.

2.3.1 Laboratory determination of impacts of oxygenated infill water

To compare the effects of using O_X to D_eO_X infill water water, a system of reservoirs shown in Figure 2.1 was designed. The set-up consists of the following:

- Four glass reservoirs (5 cm in diameter and 100cm high),
- One 20 litre Nalgene bottle,
- Four variable head and reversible flow Multiflex peristaltic pumps,
- A stainless steel manifold, tygon tubing, glass seal, argon and nitrogen gas-cylinders, DO meters, anaerobic bags, deoxygenation apparatus, etc.

Each pump head attached to the peristaltic pump was connected at one end to a glass reservoir and the other end to the manifold. The manifold was used to couple the four reservoirs together through one inlet to the Nalgene bottle, then, filled with formation water and elevated as shown in Figure 2.1 to allow gravity flow of water to the manifold. All the connections were fitted with valves for flow control. The manifold, pump, and Nalgene bottle were enclosed in an airbag filled with nitrogen gas to minimize interaction with atmospheric oxygen.

Diffusion samplers were fabricated from pre-treated regenerated cellulose from Membrane Filtration Products Inc. (MPFI). The dialysis membrane has a molecular weight cut off (MWCO) of 8000 Dalton, wall thickness of 30μm, nominal pore size of about 0.002μm, and a closed flat width of 50mm. The dry filled diameter of the membrane is 31.8mm with a filled volume of 7.94mL/cm (i.e. millilitres per cm-length of sampler[2]). A length of 30cm was cut from the roll of the membrane, rinsed properly in deoxygenated deionized (D_eO_x) water, and knotted at one end (each end knotting takes about 5cm of the cut length). The open end was then filled with D_eO_x water to make the D_eO_x-Sampler or oxygenated deionized (O_x) water (of 6mg/l DO) to make the O_x-samplers. The filled samplers were knotted at the open end for the laboratory experiments but the field samplers were fitted with a brass screw-on cap as shown in Plate 1.

Two types of reservoir water (i.e. water used to fill the glass reservoirs from the Nalgene bottle) were used for the experiment. The first type was spiked deoxygenated and sterilized deionized water from the laboratory, to test the efficiency of the system and as a control. The second type of water was spiked formation water from a contaminated site. The first reservoir water was prepared by filling a 20-litre Nalgene bottle with deionized water in the laboratory, boiled to remove air bubbles and sterilize the water. The water was then cooled over several hours to room temperature and deoxygenated by drawing the water from the bottle into the 4-litre deoxygenation chamber using a vacuum pump. Nitrogen was then bubbled through chamber under a vacuum for about ten minutes to strip out oxygen from the water. The water was then discharged into another argon-filled 20-litre Nalgene bottle. The dissolved oxygen (DO) concentration of the effluent water was checked using a calibrated DO probe and it ranged from 0.0 to 0.6mg/L. The DO was also checked with a Chemet[3] tester and found to be consistently below 1mg/l. Spiking was done by dissolving 0.92mL of each BTEX compound in 250mL of methanol, and mixing the solution with the reservoir water. The bottle was shaken to mix the BTEX, and then left in place for about two hours to allow for equilibration.

---

[2] It should be noted that the membrane is expandable and due to knotting of the sampler at both ends, the filled volume is not uniform across the sampler length.

[3] A colorimetric D0 testing vial

The spiked solution container was elevated as shown in Figure 2.1 to facilitate gravity flow to the manifold from where water was pumped to the reservoir systems at 13mL/min to prevent the development of air bubbles within the system. Prior to pumping, the glass reservoirs were filled with argon to minimize mixing of ambient air with the formation water. Three prefabricated dialysis samplers were then suspended in each reservoir by monofilament fish line, hung from the lid's hook at 10 cm interspacing. The lids were sealed to the reservoir by a combination of silicon grease and glass-seal tape. A relief pipe fitted with a control valve is provided through each lid. The valves were kept opened during infilling and when the reservoirs were full with the expulsion of all entrained air, a sample of the water was taken.

Water sampling for BTEX analysis was done by pipetting 4.4mL with a 5ml-glass syringe into a 44mL vial for analysis on a GCFID[4] system (based on EPA method 8015D). The settings for the GCFID are given in Appendix A.5. Three samples were taken from each reservoir after filling, the pump was stopped, and all the valves were closed. After each sampling interval (three to five days), three samples were taken from both the reservoir and each sampler, and the DO of the samples was measured. Sampling was done as described earlier to limit volatilization, and the DO of the reservoirs was taken by inserting the probe to approximately 0.7m into the reservoir.

Two reservoirs were sampled at each time interval, one each for D_eO_x and O_x samplers respectively. The total sampling interval was one week based on the results of preliminary experimental studies and results from the theoretical simulation. When the water from the contaminated site was used, the same basic procedure was followed with the exception of heating and air striping of the water prior to spiking it.

---

[4] Gas chromatography with a Flame-ionization detectior

Also, to evaluate mass loss of BTEX to the samplers, a batch test was conducted on the dialysis membrane material to calculate the sorption on the membrane. The batch test was conducted by first preparing standard BTEX solutions of different concentrations ranging from 0.2mg/L to 5mg/L (i.e. 0.2, 0.5, 1.0, 2.0, and 5.0mg/L) in 200ml conical flasks. Fifteen 44mL-vials were pre-weighed and the dialysis membrane was cut into uniform sections of about 5 cm-width by 6 cm-height. The cut-sections were rinsed in deionized water and placed in the pre-weighed vials in a wet state. The final weight was taken and the mass of the membrane per cm^2 of surface area was calculated. A vial set consisting of three vials were filled with each of the prepared BTEX solutions of different concentrations given above to measure non-sorption losses. A control vial set of each solution was also prepared. The vials were left in the fridge at 5°C for a week and then analyzed using GCFID in the laboratory. The processed results are given in Appendix A.3.

2.3.2 *Sampler integrity testing*

Two laboratory tests were performed on the dialysis samplers to quantitatively examine its integrity over time by measuring the sampler's strength. These included pressure and grab strength tests.

2.3.2.1 *Pressure test*

The pressure test involved pressurising the sampler with water and measuring the pressure response with time. The rationale for this test is that if there is degradation of the membrane, the degraded section will give rise to localized failure under all around pressure and the membrane will rupture at a pressure less than that of a sampler, which has not degraded.

The test consists of a syringe pump, which provides fluid at a constant rate, a data-logging system for measuring pressure and volume of water pumped with time, and a stand-clamp. A schematic of the test set-up is shown in Figure 2.2. The syringe pump has two outlets, each with a valve, which can either be used for pumping or refilling the 508ml capacity cylinder of the pump. One of the outlets was connected to the brass fitting on the dialysis sampler, which was knotted at the other end. The other outlet was connected to a jar of water to refill the pump after each stroke. During each pumping operation, the refill outlet was closed, the delivery outlet opened and the system was connected to a computer system for data logging.

The test began with the sampler fabrication in the laboratory in which one end was knotted and the other end secured to a brass fitting. Some of the samplers were deployed in the field while others were tested in moist state immediately after fabrication. The brass fitting on the sampler was connected via a threaded fitting to a tygon tube, which was connected to the outlet of the syringe pump. The sampler was lowered into water filled container to keep the membrane moist, and held in place by a stand-clamp. The syringe pump was then started and water was pumped into the sampler at a constant rate of 40mL/min. The pressure and volume of water being injected were recorded by the computer data-logger. If the membrane was still intact after the first stroke of the pump position, the valve to the sampler was closed, that of the reservoir was opened, and the pump refilled. Sampler failure was defined as the pressure at which the membrane ruptured. A benchmark test was first performed on four new samplers to provide baseline data for statistical comparison with the samplers deployed in the field.

2.3.2.2 Tensile strength test

To examine membrane degradation with time, a grab tensile strength test was also developed. The rationale for using this test is that if the membrane has degraded, there will be a significant decrease in its tensile strength due to local defects arising from degradation. However, since no previous record of the use of this test on dialysis membranes was found, there was need for baseline tests on the membrane to determine the average tensile strength and elongation prior to failure.

The test was conducted in accordance to ASTM D5034. The testing machine used was Instron-V Model 4202. The membrane was cut to a length of 15cm and maintained in wet state. The clamps were set 7.5cm apart and loading was performed with a crosshead speed of 10mm/min because of the nature of the material. The specimen was mounted between the clamps with equal projection at both ends, and a tissue paper was used to support the grip of the membrane at both ends to prevent slippage of the membrane and to improve the grip. Times to failure were typically 3 to 4 minutes.

A computer data-logger recorded the strength and elongation of the membrane. Initially, some tests were conducted on split-width samples of the membrane but when failure initialized around the split zone, subsequent tests were performed on the intact membrane. A benchmark test was also performed on the pressure-tested samplers, and the sampler failure was defined as the tensile strength at which the membrane snapped. Typical strength response for the dialysis membranes are given in Appendix A.2.

2.4 Results and discussion

2.4.1 Impacts of dissolved oxygen in the infill water

2.4.1.1 Analytical simulation

The analytical simulation results are given in Appendix A.1 and the results for 1mg/l benzene and summary results are given in Figures 2.3, and 2.4 using the predictive model for the previously described laboratory experimental setup. Figure 2.3 shows the model results for 1mg/l of benzene in the reservoir. Considering diffusion only with no oxidation, the system will come to equilibrium within three days at a concentration of 0.78 mg/L corresponding to about 22% reduction in mass concentration due to dilution only. When oxidation of benzene only was considered with an initial DO of 6mg/L in the sampler, equilibrium occurred in approximately 16 days at a concentration of 0.35 mg/L. However, when 5mg/L of Fe^{2+} oxidation was coupled with benzene oxidation, the equilibration time was approximately nine days with a benzene equilibrium concentration of 0.5 mg/L. Thus, the mass concentration losses due to degradation are 43% and 28% for benzene oxidation only and benzene with iron oxidation respectively. These losses cannot be projected to different initial reservoir concentrations in the closed system because the degradable concentration is fixed, implying that the lower the initial reservoir concentration, the greater the percentage of mass concentration losses due to degradation.

The concentrations vs. time curves in Figure 2.3 are divided into four regions based on the shape of the curves. In region "I", due to initial high concentration gradient the diffusion rate into the sampler is greater than the benzene oxidation so the curves for the reservoir and sampler concentrations approach each other rapidly. In region "II", the concentration gradient has diminished, thus, the diffusion rate is nearly the same as the rate of oxidation so the curves of the reservoir and sampler concentrations are nearly parallel. This continues until all the dissolved oxygen in the sampler is depleted, resulting in rapid equalization of reservoir concentration in region "III", which accounts for the observed jump in the diffused concentration. Finally, in region "IV", the diffused concentration comes into equilibrium with the reservoir concentration.

Figure 2.4 shows a summary of equilibration times for varying reservoir concentrations of benzene, DO and Fe^{2+}. For a given reservoir benzene concentration (i.e. 3mg/L), the time to equilibrate can be read off the graph (i.e. shown as a dotted line). At concentrations above 10mg/L, the equilibration times are nearly constant for all the models, however, as the concentration decreases below 10mg/l, the differences become apparent. If there is no oxidation, equilibration will occur for all concentrations in three days. With biodegradation only, at benzene concentrations below 1mg/L, it may take more than three weeks to achieve equilibrium. With oxidizeable iron, equilibrium is attained much faster (i.e. 5.8days for benzene concentration of 3mg/L). The equilibrium concentrations can also be read off the graph, by following the reservoir concentration horizontally across to the appropriate diagonal line, then extending a line vertically upward to read off the top scale, as shown in Figure 2.4. The simulation results are for the closed system used in the laboratory set-up.

When the model was modified to simulate the field scenario whereby the available contaminant mass in the formation is high in comparison with that of the samplers within the well, Figure 2.5 was produced for benzene formation concentration of 5μg/L (0.005mg/L), and the results for other formation concentrations are included in Appendix A.1. Figure 2.5 shows that equilibration occurs in about three days with no oxidation. If only benzene oxidation is considered, the benzene concentration after three days will be approximately 90% of the formation concentration using a realistic first order biodegradation rate constant ($\lambda=0.3\text{day}^{-1}$). A summary of the simulated results at other concentration values are given in Figure 2.6. From the results, the times to achieve equilibrium at benzene concentrations in the parts per billion (μg/L) ranges are significantly shorter in the presence of oxidizeable iron in the formation.

Moreover, a sensitivity analysis was performed by increasing the first order degradation rate "λ" of the benzene by an order of magnitude from 0.3day^{-1} to 3day^{-1} to determine its impact on equilibration. The summary of the results is given in Figure 2.7, and it can be seen that equilibration is achieved faster but the sampler concentration equilibrated at about 45% of the formation concentration until the depletion of the dissolved oxygen in the sampler by benzene, when oxidizeable ions are absent (Figure 2.5). It should be noted that multiplying the degradation rate by a factor is commensurate to dividing the half-life by the factor. The initial degradation rate of 0.3day^{-1} corresponds to half-life of 2.31days for benzene (USEPA, 2005), which is reasonable for all practical purposes, and it is very unlikely to have half-life of 0.231day in the absence of other oxidizeable ions in petroleum impacted sites.

2.4.1.2 Laboratory experiment

The results of laboratory equilibration tests for BTEX compounds spiked into deionized water are shown in Figure 2.8. From the t-test analyses of the BTEX data given in Appendix A.4, equilibration occurred within three days and there was no significant difference in concentrations obtained in the oxygenated (O_x) versus deoxygenated (D_eO_x) samplers. This was expected because the water used was sterilized. From the predictive models (Figures 2.3 and 2.4), equilibration was expected to occur in three days, which is corroborated by the results. More so, it should be noted that the consumable dissolved oxygen (DO) in the system is fixed, i.e. 2.7mg of DO was available for consumption in each reservoir system. This translates to about 0.86mg of degradable BTEX mass, and a total loss of 0.45mg/L in concentration, which the system is not sensitive enough to account for at the elevated concentrations tested.

The data from using spiked formation water from contaminated wells in the field is shown in Figure 2.9 and shows no significant difference in BTEX concentrations for both samplers (Appendix A.4). Sampling was done at five day intervals for this run due to logistics associated with the analysis in the laboratory. The initial dissolved oxygen (DO) in the reservoirs after infilling was approximately 1.2mg/L but during subsequent sampling the measured DO was consistently non-detectable. The initial DO in the apparatus translates to 2.7mg for the D_eO_x system and 4.5mg for the O_x system. Using utilisation factor of 3.14 for total BTEX, 0.86mg and 1.4mg of BTEX could be degraded to CO_2 and H_2O (ignoring mineralization to intermediates) for D_eO_x and O_x systems respectively. These mass losses are less than the resolution of the experimental system because of the high BTEX concentrations used for the tests. The mass balance calculations of the results are given in Appendix A.2 including results for individual compounds.

A statistical comparison of the measured sampler concentrations with the reservoir concentration at each time-step showed significant difference using t-test as shown in Appendix A.4. The measured initial reservoir concentration was also smaller that the projected initial concentration by back calculation. Although these differences are within 25% analytical variation, however, the observed differences may be due to volatilizations of the BTEX compounds during sampling. As earlier mentioned, the initial reservoir concentration was measured by using syringe to siphon water from the valve attached to reservoir's lid. The annulus of the valve outlet is not under full flow because the rate at which the reservoirs were filled was low (13mL/min). At each time-step, the reservoirs were sampled from the top with the lid removed. Opening the lid depressurizes the reservoir and this may enhance volatilization of the BTEX compounds.

Batch tests results on the dialysis membrane to determine its sorption to the BTEX compounds are given in Appendix B.3. The results show little sorption to the BTEX compounds based on Langmuir isotherm with an average maximum absorbable concentration (β_{max}) of 0.0016mg/g/cm^2. This translates to a maximum of approximately 1.3mg for each BTEX compounds, which is low in comparison to the overall mass of BTEX in solution. These results agree with the simulated analytical solution for benzene. However, in practice, when using the analytical results at very low concentrations near the regulatory limits, it will be prudent to allow the samplers to seat for a prolonged period of time if an oxygenated sampler is used. Moreover, mineralization of BTEX compounds in the presence of oxygen are aided by microbes, and since the pores of the dialysis membranes are very small and impermeable to microbes, the probability for microbial oxidation of the BTEX compounds within the samplers are low. However, the same cannot be deduced for oxidizeable iron which does not depend on microbes for oxidation to take place but on properties like the pH of the solution.

2.4.2 Observations on samples deployed at field sites

The following observations were made upon retrieval of some of the samplers from contaminated field sites:

- Some dark precipitates were noticed inside some of the samplers when retrieved as shown in Plate 2. It was initially thought that these might be sulphide precipitates, but when the precipitates were mixed with nitric acid (though not readily soluble in the acid) and analysed in the lab using ICS[5], they were not sulphides. Thus, they might be some organic materials or other compounds like copper II oxide, which were not analysed for in the lab.
- Some free product was seen inside the samplers in wells containing free products (Plate 3) indicating that the samplers are permeable to free product of petroleum hydrocarbons. This petroleum fraction was not analysed in the laboratory.
- Some samplers retrieved from wells where the water table had dropped below the bottom of the samplers were almost devoid of water indicating gravity drainage and evaporative water loss as observed by Morin (2004).

---

[5] ICS – Ion Chromatography System: The model used for the analysis is DIONEX ICS-2500 with a CS12A column.

2.4.3 Sampler integrity testing

For all the samplers retrieved from site, there was no visible deterioration. However, a significant challenge encountered was preventing mechanical damage during installation and retrieval.

The pressure test results are shown in Figure 2.10. The burst pressure of four unused samplers was about 31kPa ± 5kPa. After two months in the monitoring wells, the field samplers had a slightly greater average burst pressure (33.8 kPa) in comparison to the unused samplers. The FS1-2 samplers were retrieved from a well where the water level had dropped significantly, and both samplers were immersed in free product when retrieved. However, the pressure test results and field examination indicated the samplers were intact. Sample 2-FS2-1 had very low burst pressure and the mode of failure was localized and different from all other tests. There appeared to be abrasions on the sampler surface in the localised area where failure had been initiated, which may indicate mechanical damage during installation or retrieval. After four months, the field samplers were checked and showed no visible degradation so were placed back in the well except 4-FS2-2B. The burst pressure was low (19KPa), but well over 50% of the burst pressure of the new sampler. After six months, the remaining samplers were retrieved and tested as well. The results obtained are similar to that after four months and within 2.1 standard deviations of the new samplers.

The results from tensile strength tests are summarized in Figure 2.11. The tensile strength of new membranes was 3.3±0.5kgf/cm-width. The tensile strength after two months averaged 2.9kgf/cm-width and was generally within the expected range of intact membranes except sample FS2-1. This was expected because of the local failure that was noticed in the sample in the previous pressure test. The average tensile strength results for the samplers after four and six months were lower than that obtained after two months and within 0.06 standard deviations from the new samplers. The average ambient temperature within the wells was 2°C over the six month period and there were layers of ice above the well screen, which damaged some of the samplers during retrieval from the well.

2.5 Conclusions and Recommendations

2.5.1 Conclusions

These results indicate that regenerated cellulose diffusion samplers may be highly suitable for long-term monitoring (up to six months), in sampling groundwater at upstream oil and gas sites associated with natural attenuation assessment. For a closed system (as simulated in the laboratory), the theoretical simulation showed no significant adverse impact on BTEX concentrations if oxygenated water is used with biodegradation occurring at BTEX concentration greater than 10mg/L. However, as the BTEX concentration is lowered to 1mg/L, it showed significant impact resulting in prolonged equilibration time and about 43% loss in benzene concentration in addition to the 22% reduction in concentration due to dilution. In the presence of 5mg/l oxidizeable ferrous ion, the DO is scavenged more rapidly and the time to equilibrate is significantly shortened.

The results of open system simulation, which is akin to field conditions, showed approximately 90% equilibration will occur after three days of sampler deployment even at 1ppb (0.001mg/L) concentration range. The presence of oxidizeable ferrous ion will cause equilibration to occur within a week of sampler deployment. However, in the absence of oxidizeable ion, it may take months to achieve equilibration at µg/l (ppb) concentration range. The good news is that 90% equilibration will occur after three days of sampler deployment. Thus, even with the 10% loss at low concentration (in the μg/L range), it is well within analytical variability associated with sampling. Therefore the results are quite acceptable.

The laboratory results corroborated the equilibration time calculations of the model, and also showed that the use of oxygenated infill-water in the sampler had no adverse effect in sampling for petroleum hydrocarbons (PHCs) at high BTEX concentrations. However, there is need for tests at low BTEX concentrations in the ppb range to confirm the simulation results.

The burst pressures and tensile strengths of the samplers were within the expected range of the intact samplers after two months and there was no observable physical degradation of the samplers in the field. After 4 months there was no visible degradation, however, there was a reduction of 36% and 19% in the burst pressure and tensile strength respectively.

It should be noted that the results obtained from this study are site specific, however, they are deemed reasonable for PHC contaminated sites with similar groundwater conditions. Higher temperatures or the presence of other chemicals, particularly, chlorinated solvents may give different results.

2.5.2 Recommendations for future research

- More field testing should be carried out under different conditions including higher temperature, presence of chlorinated solvents, and other in-situ chemical conditions.
- The permeability of dialysis membrane to microbes should be undertaken as this will affect the integrity of samples obtained and the membrane itself over time.
- More laboratory tests at low BTEX concentrations should be undertaken to evaluate the simulation results.

2.6 Figures

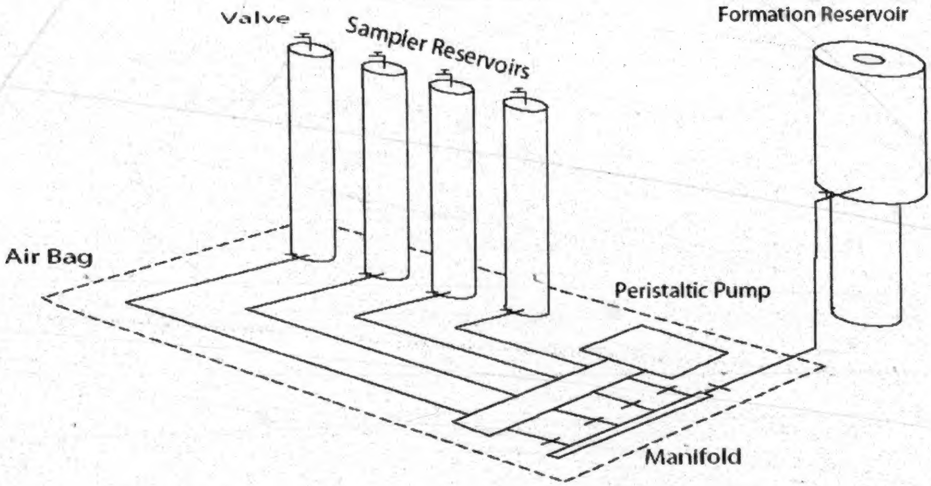
Valve
Sampler Reservoirs
Formation Reservoir
Air Bag
Peristaltic Pump
Manifold

Figure 2.1 Schematic diagram of Laboratory set-up to determine the impacts of infill deionised water.

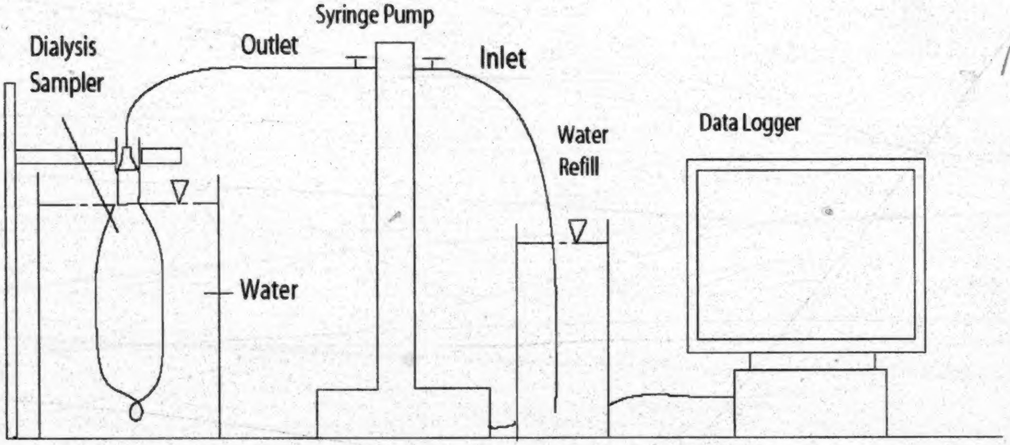
Syringe Pump
Dialysis Sampler
Outlet
Inlet
Water Refill
Data Logger
Water

Figure 2.2 Pressure test schematic set-up for integrity test.

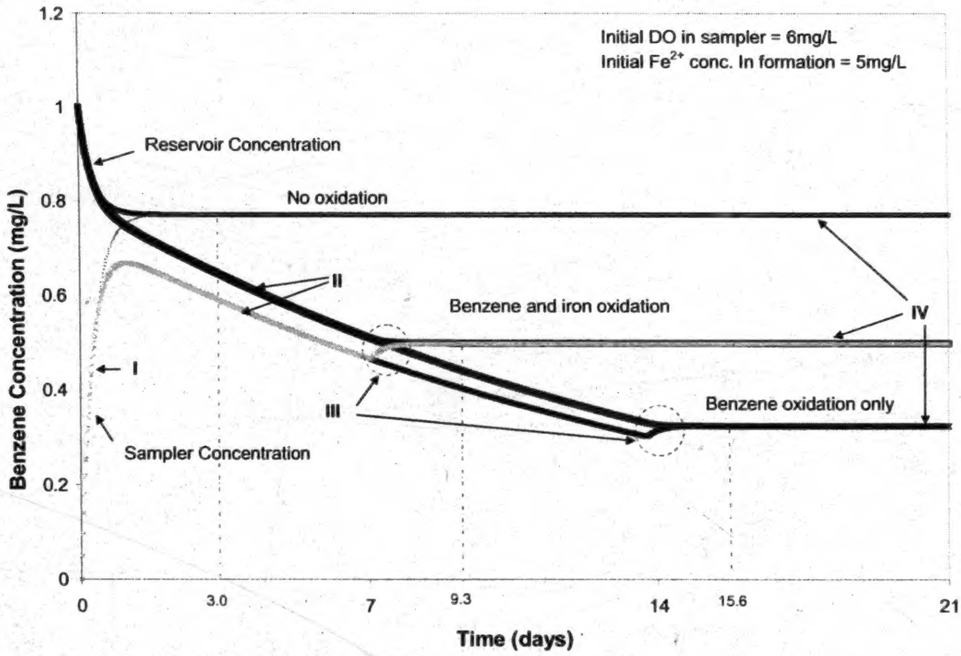

Figure 2.3 Simulation results for 1mg/L of benzene in laboratory test apparatus.

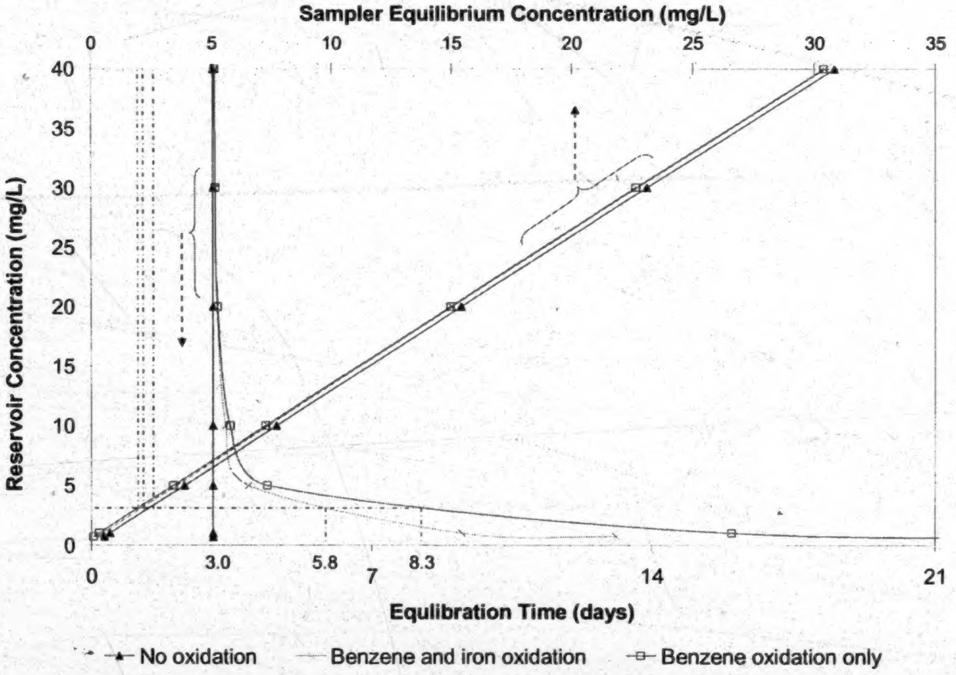

Figure 2.4 Summary of analytical simulation for benzene for the experimental set-up.

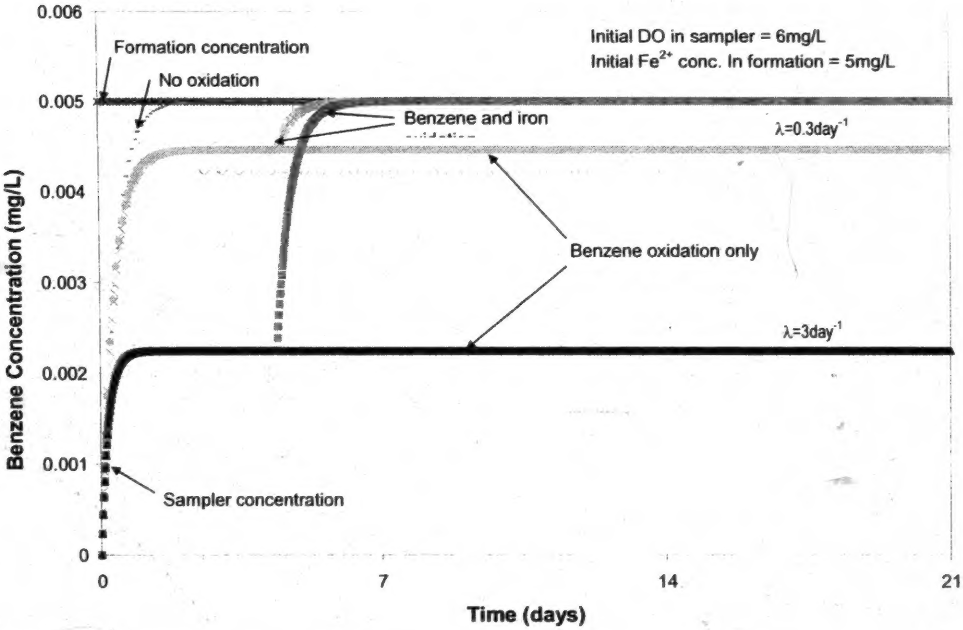

Figure 2.5 Simulation results for 0.005mg/L benzene for an open system.

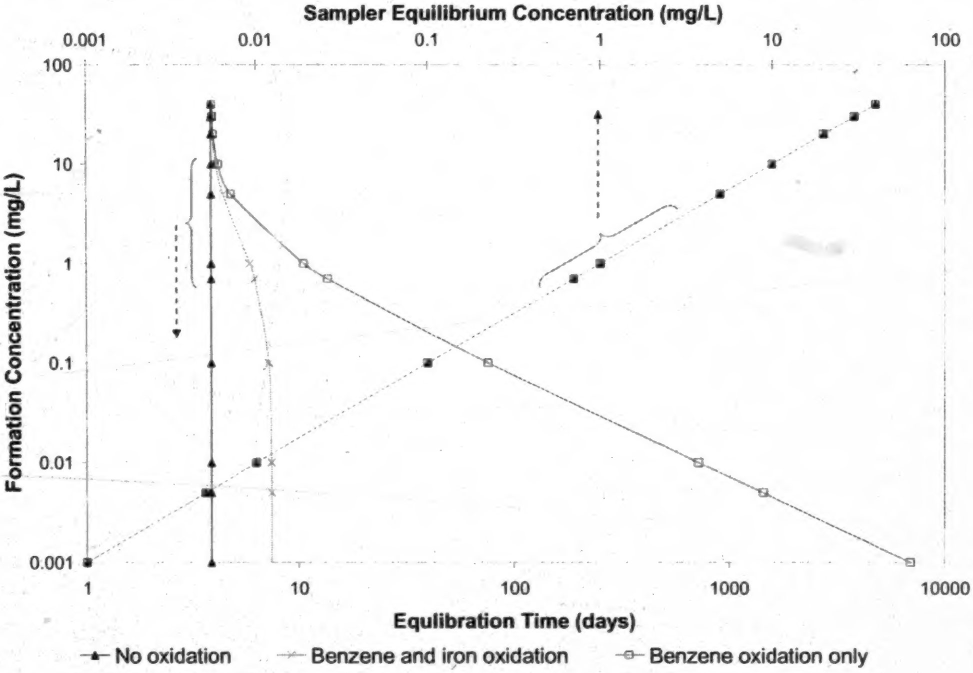

Figure 2.6 Summary of analytical simulation for an open system.

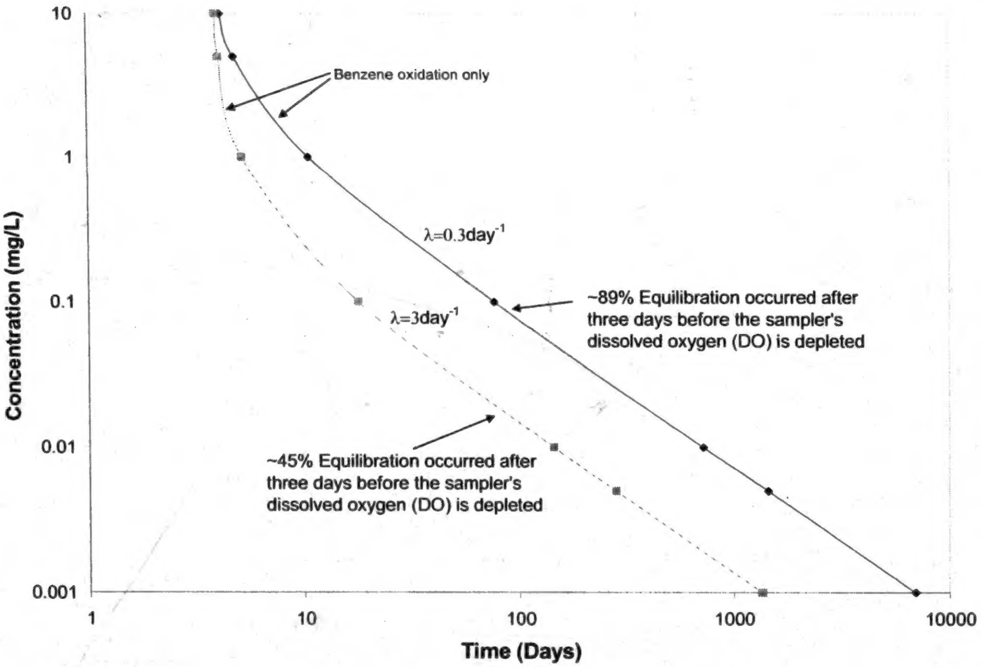

Figure 2.7 Summary of varying biodegradation rate (λ) for an open system.

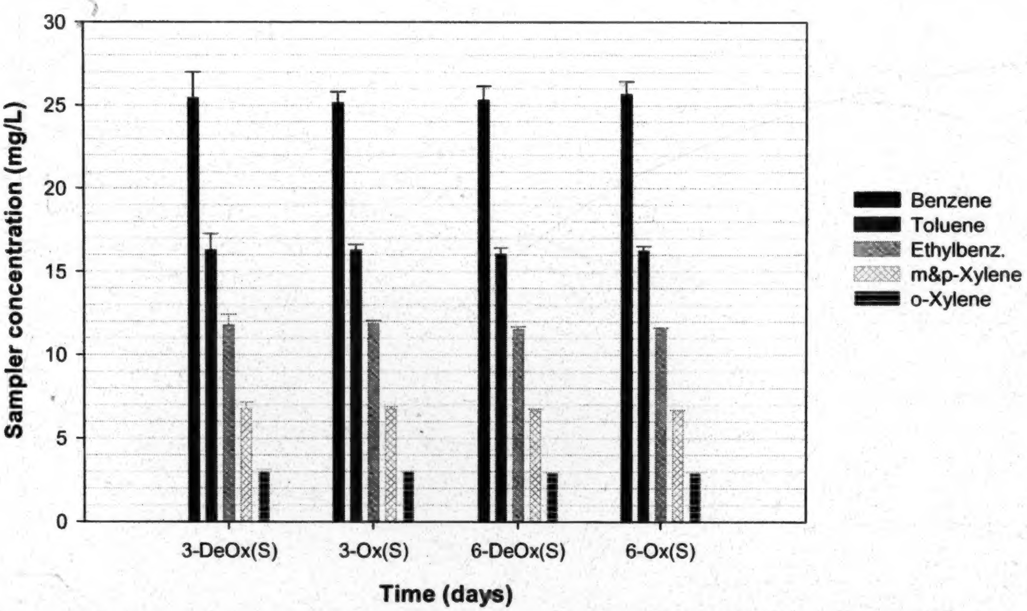

Figure 2.8 Summary of laboratory experiments for BTEX compounds in spiked deionised water. (Error bars indicate standard error associated with 95% confidence interval).

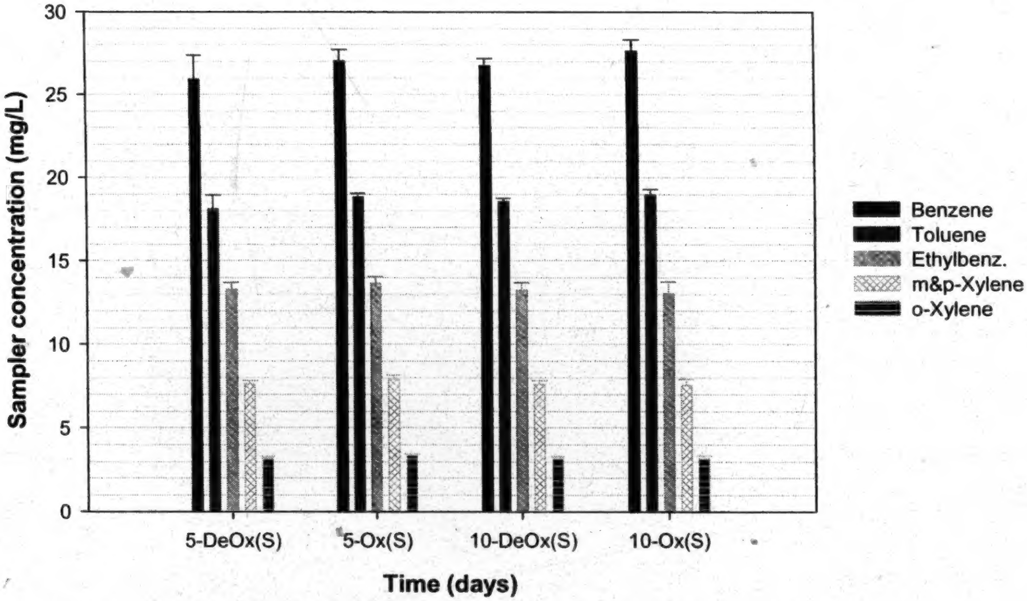

Figure 2.9 Summary of laboratory experiments for BTEX compounds in spiked formation water. (Error bars indicate standard error associated with 95% confidence interval).

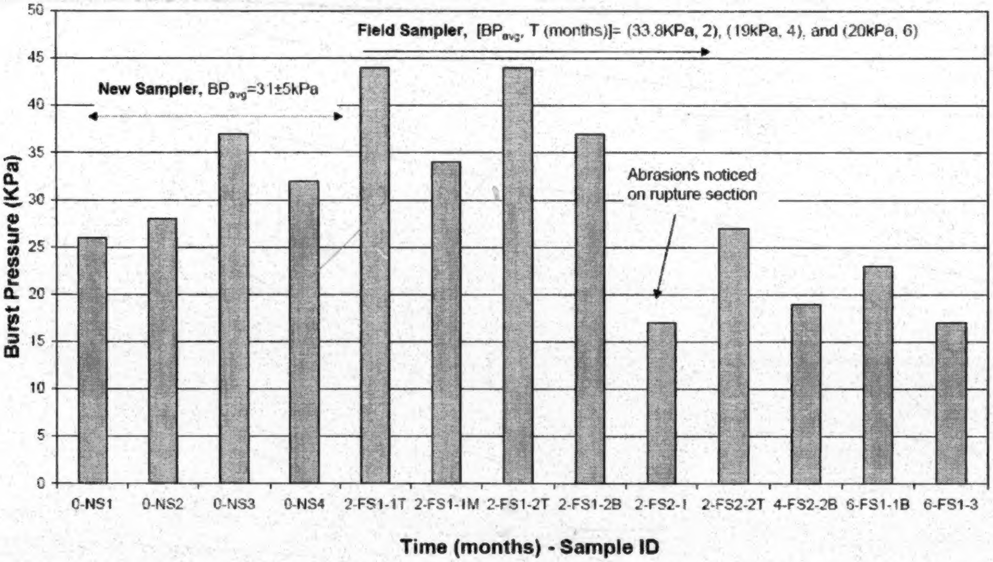

NS - New Sample FS - Field Sample T - Top M - Middle B - Bottom
Prefix before sample ID indicates duration of installation (months), and suffixes after ID indicate site number, well number and position respectively

Figure 2.10 Summary of diffusion samplers burst pressure (BP) results.

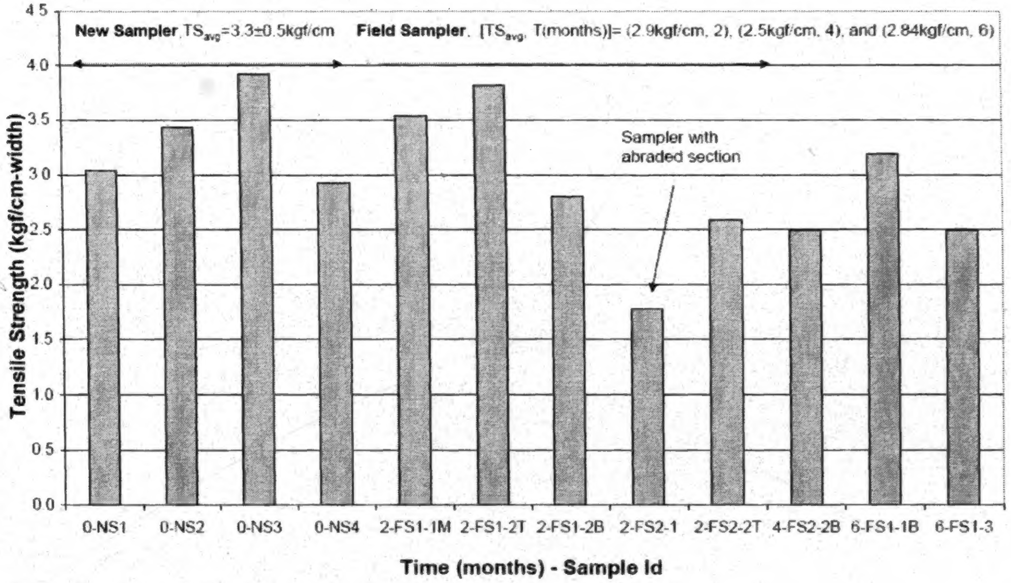

NS - New Sample FS - Field Sample T - Top M - Middle B - Bottom
Prefix before sample ID indicates duration of installation (months), and suffixes after ID indicate site number, well number and position respectively

Figure 2.11 Summary of tensile strength test results.

2.7 Plates

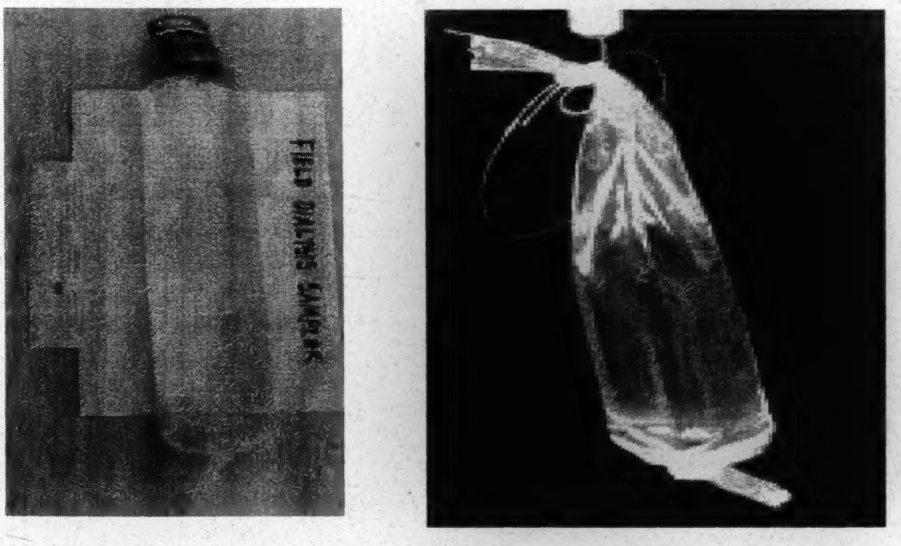

(a) (b)

Plate 1 (a) Field sampler (b) Laboratory sampler.

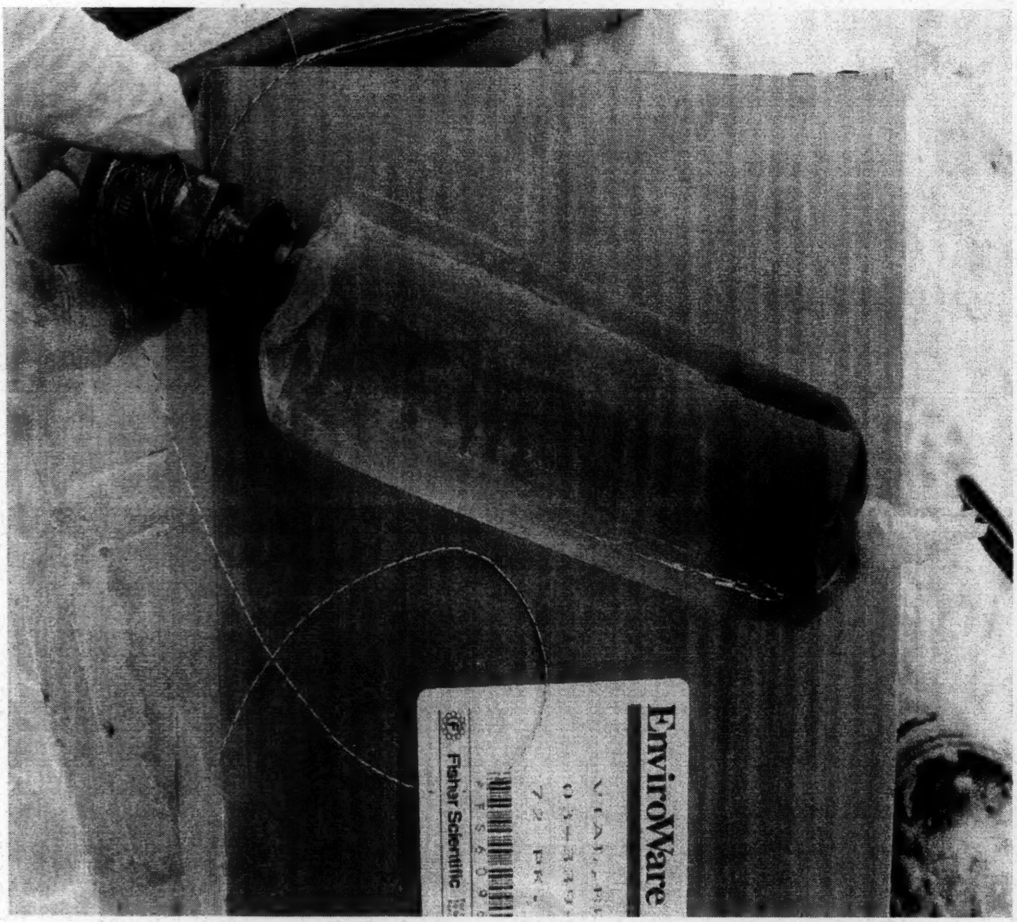

EnviroWare
Fisher Scientific

Plate 2 Field dialysis sampler showing dark substances when retrieved after two months.

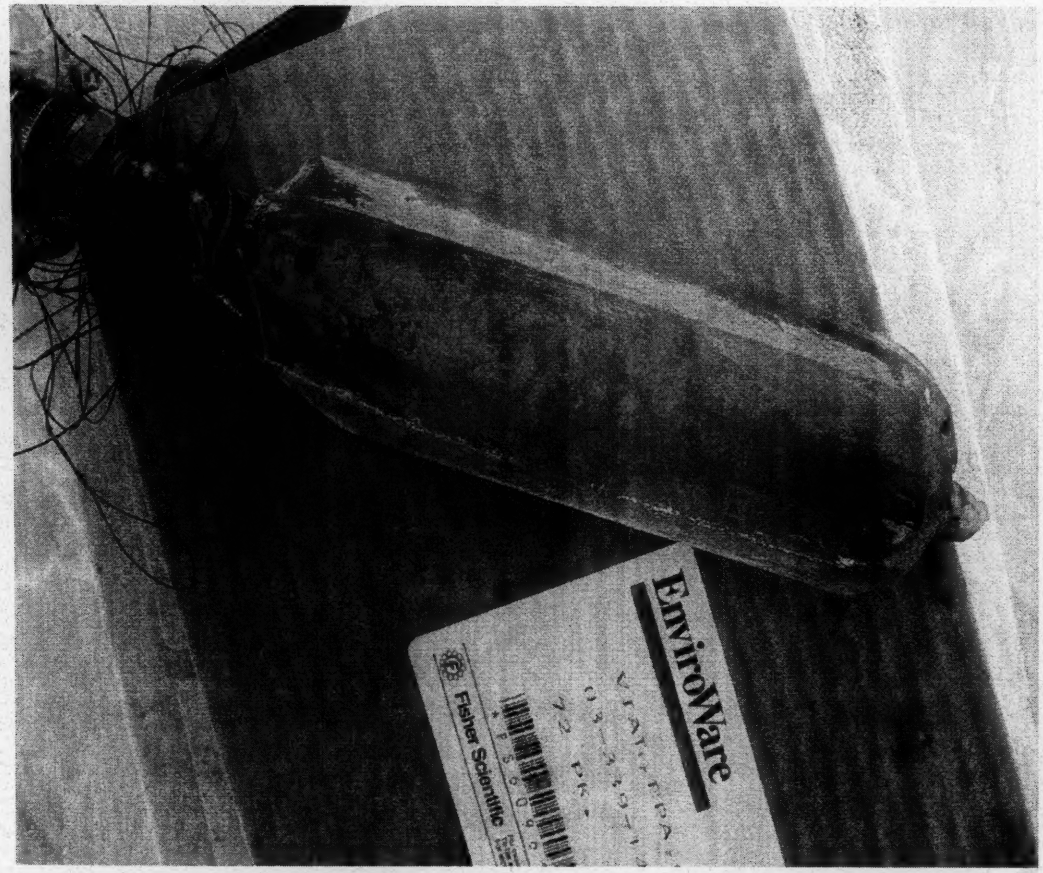

Plate 3 Field dialysis sampler showing some free phase petroleum hydrocarbon (PHC) when retrieved after two months from site.

References

Bopp, S., 2004. Development of passive sampling device for combined chemical and toxicological long-term monitoring of groundwater. Thesis, Der Mathematisch-Naturwissenschaftlichen Facultat der Universitat Rostock, UFZ-Bericht, Germany. ISBN 0948-9452.

California EPA 1997. Utilization of non-purge approval for sampling of monitoring wells impacted by petroleum hydrocarbon, BETX, and MTBE. Guidance document, Jan 31, 3 p. File 1123.64.

Diog, L., and Liber, K., 2000. Dialysis minipeeper for measuring pore-water metal concentrations in laboratory sediment toxicity and bioavailability tests: Environmental Toxicology and Chemistry, vol 19, no. 12, p. 2882-2889.

Divine, C.E., and McCray, J.E., 2004. Estimation of membrane diffusion coefficients and equilibration times for low-density polyethylene passive diffusion samplers. Environ. Sci. Technol., vol 38, no 6, pp. 1849-1857.

Ehlke, T.A., Imbrigiotta, T.E., and Dale, J.M., 2002. Laboratory comparison of polyethylene and dialysis membrane diffusion samplers. Groundwater Monitoring and Remediation, vol 24, no 1, pp. 53-59. National Groundwater Association, New Jersey.

Imbrigiotta, T.E., Ehlke, T.A., Lacombe, P.J., and Dale, D.M., 2002. Comparison of dialysis membrane diffusion samplers and two purging methods in bedrock wells. Third International Conference on Remediation of Chlorinated and Recalcitrant Compounds, Battelle, May 20-23, 2002, Monterey, CA.

Langmuir, F., 1997. Aqueous Environmental Geochemistry, Prentice Hall, U.S.A.

Magaritz, M., Wells M., Amiel, A.J., and Ronen, D., 1989. Application of a multi-layer sampler based upon the dialysis cell technique for the study of trace metals in ground water. Applied Geochemistry, vol 4, pp. 617–624.

Morin, D.M., 2004. Critical analysis of monitoring technologies for monitored natural attenuation at upstream oil and gas sites in Alberta. Unpublished M.Sc. thesis at the University of Alberta, Canada.

Parker, L.V., 1994. The effects of ground water sampling devices on water quality: A literature review. Ground Water Monitoring and Remediation, vol 14, no 2, pp. 130–141.

Parker, L.V., and Clark, C.H., 2003. Study of five discrete interval-type groundwater sampling devices: U.S. Army Corps of Engineers Cold Regions Research and Engineering Laboratory, ERDC/CRREL TR-02-12, 56 p.

Rifai, H. S., and Newell, C.J, 2002. Estimating First Order Decay Constants for Petroleum Hydrocarbon Biodegradation in Groundwater, American Petroleum Institute, Soil/Groundwater Technical Task Force, Washington, DC.

Sanford, W.E., Shropsphire, R.G., and Solomon, D.K., 1996. Dissolved gas tracers in groundwater: Simplified injection, sampling, and analysis. Water Res. Vol 32, no 6, pp. 65.

Tunks, J., Guest, P., and Santillan, J., 2000. Diffusion sampler evaluation of chlorinated VOCs in ground water: Proceedings, Second International Conference on Remediation of Chlorinated and Recalcitrant Compounds, Monterey, California, May 22-25, vol 2, no. 1, pp. 369-376.

US EPA, 2005. Technical Factsheet on Benzene. http://www.epa.gov/OGWDW/dwh/t-voc/benzene.html, last accessed on September 10, 2005.

Vroblesky, D.A., and Pravecek, T., 2002. Evaluation of passive diffusion bag and dialysis samplers in selected wells at Hickam Air Force Base, Hawaii, July 2001: U.S. Geological Survey Water Resources Investigations Report 02-4159, 38 p.

Vroblesky, D.A., and Hyde, T.W., 1997. Diffusion samplers as an inexpensive approach to monitoring VOCs in ground water: Ground Water Monitoring and Remediation, vol. 17, no. 3, pp. 177-184.

Vroblesky, D.A., Petkewich, M.D., and Campbell, T.R., 2002. Considerations for sampling inorganic constituents in ground water using diffusion samplers: Proceedings, third International Conference on Remediation of Chlorinated and Recalcitrant Compounds, Battelle, Monterey, CA. ISBN:1-57477-132-9.

3 Modeling of Contaminant Movement across Well Open Interval

3.1 Introduction

Diffusion samplers are capable of providing quality samples of the water surrounding them (Vroblesky et al, 2002). However, in monitoring wells with relatively long screens (i.e. 3m) the question that arises is how accurately the monitoring well water represents the formation surrounding it. The use of diffusion samplers to obtain representative groundwater samples depends on the free movement of water across the well screen or open interval (Vroblesky, 2001). Earlier studies have shown there is free movement of water across the well open interval even in low permeable formation (Kearl et al, 1992; Powell and Puls, 1993; Robin and Gillham, 1987). To ensure proper use of diffusion samplers, there is a need to understand conditions that may lead to non-representative water samples within the well open interval due to different flow and stratigraphic conditions. This study used numerical modeling to investigate various scenarios as described below:

1. If the well screen is less permeable than the formation adjacent due to inadequate well development, or bacterial fouling, there may be flow divergence around the well screen under ambient conditions, potentially causing inadequate exchange across the well screen.
2. If the well screen cuts across zones of differing hydraulic conductivity and variable contaminant concentration due to stratigraphic conditions, water within the well screen may not be representative of the contaminated formation due to different formations contributing flow and contaminant through it, leading to a stratified chemical gradient within the well screen.
3. If a diffusion sampler is placed above or below the well screen, the concentration obtained may not be representative depending on how long the contaminated groundwater has been

there, the position of the sampler relative to the well screen and other physiochemical and biological processes ongoing.

3.1.1 Objectives of Study

The objectives of this study are:

- To examine the effects of decreasing permeability of the sand pack adjacent to the well open interval on the free movement of water and contaminant in the well,
- To determine the effects of a high permeability seam layer adjacent to the well open interval on the distribution of contaminants in the well, and
- To examine the impact of varying the contaminant distribution in the formation on the contaminant distribution in the well.

3.1.2 Scope of Work

Numerical modeling was conducted using SVFLUX and CHEMFLUX[6] software to simulate movement of a conservative contaminant across and within the well under different flow and stratigraphic conditions. SVFLUX was used for the 3-D seepage analysis, and the velocity gradients obtained were exported to CHEMFLUX, for the simulation of contaminant transport.

3.2 Governing Equation and Assumptions

A concise description of the underlying theories on the numerical methods used by the FLEXPDE solver in SVFLUX and CHEMFLUX software are discussed in this section. These theories can be broadly divided into seepage and contaminant transport. SVFLUX uses seepage theory in solving the hydraulic aspect and CHEMFLUX uses the flow field generated from the

---

[6] SVFLUX and CHEMFLUX are developed by SoilVision Systems Ltd. The SVFLUX and CHEMFLUX versions used are 3.19.0002 and 3.02.0001 respectively. The solver used by these programs is FLEXPDE version 3.10a professional from PDE Solutions Inc.

SVFLUX output coupled with additional boundary conditions to solve the contaminant aspect of the problem.

3.2.1 Seepage Theory

The general governing equation in solving the seepage aspect of the problem in three-dimensions is given by eq.1 below (Stianson, 2002):

$$\frac{\partial}{\partial x}\left(K_x(\varphi)\frac{\partial h}{\partial x}\right)+\frac{\partial}{\partial y}\left(K_y(\varphi)\frac{\partial h}{\partial y}\right)+\frac{\partial}{\partial z}\left(K_z(\varphi)\frac{\partial h}{\partial z}\right)=m_w^2\gamma_w\frac{\partial h}{\partial t} \qquad [1]$$

Where

h = Total head

$K_x(\varphi)$ = Hydraulic conductivity in x-direction

$K_y(\varphi)$ = Hydraulic conductivity in y-direction

$Kz(\varphi)$ = Hydraulic conductivity in z-direction

m_w^2 = Slope of the soil water characteristic curve

γ_w = Unit weight of water

φ = Water content

For saturated steady state seepage,

$\frac{\partial h}{\partial t} = 0$, and $K_i = f(K_{sat})$, where $i = \{x, y, z\}$ and K_i is the hydraulic conductivity in the i-direction

For saturated steady state with non-linear hydraulic conductivity,

$\frac{\partial h}{\partial t} = 0$, and $K_i = f(K_{sat}, \varphi)$, where $i = \{x, y, z\}$ and K_i is the hydraulic conductivity in i-direction

For unsaturated steady state seepage, the general equation remains unchanged as written above. Moreover, where there is the need for rotation of axes, the SVFLUX solver performs the rotation; however the equations for the translation are outside the scope of this report.

3.2.2 *Chemical Transport*

In solving for the contaminant transport, CHEMFLUX uses the flow field seepage velocity output in the governing partial differential equation [2] given below for the contaminant transport.

$$\frac{\partial}{\partial i}\left(D_{ij}\frac{\partial C}{\partial j}\right)-V_i\frac{\partial C}{\partial i}-\lambda_1 C-\frac{\lambda_2\rho_d C^*}{\theta}=R\frac{\partial C}{\partial t} \qquad [2]$$

$i,j=\{x,y,z\}$ And $V_i=\frac{v_{d\,i}}{\theta}$

Where,

D_{ij} = Coefficient of hydrodynamic dispersion in i,j -direction

V_i = Seepage velocity in i -direction

$v_{d\,i}$ = Discharge velocity in i -direction

λ_1 = Dissolved half life

λ_2 = Sorbed half life

C = Dissolved concentration

C^* = Sorbed concentration

ρ_d = Bulk density

R = Retardation factor of the sorption isotherm

θ = Volumetric water content

The solution of the transport equation above depends on the imposed boundary conditions on the problem.

3.2.2.1 Dispersion

The dispersion term of the equation consists of both the molecular diffusion and mechanical dispersion, which are embedded in the hydrodynamic dispersion coefficient. Molecular diffusion is the mixing due to a concentration gradient and the mechanical dispersion accounts for the mixing due to variation in velocities at the pore scale. The hydrodynamic dispersion coefficient in three-dimensional are given below (Stianson, 2002):

$$\begin{pmatrix} D_{xx} & D_{xy} & D_{xz} \\ D_{yx} & D_{yy} & D_{yz} \\ D_{zx} & D_{zy} & D_{zz} \end{pmatrix}$$

$$D_{xx} = (\alpha_L - \alpha_T)\frac{V_x^2}{|V|} + \alpha_T|V| + D^*, \qquad D_{yy} = (\alpha_L - \alpha_T)\frac{V_y^2}{|V|} + \alpha_T|V| + D^*,$$

$$D_{zz} = (\alpha_L - \alpha_T)\frac{V_z^2}{|V|} + \alpha_T|V| + D^*, \qquad D_{xy} = (\alpha_L - \alpha_T)\frac{V_x V_y}{|V|} = D_{yx},$$

$$D_{xz} = (\alpha_L - \alpha_T)\frac{V_x V_z}{|V|} = D_{zx}, \qquad D_{yz} = (\alpha_L - \alpha_T)\frac{V_y V_z}{|V|} = D_{zy}$$

$$D^* = \tau D_o, \qquad |V| = \sqrt{\left(V_x^2 + V_y^2 + V_z^2\right)} \qquad [3]$$

Where,

α_L = Dispersivity in the longitudinal direction

α_T = Dispersivity in the transverse direction

V_i = Seepage velocity in i-direction

D^* = Effective diffusion coefficient

τ = Tortuosity

D_o = Free solution diffusion coefficient

The dispersivity term depends on the direction of flow, anisotropy, heterogeneity and the scale of the problem, and there are different equations to estimate dispersivity in different directions, which are outside the scope of this report but considered in the CHEMFLUX analysis. The equation for the dispersive flux through a given area is given below:

$$Q_D = Di_c A \qquad [4]$$

Q_D = Dispersive flux,

D = Coefficient of hydrodynamic dispersion

$i_c = \frac{\partial C}{\partial j}\{j = x, y, z\}$ = Concentration gradient

A = Cross sectional area

3.2.2.2 *Advection*

Advection is the movement of dissolved chemicals due to groundwater flow. If the advective flux is significantly greater than the diffusive flux, then, advection dominates the chemical movement. Otherwise, it is diffusion driven. For advection-dominated problem, there is some degree of numerical dispersion and oscillation using numerical methods due to truncation errors. To overcome this, the CHEMFLUX solver uses automatic mesh generation and time-step refinement to reduce the effect of the truncation errors (Stianson, 2002). The equation for the advective flux through any given section is given below:

$$Q_A = v_{d\,i} CA \qquad [5]$$

Q_A = Advective flux,

v_{d_i} = Discharge velocity in i-direction

C = Concentration

A = Cross sectional area

3.2.2.3 Sorption and decay

Sorption is the process by which the dissolved chemical in groundwater clings to a solid surface with a consequential decrease in solute concentration in the groundwater. CHEMFLUX solver assumes an instantaneous model whereby the sorption reaction is assumed fast enough relative to the groundwater flow, for equilibrium conditions to exist between the aqueous phase and solid phase concentrations. However, if the sorption process is slow relative to the fluid flow in porous media, equilibrium conditions may not exist and there may be the need to use a kinetic model to describe the process. Nevertheless, CHEMFLUX incorporates different sorption isotherms, including; linear, Fredlund, Langmuir, and user defined isotherms, to define the relationship between the sorbed and dissolved solute concentrations at a constant temperature. Each isotherm has its own retardation factor that is used in the chemical transport equation. The mathematical relationships of each isotherm and the corresponding retardation factor are outside the scope of this report.

Decay is the loss in solute concentration in adsorbed or dissolved phase, or both with time. The decay term is expressed using the half-life constants shown in the chemical transport equation. CHEMFLUX allows the entry of two separate half-lives as shown in the chemical transport equation because according to Fetter (1993), there may be differences in the half-life for sorbed and dissolved phase due to some biological activities.

3.2.3 Assumptions

Assumptions in the analyses include those inherent in the development of the seepage and transport theory, the numerical methods and the definition of the conceptual models. Some of the main assumptions are listed below but the validity of these assumptions is outside the scope of this study.

- Darcy's law holds for flow in the porous media,
- Fick's law is valid for the diffusive contaminant transport,
- The hydraulic gradient across the flow field is constant with both time and depth,
- The materials are isotropic with respect to hydraulic conductivity, and
- A non-retarding contaminant (i.e. conservative contaminant) is assumed and the only processes in operation are advection and hydrodynamic dispersion.

3.3 Conceptual Model

The geometry, material properties and boundary conditions used in the simulation to achieve desired objectives are highlighted in this section.

3.3.1 General domain

The domain used in building the basic structure of the models used for the simulation is shown in Figure 3.1, and the basic dimensions of the domain components are given in Table 3.1. The size of the domain was chosen based on the preliminary calculation of the radius of influence of the well within the formation, which was less than 0.6m from the centre of the well. A section through the domain perpendicular to the Y-axis (at Y=5) is used to define the basic configurations of the models. The models are divided into three Cases as shown in Figure 3.2. The difference in these cases is the variation in thickness of the seam layer from 3m to 0.1m.

In all the cases, homogeneous sand underlies the upper clay layer. The well screen is at the middle of the formation with impermeable strata beneath the domain. A thickness of 0.002m was assumed for the well casing, and a void was used to define the impermeable wall thickness above and below the well screen. Within the sand formation into which the well is installed, there is a horizontal seam layer with a hydraulic conductivity ranging from one to two orders of magnitude greater than that of the formation.

In evaluating the effect of the permeability of the sand pack on the flow field across the well open interval in Case III, the seam layer property was set equal to that of the sand above and below it (Table 3.2), and the sand pack's permeability was varied from 100 to 0.1 times that of the sand formation (K_f=1E-06m/s, where K_f is the permeability of the sand formation). However, when evaluating the impacts of seam layer thickness on contaminant flow within the well (Case III-CHA), the seam layer property was set back to its original value (Table 3.2).

3.3.2 Material properties

The properties of the materials used in the definition of the domain are given in Table 3.2. The well was assigned a material property with a porosity of one because there is no way to specify a water column within the domain in the software package. The hydraulic conductivity of the well was assumed to be equal to that of the sand pack divided by its porosity, for continuity of flow. Although in the seepage simulation for steady state, porosity is not used. It is used in the computation of the seepage velocity used for the CHEMFLUX analysis.

The well casing was replaced with a void section, otherwise in the 3D CHEMFLUX analyses, the mesh density in the well casing will be very high leading to numerical instability and increased computation time due to the adaptive mesh generation of the of the FLEXPDE solver.

3.3.3 Boundary Conditions

Sectional domain boundary conditions (BCs) for the conceptual models are given in Table 3.3. A constant hydraulic gradient ranging from 0.6 to 0.003 was applied across the model domain in the x-direction, and a zero flux boundary condition was applied at the opposite sides of the domain (i.e. x=4.0 and x=6.0). A zero flux boundary was also specified around the well casing and no boundary condition was applied between the interfaces of the main soil layers, including the open interval of the well with the sand pack, so that the flow field and contaminant transport will be governed by the material properties. From the layout of the simulation matrix (Figure 3.3), the flow analyses when the seam layer permeability is the same as the formation (i.e. Hn-1), have the same solution for Cases I and II. The flow analyses were done for steady state, and a maximum time frame of 100days was chosen for the chemical transport transient analyses, which is approximately equal to a quarterly sampling period. Illustrative views of the concentration boundary conditions simulated are shown in Figure 3.4.

Figure 3.4 shows the longitudinal mid-section of the domain used for the simulation in the direction of flow. Figure 3.4(a) highlights the CHEMFLUX boundary conditions imposed on different segments of the domain. For CHA conditions, constant concentration of 1mg/L is specified at the seam layer segment only and no boundary (NB) condition was specified in all other points and segments within the domain (Table 3.3). It should be noted that "NB" condition implies that the initial concentration at that point or segment is zero and not constant. When a concentration boundary is applied at a segment, it implies that the concentration at that segment will always be the value specified, but when applied at discrete points within the domain, the value specified is treated as finite, which is similar to slug input at that point. The CHB boundary condition (BC) is similar to that of CHA except that a concentration of 1mg/L was specified in the sand formation. The CHC boundary condition is similar to CHB but instead of concentration of 1mg/L in the sand formation, it was replaced with a concentration gradient ranging from 1 at the seam layer boundary to 0 at the edge of sand formation within the well screen.

The CHAS and CHCS boundary conditions are extensions of CHA and CHC respectively, but a constant concentration of 1mg/l was applied to both upper and lower surface of the seam layer as highlighted in Figure 3.4(b). In addition to the surface concentration boundary condition in CHAS and CHCS, two more simulations were modeled in which finite concentration gradient was specified within the seam layer and sand formation.

3.4 Results

The results are divided into two sections. The first section deals with the velocity flow field of the models, and the second section deals with the contaminant movement within the well open interval. Prior to invoking the contaminant transport, it was necessary to ensure the flow field behaviour was being properly developed. The next session summarizes the important results of that work.

3.4.1 Results of velocity flow field

The flow fields around the well open interval for varying conductivity of the sand pack with 3m seam layer thickness (Case III) are given in Figure 3.5. Enlarged plots of the flow fields are given in Appendix B.1. The figure shows the convergence of flow around the well open interval when the sand pack has a higher permeability than the formation and divergence of flow when the sand pack permeability was less than that of the formation. There appears to be more convergence of flow into the well within the sand pack in Figure 3.5(b) with sand pack permeability ratio "n" of 10 than Figure 3.5(a) with "n" value of 100. This is so because the permeability contrast between the well and sand pack in (b) is greater than that of (a). The outputs of the seepage velocity were subsequently used for the contaminant transport simulation.

A summary of the discharge velocity profiles for Cases I and II (with gradient of 0.003) is shown in Figure 3.6. The elevation was plotted on the vertical axis and the discharge velocity on the horizontal axis. The velocity profiles at higher gradients (of 0.6 and 0.2) have a similar shape. The effects of increasing permeability with a metre thick seam layer (Case I) on velocity flux across the well open interval are more pronounced than that with 0.1m seam layer (Case II) due to higher sectional area of the seam layer.

3.4.2 Results of contaminant transport

The plots of results of the contaminant transport simulations for all the models are given in Appendix B.2. Figure 3.7 shows a typical example of the results from one of the simulations. The elevation from the bottom of the well is plotted on the vertical axis and the concentrations at different time steps are plotted on the horizontal axis. The well screen is located between 2 and 5 metres as shown. At the interface between the well screen and the well casing, some negative concentrations were observed. Numerical instability accounts for the observed negative concentrations as discussed in the next section. The shape of the concentration profile is similar to the velocity profile for each simulation except for the case when the seam layer has the same permeability with the formation. Faster contaminant movement was observed at higher hydraulic gradients as the seepage velocity was increased. The plots of the concentration profile at middle of the well open interval are given in Appendix B.3 for different dispersivity coefficients.

To examine the effect of seepage velocity on contaminant movement in the 0.1m thick seam layer (Case II CHA simulations), Figures 3.8 to 3.10 summarize data contained in

Appendix B.2. Figure 3.8(a) shows the effects of seepage velocity on contaminant concentration at the end of 100days. The plot shows increasing contaminant movement as the seepage velocity in the seam layer and sand formation increases. A plot of effect of the seam layer velocity on time to achieving 90% equilibration (T_{90}) of contaminant concentration is given in Figure 3.8(b). The data used for the plot is that with the highest seepage velocity in the sand formation shown in Figure 3.8(a). The seepage velocity is very high but the aim is to show a relationship between the seepage velocity in the seam layer and T_{90}, which is exponential as shown. If lower seepage velocities were used, it will take longer iteration beyond the 100days interval set for the simulation. Figure 3.9 illustrates the location of seven different points along the seam layer and Figure 3.10 compares the differences in concentration at these points at the end of 30 and 90 days for different seepage velocities. The velocity flow fields around the well at different permeability ratios are shown in Figure 3.11, and the lateral extent of influence of the well on the flow field is shown in white. This zone of influence is further discussed in detail in the discussion section.

The results shown in Figures 3.6 to 3.10 are for cases where the contaminant concentration is zero at time equals zero out to a distance of one metre away from the well screen as described in section 3.3.3. These conditions are extreme and are less likely to be encountered in the field. Figure 3.12 shows the concentration profile within the well for a more likely field boundary conditions in which the soil immediately adjacent to the well is already contaminated (CHAS & CHCS). It could be seen from that there is no significant difference in the concentration profiles for CHAS and CHCS boundary conditions, and the monitoring well is shown to equilibrate with the formation in three days where the concentration in the well is zero at time equals zero, even with the very slow seepage velocities modeled.

The effects of contaminant distribution in the formation on its movement within the well are shown in Figure 3.13. Figure 3.13(a) shows the normalized contaminant distribution for a 0.1m thick seam layer after 100 days as the contaminant concentration in the soil adjacent to the seam layer changes. In these simulations, the concentration everywhere in the domain is equal to zero at time equals to zero. As earlier discussed in section 3.3.3, for CHA condition, the concentration at the seam layer boundary one meter away from the middle of the well equals 1mg/L but zero at all other points and boundary at the initial start time (t-time=0). For CHB condition, the concentration at the sand formation equals 1mg/l in addition to CHA condition. CHC condition is similar to CHB but a linear concentration gradient (M) was specified at the sand formation instead of one in CHB condition. The concentration gradient ranged from one at the seam layer boundary to zero at sand formation corresponding to the edge of the well screen (Table 3.3). Figure 3.13(b) shows the results when the concentration equals to 1mg/L at the seam layer boundary at the initial start time, but where the concentration in the soil adjacent to the seam layer equals zero or M (gradient) at time equals zero (Figure 3.4). The figure shows more movement of contaminant into the well as the initial area covered by the contaminant increases.

Figure 3.14 shows the effects of varying the transverse dispersivity on contaminant distribution within the well. As the transverse dispersivity decreases, there was a decrease in the vertical movement of contaminant mass, resulting in greater horizontal mass transport of the contaminant. High seepage velocity was simulated for this scenario to overcome the development of negative concentrations at the top of the well screen.

The impact of varying the thickness of the seam layer on well equilibration is shown in Figure 3.15. The figure shows faster equilibration as the seam layer thickness increases due to increased advective flux within the formation.

To examine the impact of well response on diffusion sampler response, the diffusion equation for the dialysis sampler (in Chapter 2) was coupled to the CHEMFLUX output. Using the concentration profile at the middle of the well open interval for a 1m seam layer model with constant concentration of 1mg/L at the seam layer boundary and zero in the adjacent formation (i.e. Figure 3.7) resulted in the data shown in Figure 3.16. A logistic three-parameter equation[7] was obtained using SIGMAPLOT to describe the curve function of the concentration output from CHEMFLUX, using data at ten day intervals. This equation was then coupled with the diffusion equation for the dialysis sampler developed earlier using a diffusion coefficient (Dm) of 0.0173cm^2/d. It was assumed that the sampler was placed in the well at time equals 60 days. However, irrespective of when the sampler is placed in the well, the same time lag of three days was obtained for the sampler to achieve equilibration with the water in the well, even if a different concentration profile was used for the well water. Reduction of the diffusion coefficient (Dm) for the dialysis sampler by a factor of 2, 5, and 10 resulted in times to equilibrate of 7, 18, and 38days respectively as approximated from Figure 3.16.

3.5 Discussion

3.5.1 Flow field around the well

In Case III with a 3m thick seam layer, attraction of flow towards the well occurs when the permeability of the sand pack is more than the formation. This flow attraction decreases as the ratio of the sand pack permeability to that of the formation decreases as shown in Figure 3.5.

---

[7] $y = if(x \le 0, if(b < 0, 0, a), if(b > 0, \frac{a}{\left(1 + \left|\frac{x}{x_0}\right|^{b}\right)}, \frac{a\left|\frac{x}{x_0}\right|^{b}}{\left(1 + \left|\frac{x}{x_0}\right|^{|b|}\right)}))$; a, b & x_0 are fitted numerically.

When the permeability of the sand pack was less than the formation, flow diverges around the well open interval resulting in less flow through the well. Therefore, the discharge velocity within the well may be less than that within the formation if the sand pack permeability is reduced due to processes like clogging, or bio-fouling. This will invariably affect the advective movement of contaminant across the well and thus the associated response of a diffusion sampler.

The observed negative velocities at the edges of the well screen boundaries between elevation 2 and 5m in Figure 3.6 are due to numerical instability. Although some eddy currents may be expected at these regions, the magnitude of the negative flow will be far less than that simulated. This numerical instability arises due to steep gradients in flow at the well-screen/well-casing boundary as opposed to continuity of flow in space. A much finer grid was initially used in such regions to attempt to alleviate negative velocities, but the run times for the simulation become high, thus, the automatic mesh generation function was disabled. Figure 3.6 shows higher velocity at the middle of the well screen when the seam layer hydraulic conductivity was increased, however, it should be noted that the velocity presented is the discharge (Darcy) velocity. When discharge velocity is converted to the seepage velocity in the soil pores, it will be 2.5 to 3 times greater. In the models with 1m and 0.1m seam layers (i.e. Cases I and II respectively), there is increase in flow velocity at the centre of the well and the effects of increasing permeability of the seam layer are more pronounced in Case I with a one metre seam layer than Case II with 0.1m seam layer due to the increase in flux through the open interval. The same results were obtained for the two cases when the permeability of the seam layer equals that in the formation.

In summary, these simulations conform to past studies (Powel and Puls, 1993; Kearl et al, 1992) showing flow across the well open interval depends on its configuration. If the sand pack has hydraulic conductivity of about an order of magnitude less than that of the formation, there will be less flow into the well. An understanding of the hydraulic conductivity function of the sand pack with time may be very useful in predicting a decrease in free flow across the well, which the diffusion samplers are dependent on. The presence of high permeability seam layer across the well open interval may cause variable flow across the well which may lead to concentration gradients within the well.

3.5.2 Contaminant movement within the well

3.5.2.1 Numerical Instability

The concentration profile in Figure 3.7 (which is a sample of those given in Appendix B.2) showed some negative concentrations at early time at the edge of the well screen. These arose from the assumption that the solution can be approximated by a polynomial equation (quadratic in FLEXPDE's default) over each cell with continuity of volume at the cell interfaces. However, discontinuities or steep transitions with insufficient mesh density cannot be adequately modeled by such an approximation unless a very dense grid is used at such regions. The adaptive mesh generation of the solver was turned off to save time (note: when the adaptive mesh generation was turned on, the runtime was greater than two weeks, thus, the resulting coarser grid gave some inappropriate values at regions with steep gradients). Nevertheless, the shapes of the concentration profiles were similar to the velocity profiles for each simulated scenario.

3.5.2.2 Effects of seepage velocity on contaminant movement

The effects of seepage velocity on equilibration time are summarized in Figure 3.8 from the concentration profiles for different seepage velocities given in Appendix B.2.1. As the velocity of the seam layer increases, the advective flux and the dispersive flux due to mechanical mixing increase, thereby hastening the contaminant movement through the well. This is evident by comparing the velocity profiles at different seepage velocities in the sand formation in Figure 3.8(a).

Figure 3.10 shows how the seepage velocity in the seam layer affects equilibration of the well with the surrounding formation and the difference between the well concentration at different points upstream and downstream of the well at the end of 30 and 90 days respectively. Before further discuss of these results, it is prudent to resolve what points in the formation relative to the monitoring well are of interest when sampling.

To address this issue, the recharge zone of the well has to be known, which can also be termed its zone of influence. This zone of influence is quite different from the radius of influence during well draw-down because purging is not a requirement for the use of diffusion samplers. This zone of influence may be defined as the maximum distance from the well screen at which a streamline passing through it experiences curvature or attraction to the well (Figure 3.11). This zone of influence is a function of the permeability contrast between the well screen or sand pack and the surrounding formation. In most studies, this zone of interest is considered as the formation immediately adjacent to the well screen without apportioning a distance from the well screen at which the sampled concentration will be representative of the formation.

For the modelled conditions where concentration equals zero everywhere in the domain at initial start time (t=0) and seam layer boundary concentration (C_{sl}) equals 1mg/L (i.e. CHA conditions) shown in Figure 3.10, it is insightful to compare the concentration in the well with other points in the formation. If the zone of interest is taken as the formation immediately adjacent to the sand (i.e. points C & C'; Figures 3.9 & 3.10), a diffusion sampler will provide a concentration within 85-90% of the formation concentration even in a low permeable formation at any time of interest as long as the sand pack is more permeable than the surrounding formation.

From Figure 3.11, the apparent average of zone of influence is approximately 0.35m from the centerline of the well at permeability ratios "n" greater than ten. At 0.5m upstream and downstream from the well's centerline (i.e. points A & A'; Figure 3.9), the plots showed that as time progresses, the concentration difference between the well and formation becomes smaller. At seepage velocities less than 20m/year, the differences in concentration values after 90 days are 20-100% at points 0.5m from the well's centerline. However, it should be noted that points at 0.5m from the centerline of the well is well outside its zone of influence (Figure 3.11). Comparison of points within the modified zone of interest (i.e. points B-B') showed that concentration in the well after 90 days are within 50% of formation concentration for seam layer seepage velocity "V_{sl}" equals 5m/year, and within approximately 25% for V_{sl} = 16m/year. With higher seepage velocities, the difference becomes insignificant.

However, it should be noted that the above-simulated condition is an extreme condition because monitoring wells are most often sited within the contaminant impacted area, so the boundary condition (BC) of zero concentration in the formation adjacent to the wells is not often appropriate. The conditions of reasonable concentrations in the formation are better simulated in the CHAS and CHCS simulations (Table 3.3; Figure 3.4) shown in Figure 3.12, where a surface concentration boundary condition was imposed on the thin seam layer surrounding the well, and in this instance the well equilibrated with the formation in approximate three days.

3.5.2.3 Impacts of contaminant distribution within the formation

Variations in the contaminant distribution within the formation for the model with a 0.1m thick seam layer (Case II) are summarized in Figure 3.13 for small seepage velocity (V_{sl} =2.34m/y). There was more movement of contaminant through the well when the initial constant concentration in the seam layer of 1mg/l was extended to that of the formation (CHB). This is expected because the dispersive mass loss to the surrounding formation will decrease. When a constant surface concentration is placed in the seam layer directly around the sand pack (Figures 3.12 & 3.13(b)), the well concentration reached concentration ratio (C/C_o) of one within three days in the formation immediately adjacent to the seam layer and diffusion continued along the well column with time. As time progresses, the concentration over the well length continues to increase vertically but at a very slow rate and there was no significant change with varying permeability of the formation because vertical chemical transport in the well is due to diffusion only.

In all the simulations, there were concentration gradients within the well reflecting the concentration profile in the formation. The concentrations peak at the middle of the well open interval, even when the permeability of the seam layer is the same as the formation. This was expected because the velocities were highest at the middle of the open interval due to flow convergence and the centre of mass of the initial concentration boundary is at the same elevation as the centerline of the well screen. Monitoring wells are most often sited in contaminated zone in which plume migration is already in progress, thus, depending on the source function of the contaminant, its spatial distribution, and how long the contaminant has been in place, the well concentrations may equilibrate with that of the formation within three days for steady state flow conditions.

3.5.2.4 Impacts of varying transverse dispersivity and seam layer thickness

Variation of the dispersivity coefficient affects the mechanical dispersive component of the hydrodynamic dispersion coefficient. A decrease in the transverse dispersivity decreases the lateral migration of the contaminant but enhanced its longitudinal movement as shown in Figure 3.14. Figure 3.14(a) shows that with a very low transverse dispersivity (α_T) little contaminant mass is seen at the top of the well screen. Comparing Figures 3.14(a) and 3.14(b) shows that for the condition modeled α_T has significant impact at the top of the well screen but less impact at the screen center. Time to 90% equilibration decreased from 60 to 20 days as α_T decreased from 1.0m to 0.02m. This is reasonable because as the transverse dispersivity is decreased; mass loss to the surrounding formation from the seam layer also decreases, thereby enhancing the longitudinal movement of the contaminant. Increase in the thickness of the seam layer brings about commensurate increase in the advective flux, which is dependent on the sectional area of the contaminated zone in the direction of flow. This explains why the time to equilibration for a 3m-thickness seam layer is very short in comparison to that with 0.1m as summarized in Figure 3.15.

3.5.2.5 Coupled diffusion equation with contaminant movement

When the diffusion equation for the dialysis sampler was coupled with the concentration profile at a point in the well, the sampler was shown to come into equilibrium with the water in the well screen in approximately three days (Figure 3.16). Therefore, sampled concentration will provide a real time concentration of the well rather than a time averaged concentration over a longer period. Chapter 2 showed that the time for the sampler to come to equilibrium is affected by surface area and volume of the sampler deployed in the well. Any process that induces precipitation or settling of colloidal matter on the surface of the membrane, or encasement of the sampler in a protective shell that limits the exposed surface area, may increase the time to achieve equilibrium on site.

In summary, it can be seen that the hydraulic properties of the formation adjacent to the well open interval dictate how contaminant moves across the well within a given time frame. As the seepage velocity increases, the advective and dispersive fluxes increase, thereby enhancing contaminant exchange between the well and the formation in lesser time. Depending on the initial contaminant distribution across the adjoining layers of the formation, there is tendency for the development of concentration gradients within the well. In practice, it is advisable to always sample at discrete intervals within the well to provide insight to layers contributing flow and contamination within the formation, and to provide an idea of the initial contaminant distribution. More so, the use of diffusion samplers is suitable where there exists a more conductive contaminated seam layer if the zone of interest is the formation immediately adjacent to the well screen as earlier discussed. If the zone of interest is further upstream (say 0.5m), diffusion samplers may be suitable for quarterly sampling when the seam layer seepage velocity is greater than 20m/y. At seepage velocity below 20m/year, there may be the need for alternate sampling technique (i.e. purging) to facilitate adequate exchange between the well and the formation. However, for most realistic conditions in the field, diffusion samplers are suitable even at seepage velocity less than 3m/year.

3.5.3 Practical Considerations

In all the simulations, the well concentration closely reflects the formation concentration, and given that it may be difficult to completely understand the variability involved, it would be prudent to install a number of passive diffusion samplers over the well screen interval for the first year of monitoring. When the depth of highest concentration has been discerned, subsequent sampling may be restricted to this zone if no other environmental drivers (i.e. large recharge events or large ground water table "GWT" changes) adversely affect this response. Alternatively, if an average well concentration is desired, the diffusion sampler volumes may be homogenized to give average concentrations. It must be noted that this work neglects any biological changes that may occur in the well or the sand pack.

This work only considered horizontal flow into the well and associated mechanical dispersion and diffusion of dissolved chemicals in the groundwater within the well. Diffusion of oxygen into the well in the water near the groundwater surface will impact the groundwater chemistry in the upper region of the well. Other processes that can affect the groundwater chemical concentration (i.e. pH) may also have to be considered in the context of using dialysis diffusion samplers.

3.6 Conclusions and Recommendations

3.6.1 Conclusions

From the simulation results, the following conclusions can be drawn:

- Diffusion samplers are suitable for sampling wells intercepting thin permeable seam layers. The sampler concentration will be representative of the formation immediately adjacent to the well screen, so the sampler location should be adjacent to the seam layer.
- A concentration gradient will develop within the well even if homogeneous formations with uniform permeability are adjacent to the well open interval, and the concentration gradient within the well will reflect that within the formation.
- Higher seam layer thickness, initial contaminant concentration distribution, and seepage velocity will cause more movement of contaminant within the well.
- Dialysis diffusion samplers will equilibrate with concentration in the well in a matter of days, and then closely follow concentration changes in the well.
- There will be divergence of flow around the well if the permeability of the sand pack is less than the surrounding formation, which will reduce the free exchange between the well and the formation.

- SVFLUX and CHEMFLUX provide good insight into the movement of contaminant across a well open interval, however, at steep transition in gradient or material properties, some numerical turbulence is observed.

3.6.2 Recommendations for Future Research

- The change in permeability of sand pack with time should be investigated to determine how diffusion sampler may respond with age.
- A model incorporating biological and geochemical conditions for known field conditions should be simulated to improve understanding of well response with the surrounding formation for such conditions.

3.7 *Figures*

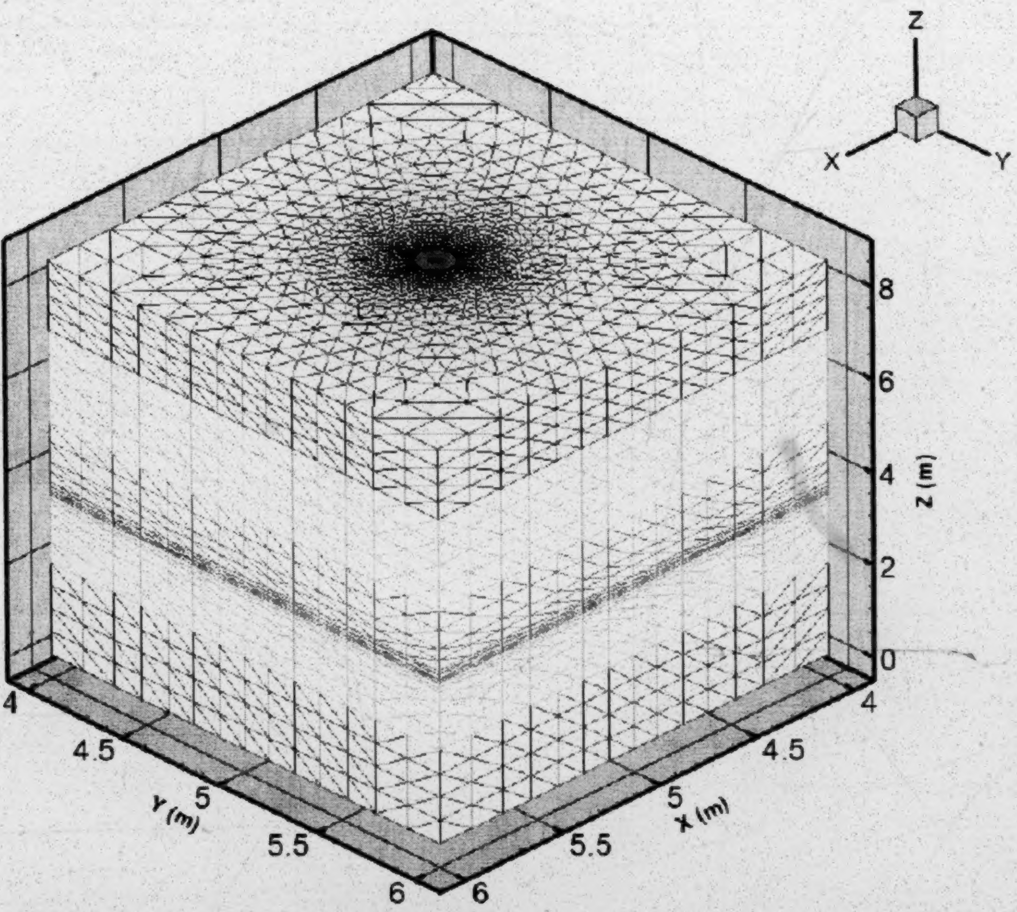
Z
X
Y
8
6
4
2
0
Z (m)
4
4.5
5
5.5
6
Y (m)
4
4.5
5
5.5
6
X (m)

Figure 3.1 Domain used for the definition of the conceptual model (Note: The well and sand pack are located at the middle of the domain, and the scale is X=Y=5Z).

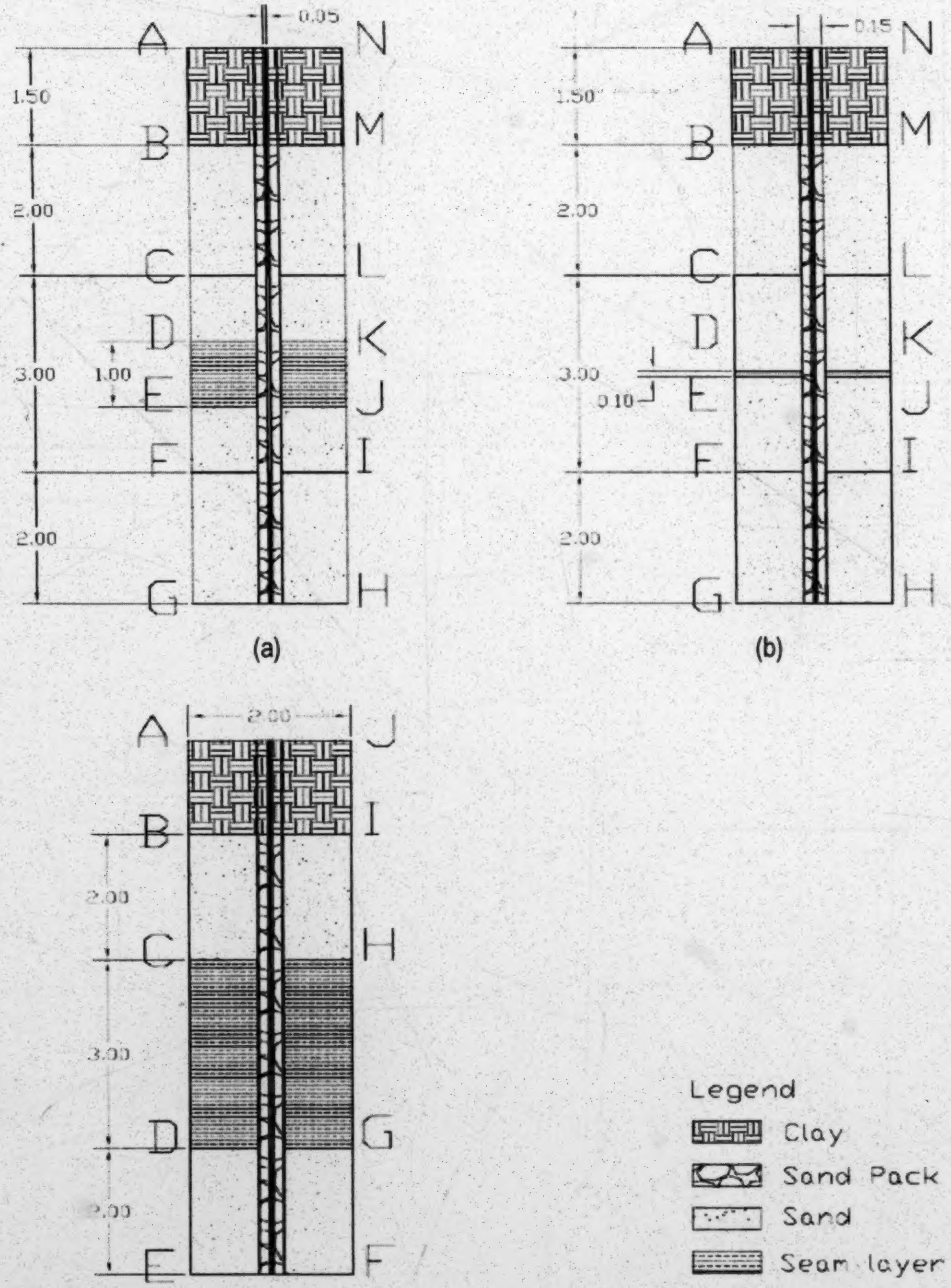

0.05
A
N
1.50
B
M
2.00
C
L
D
K
3.00
1.00
E
J
F
I
2.00
G
H
0.15
A
N
1.50
B
M
2.00
C
L
D
K
3.00
0.10
E
J
F
I
2.00
G
H
2.00
A
J
B
I
2.00
C
H
3.00
D
G
2.00
E
F
Legend
Clay
Sand Pack
Sand
Seam layer

(a) (b) (c)

Figure 3.2 Sectional drawings of the model used showing the stratigraphy of the soils used for the simulations: (a) Case I (b) Case II (c) Case III (All dimensions in metres).

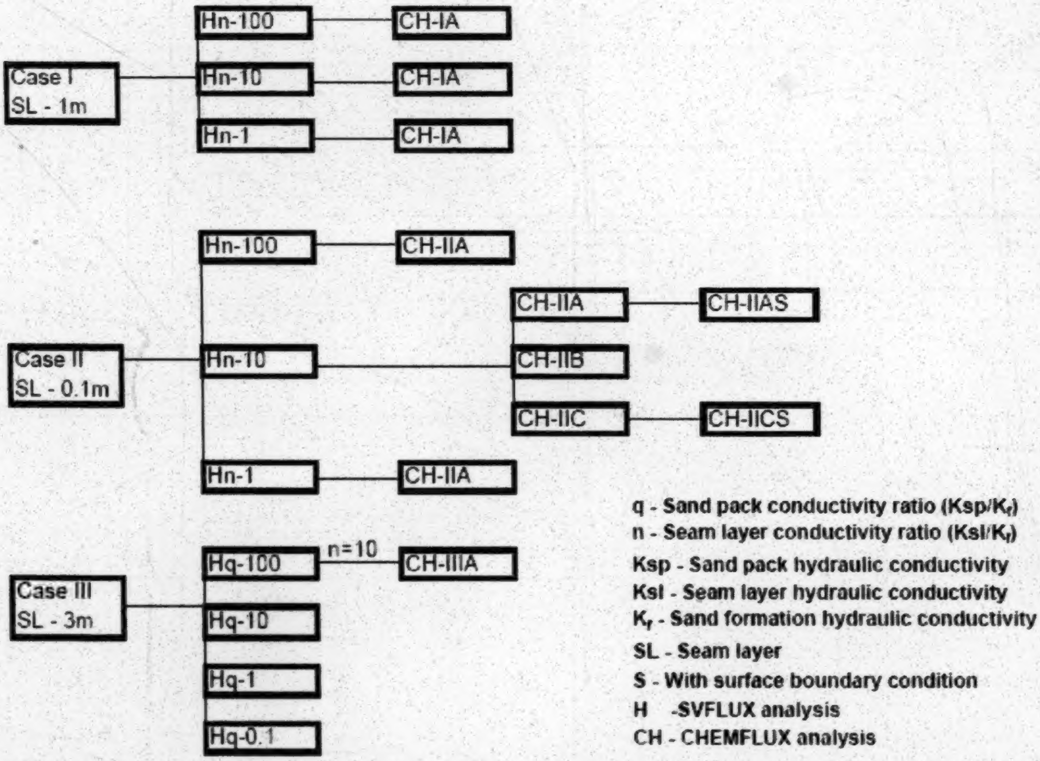
Case I
SL - 1m
Hn-100
Hn-10
Hn-1
CH-IA
CH-IA
CH-IA
Case II
SL - 0.1m
Hn-100
Hn-10
Hn-1
CH-IIA
CH-IIA
CH-IIB
CH-IIC
CH-IIAS
CH-IICS
CH-IIA
Case III
SL - 3m
Hq-100
Hq-10
Hq-1
Hq-0.1
n=10
CH-IIIA

q - **Sand pack conductivity ratio (Ksp/K_f)**
n - **Seam layer conductivity ratio (Ksl/K_f)**
Ksp - **Sand pack hydraulic conductivity**
Ksl - **Seam layer hydraulic conductivity**
K_f - **Sand formation hydraulic conductivity**
SL - **Seam layer**
S - **With surface boundary condition**
H -**SVFLUX analysis**
CH - **CHEMFLUX analysis**

Figure 3.3 Layout of the simulation matrix for the models (Note: The suffix A, B, and C corresponds to the CHEMFLUX boundary condition given in Table 3.3 imposed on the model).

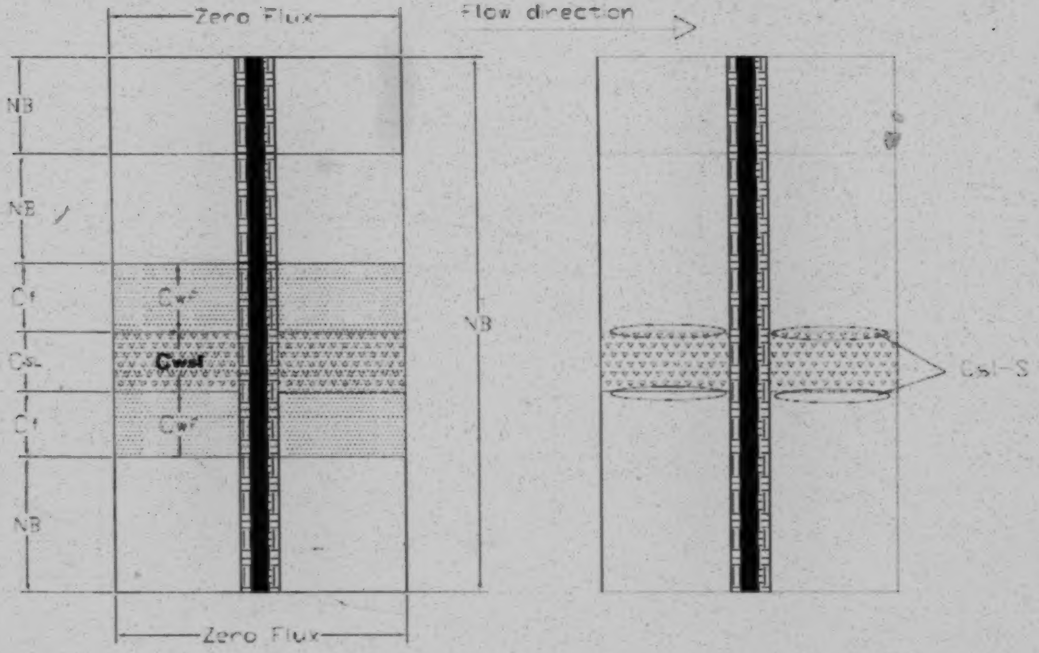
Zero Flux
Flow direction
NB
NB
Cf
Cwf
CSL
Cwsf
Cf
Cwf
NB
NB
Csl-S
Zero Flux
Legend
Sand Pack
Sand Formation
Seam layer
Well

(a) (b)

C_f	Formation boundary concentration
C_{SL}	Seam layer boundary condition
C_{wf}	Finite initial concentration in the formation
C_{wsl}	Finite initial concentration in the seam layer
$C_{sl\text{-}S}$	Seam layer surface concentration condition
NB	No boundary condition
M	Concentration gradient ranging from one in the seam layer to zero in the formation at the well screen limit

Concentration (mg/L)	Conditions				
	CHA	CHB	CHC	CHAS	CHCS
C_f	0, NB	1	M	NB	M
C_{SL}	1	1	1	1	1
C_{wf}	0, NB	0, NB	0, NB	0, M	0, M
C_{wsl}	0, NB	0, NB	0, NB	1, M	1, M
$C_{sl\text{-}S}$	0, NB	0, NB	0, NB	1	1

Figure 3.4 Illustrations of the concentration boundary conditions. (a) shows the sectional view of the boundaries and (b) is a detail of the surface boundary in (a) [For no boundary condition, the initial concentration is taken as zero].

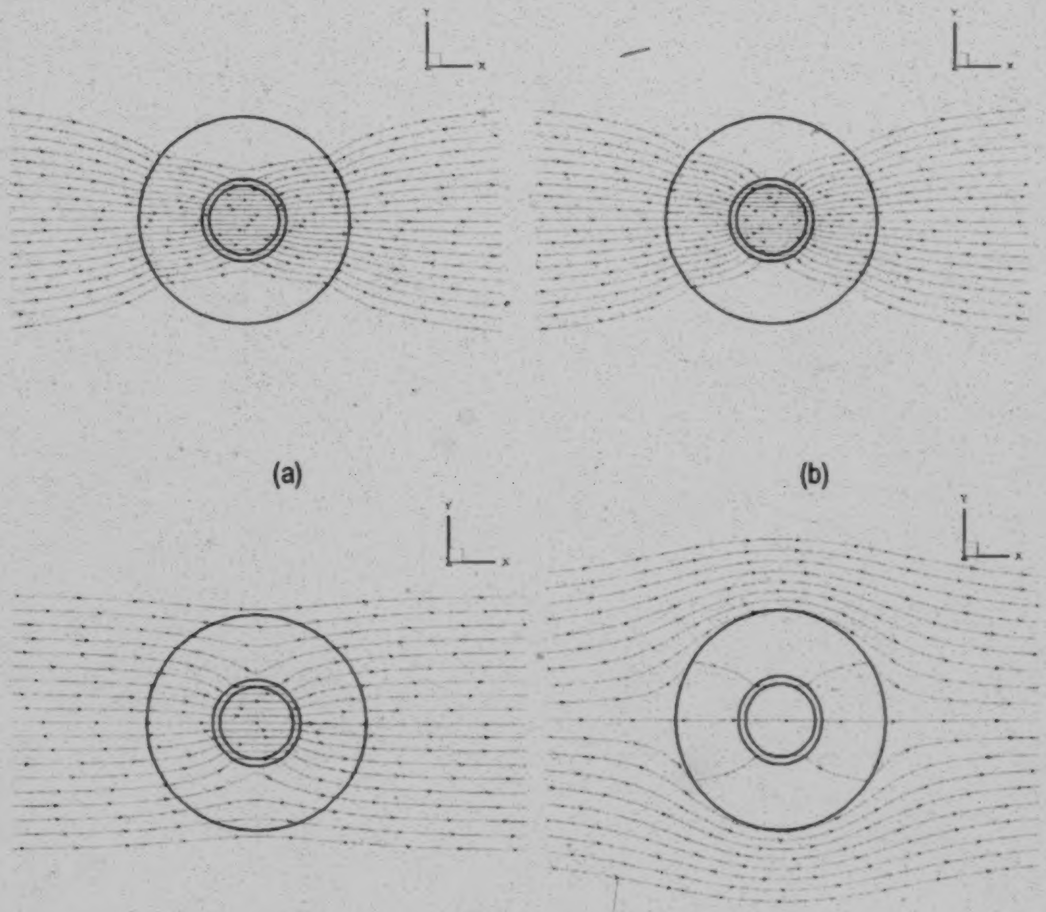

(a) (b)

(c) (d)

Figure 3.5 Velocity flow field at the middle of the well open interval under different sand pack permeability ratio with the formation. (a) Ksp/K_f = 100; (b) Ksp/K_f = 10; (c) Ksp/K_f = 1; and (d) Ksp/K_f =0.1. [Ksp = Sand pack permeability; K_f = Formation permeability (10^{-6}m/s); the streamlines are at 0.01m equidistant from the centerline of the well.

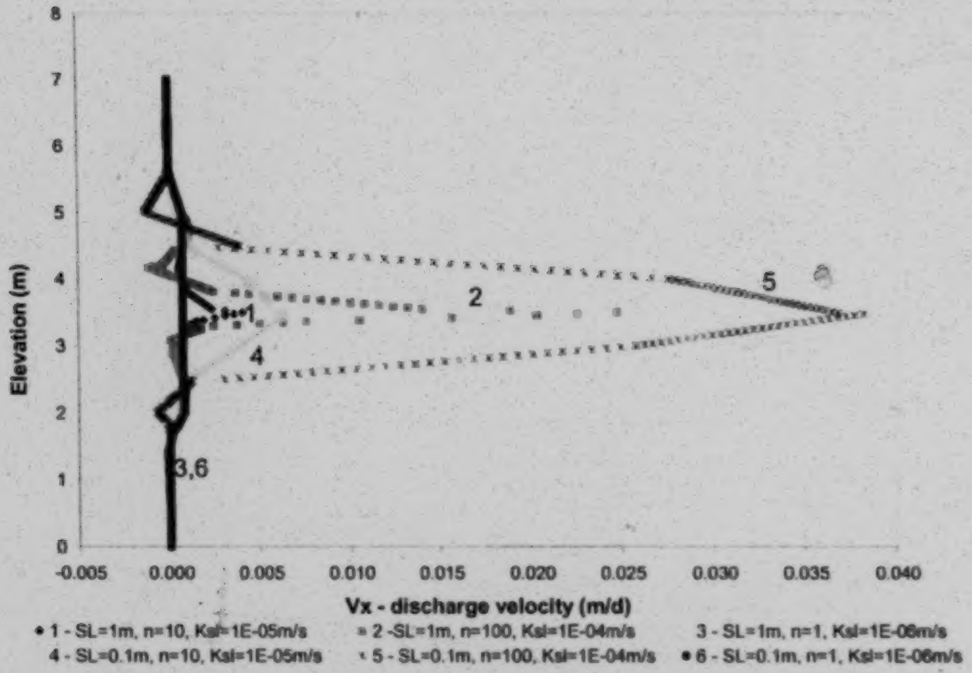

Figure 3.6 Velocity profiles within the well for hydraulic gradient of 0.003 ($n=Ksl/K_f$).

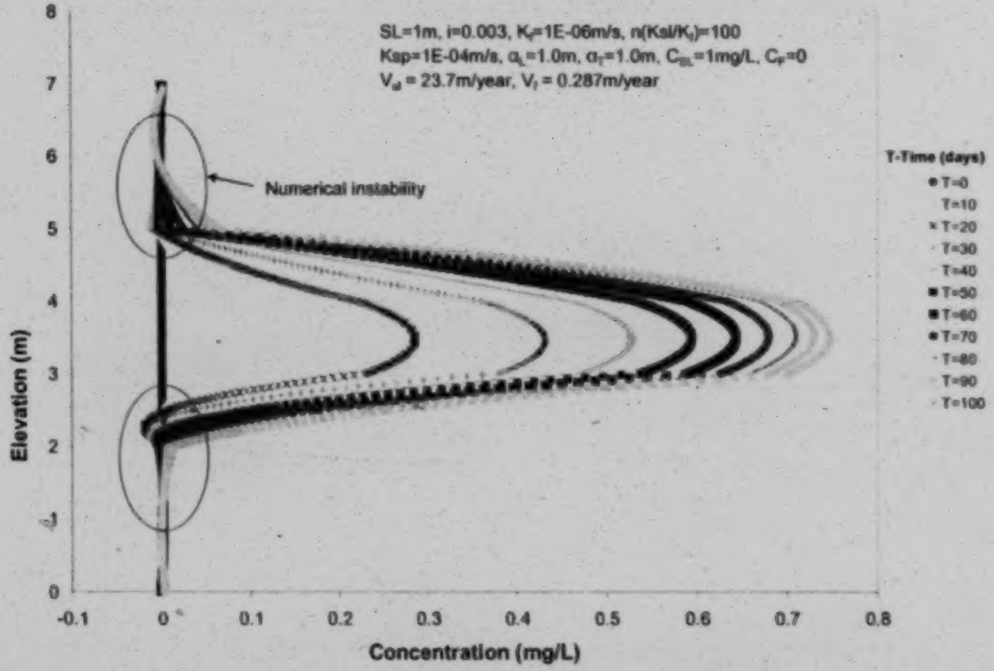

Figure 3.7 Example of concentration profile within the well (Case I-Hn100-CHA).

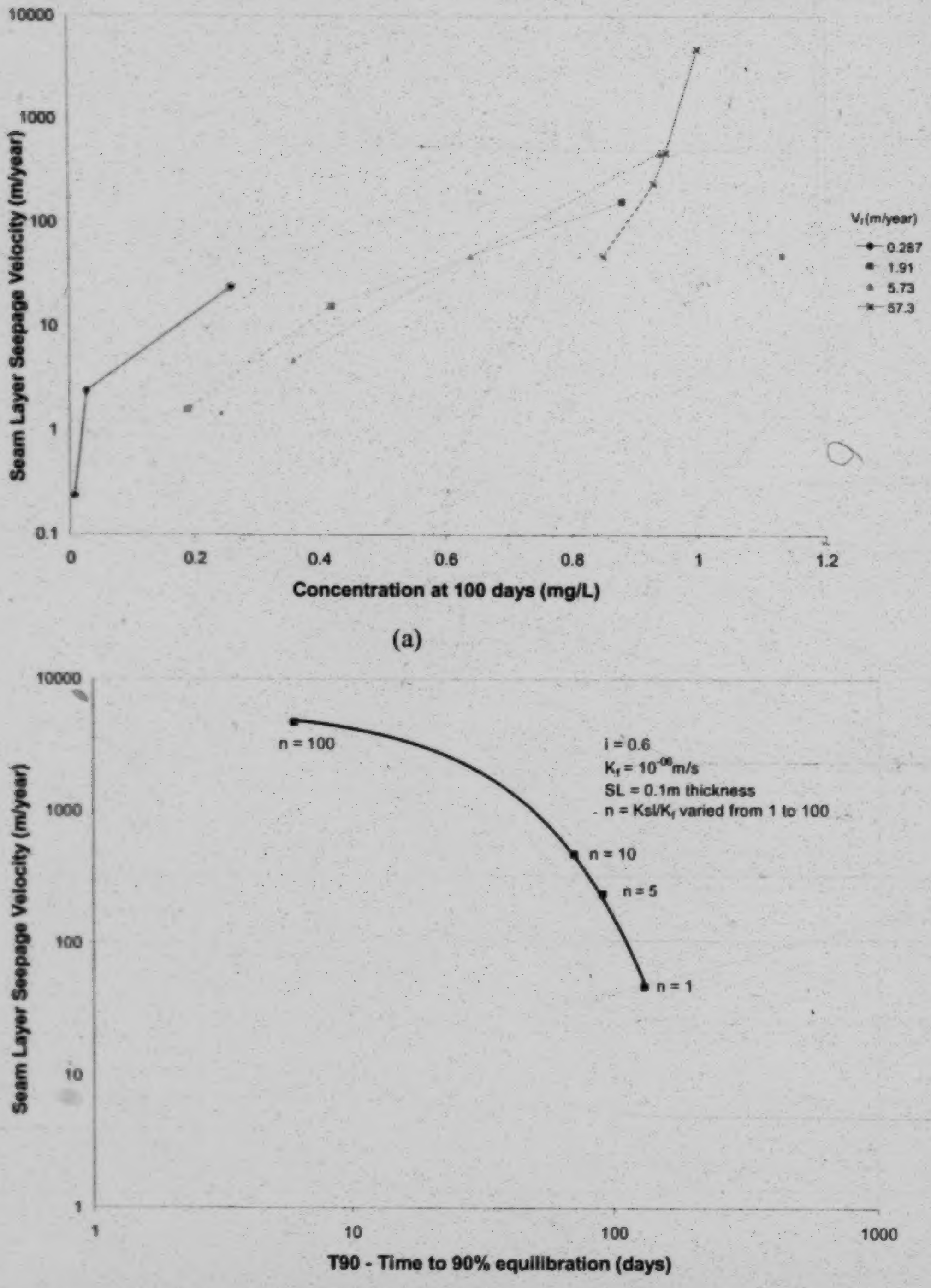

Figure 3.8 Effects of seepage velocity on contaminant movement Case II-CHA (a) Seam layer seepage velocity versus concentration at 100days (b) seam layer velocity versus T_{90} for V_f at 57.3m/year (Note: V_f is the seepage velocity of the sand formation).

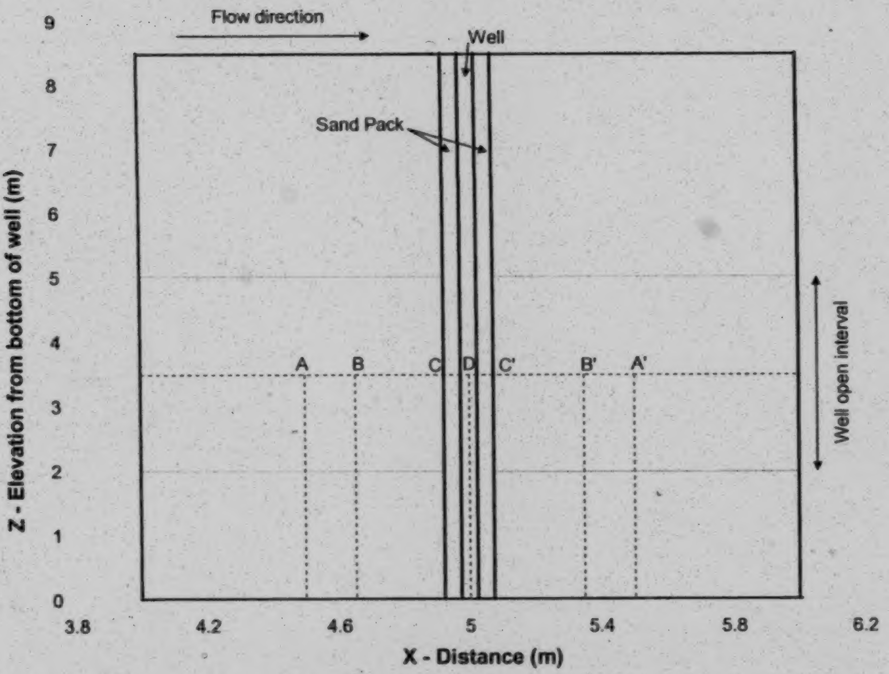
Flow direction
Well
Sand Pack
A
B
C
D
C'
B'
A'
Well open interval
Z - Elevation from bottom of well (m)
0
1
2
3
4
5
6
7
8
9
X - Distance (m)
3.8
4.2
4.6
5
5.4
5.8
6.2

Figure 3.9 Illustration of points plotted within the domain in Figure 3.10(a) and (b).

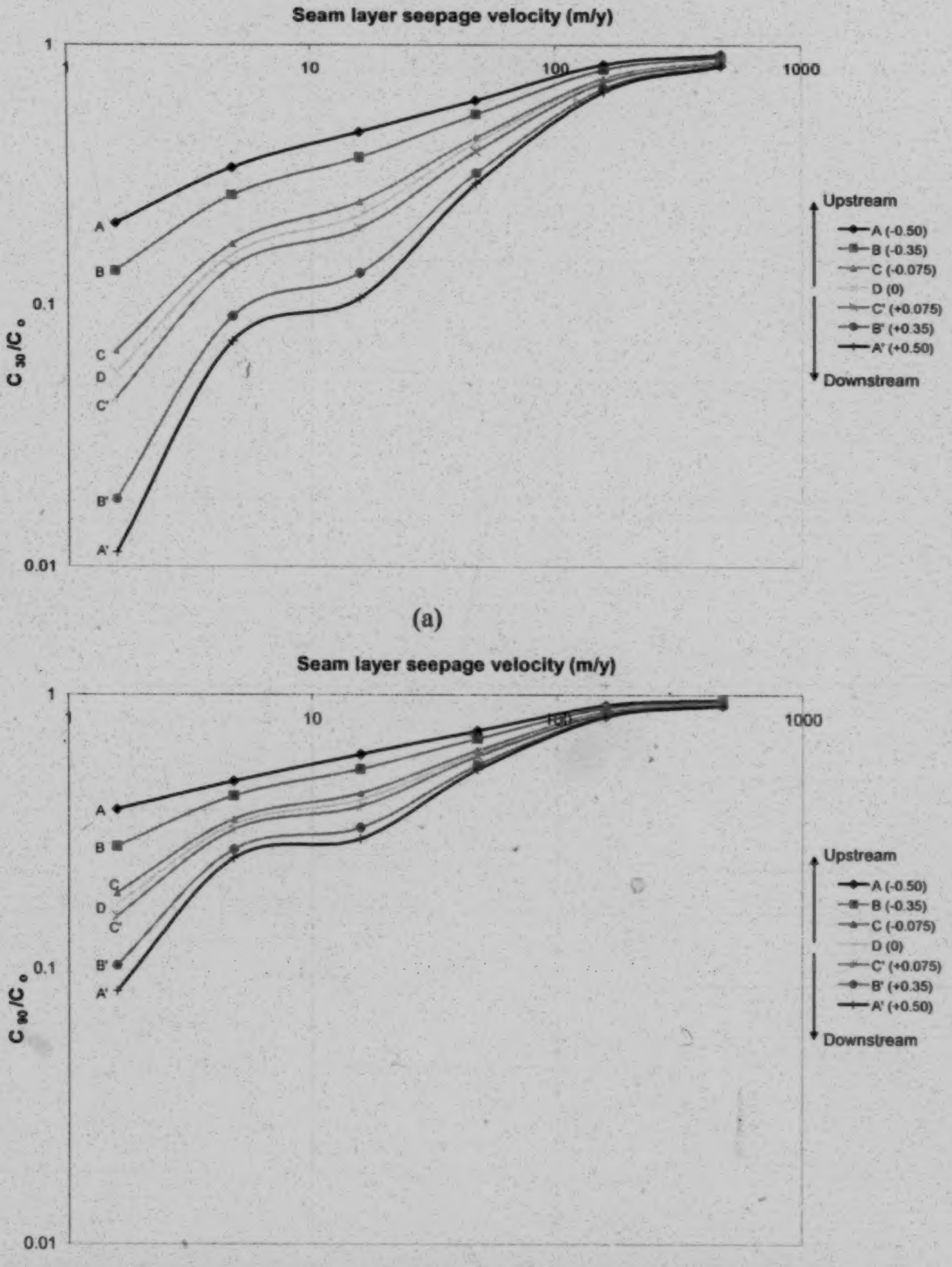

(a)

(b)

Figure 3.10 Comparison of concentration ratios at the midpoint of the well (a) Concentration ratio at the end of 30 days vs. seam layer seepage velocity,(b) Concentration ratio at the end of 90 days vs. seam layer seepage velocity at different points shown in (a), upstream and downstream of the well's centerline.

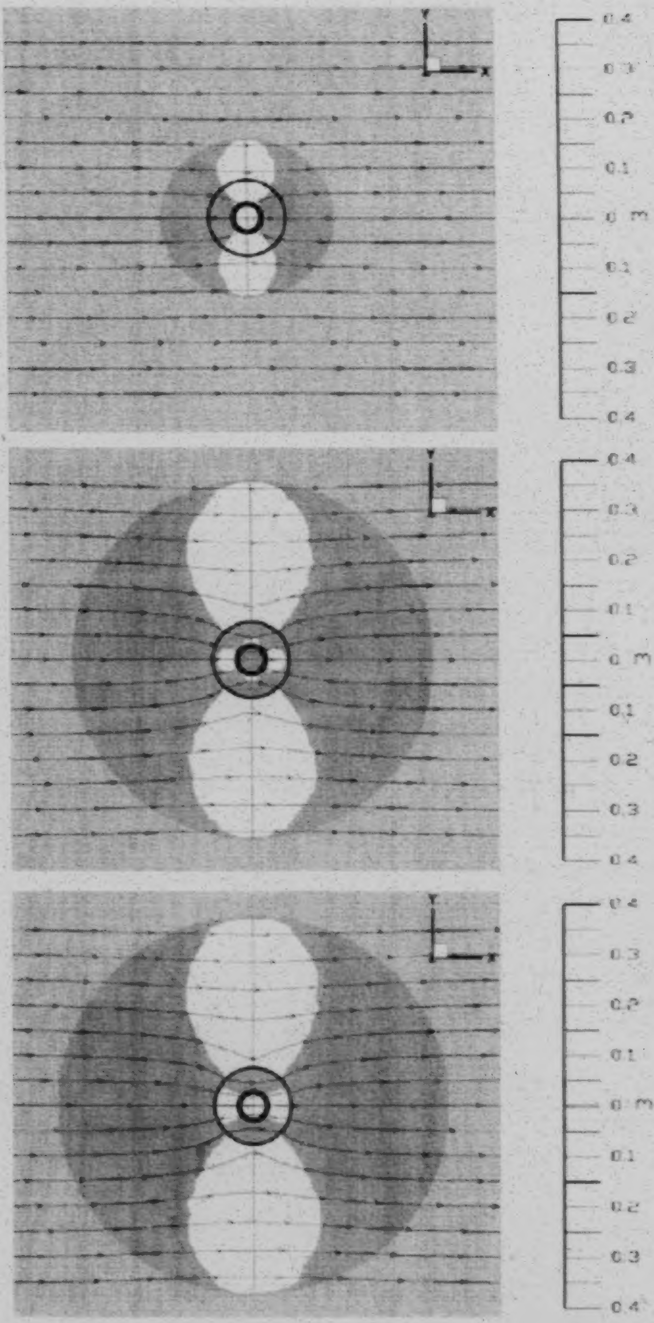

The streamlines are at 0.5m
equidistance from the centerline
of the well open interval
(Z=3.5m, X:Y = 1)
K_f = 1 E -06m/s
Kw = 3.3 E-04m/s
Ksp/K_f = n = 1
Z_f = Zone of Influence
≈0.15m

K_f = 1 E -06m/s
Kw = 3.3 E-04m/s
Ksp/K_f = n = 10
Z_f = Zone of Influence
≈ 0.35m

K_f = 1 E -06m/s
Kw = 3.3 E-04m/s
Ksp/K_f = n = 100
Z_f = Zone of Influence
≈ 0.35m

Figure 3.11 Zone of Influence at the middle of the well open interval

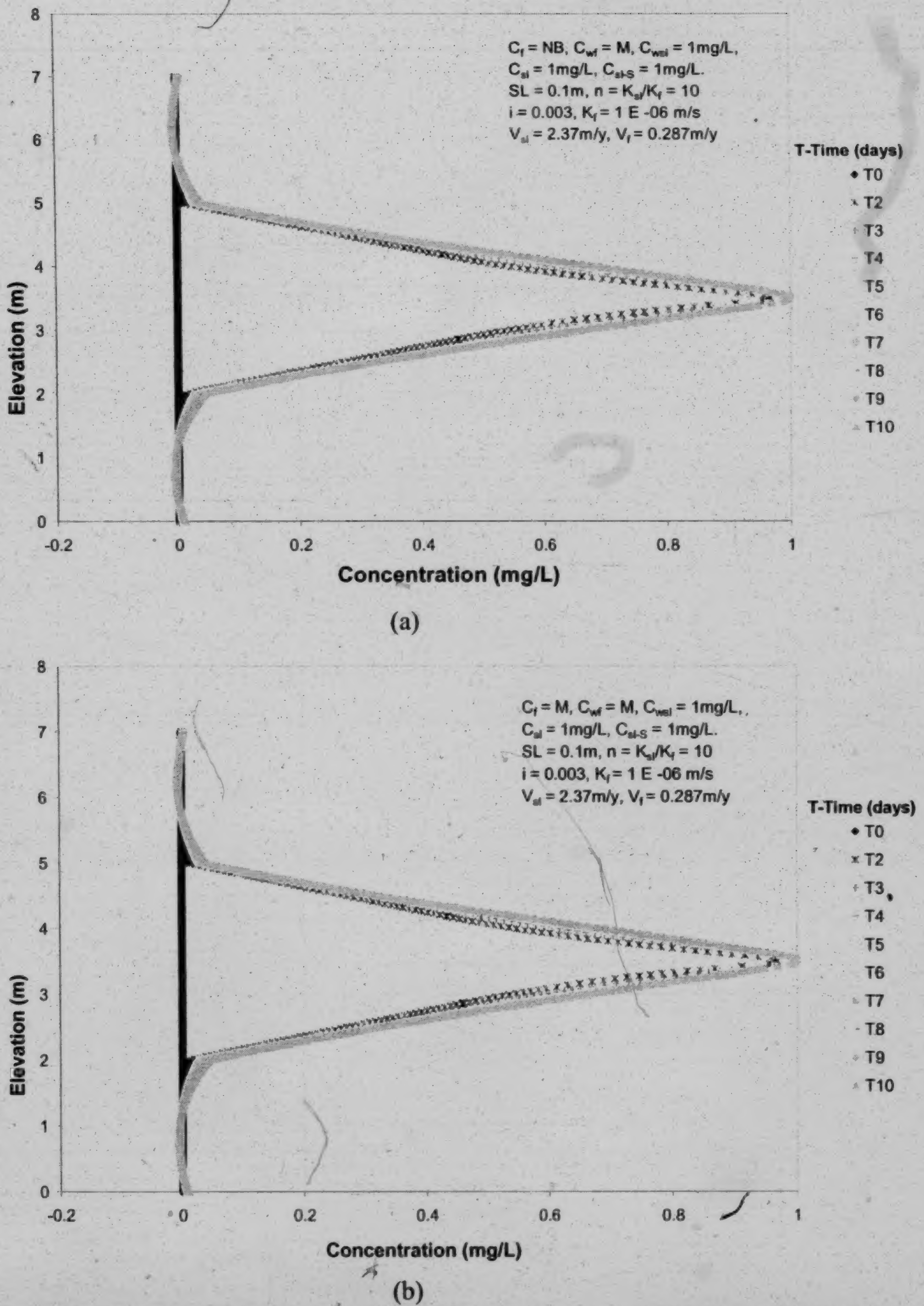

(a)

(b)

Figure 3.12 Concentration profile within the well for the boundary conditions in which monitoring well is sited in already contaminated soil. (a) CHAS –profile without formation concentration gradient, (b) CHCS – profile with formation concentration boundary.

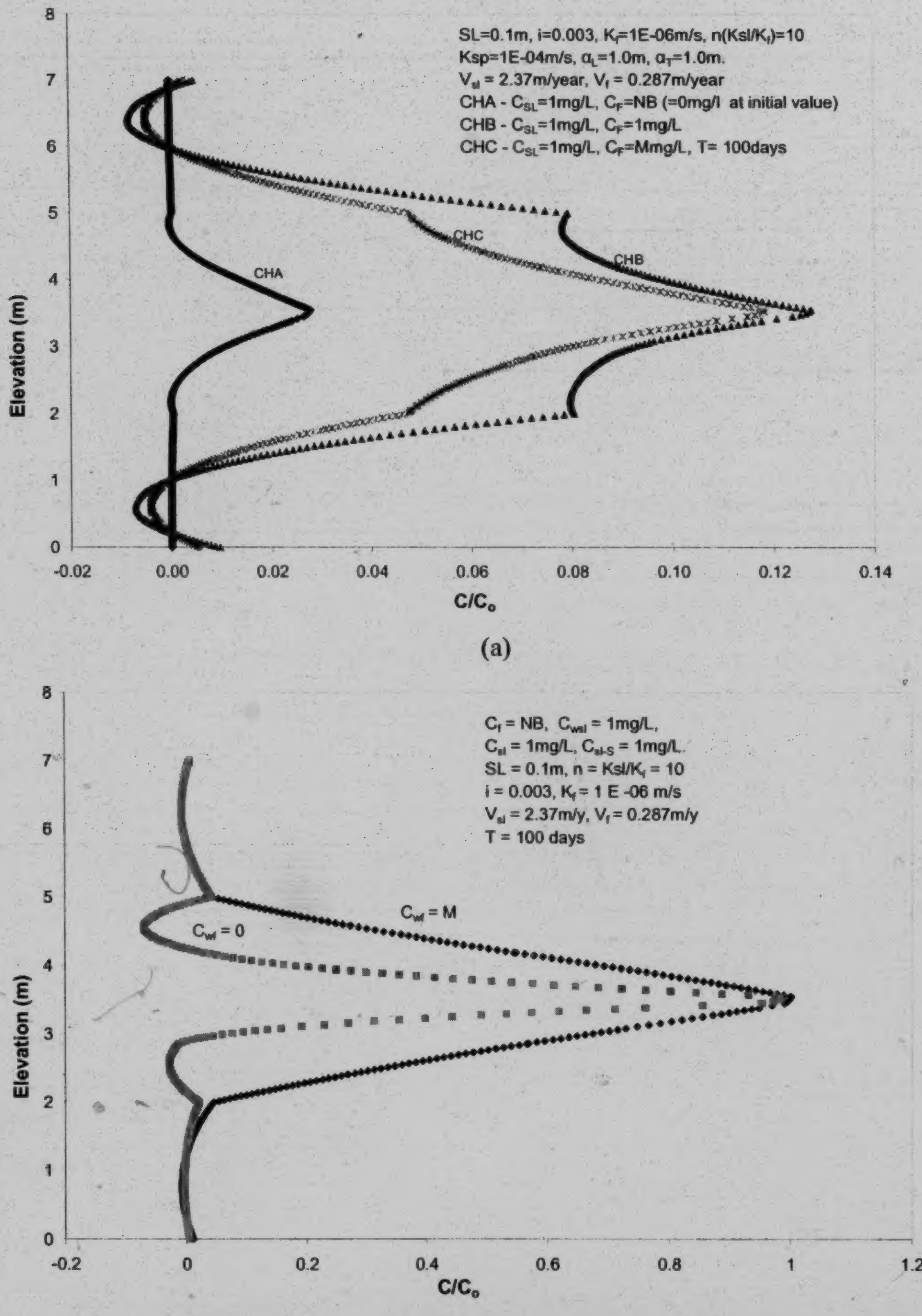

(a)

(b)

Figure 3.13 Effects of initial concentration distribution on contaminant movement within the well. (a) Simulations with C_{wsl}=0 & $C_{sl\text{-}S}$=0; (b) Simulations with $C_{sl\text{-}S}$=1 (CHAS).

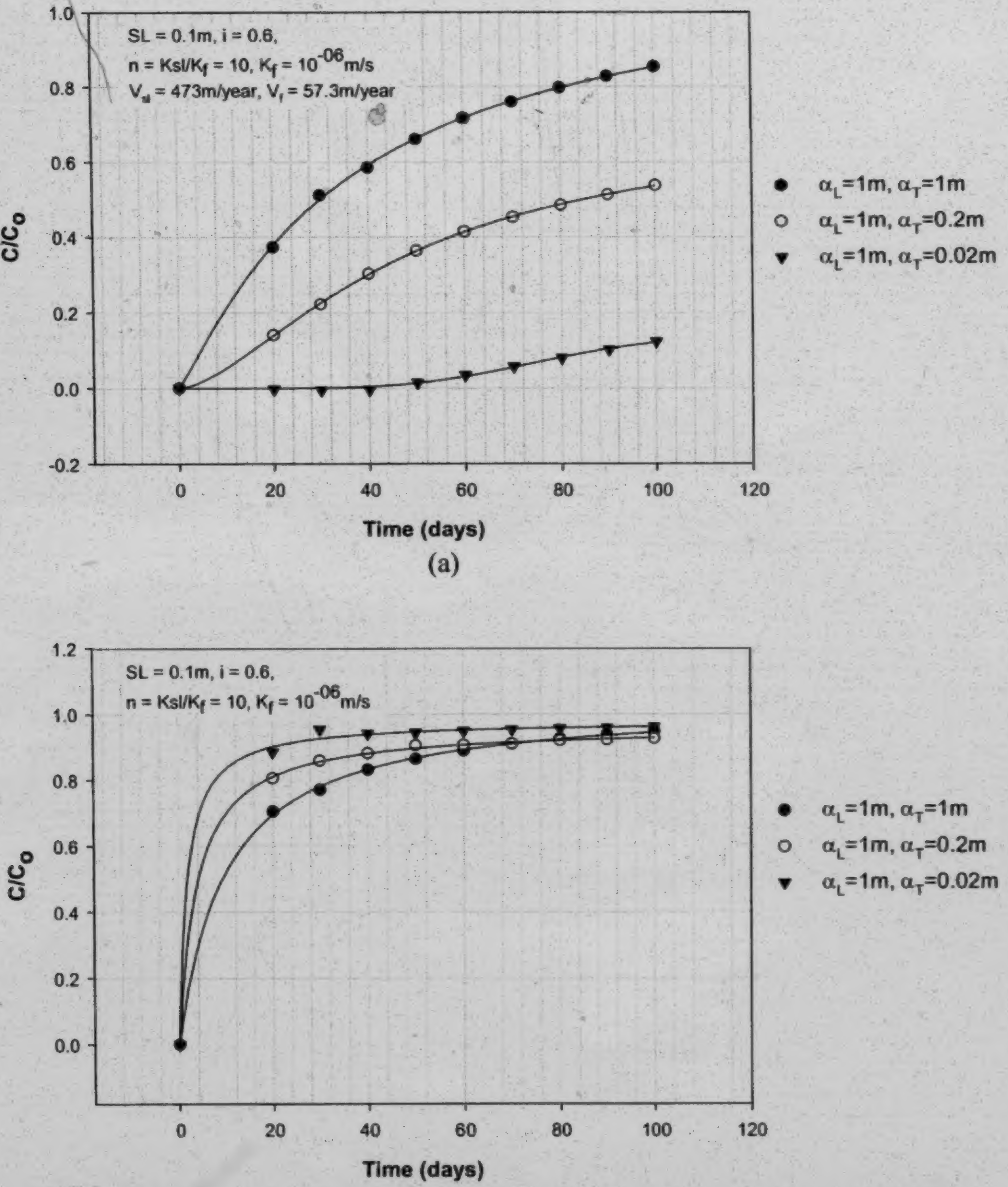

(a)

(b)

Figure 3.14 Effects of varying dispersivity coefficients using CHA boundary conditions. (a) Concentration profile at the top of the well screen: (b) Concentration profile at the middle of the well screen.

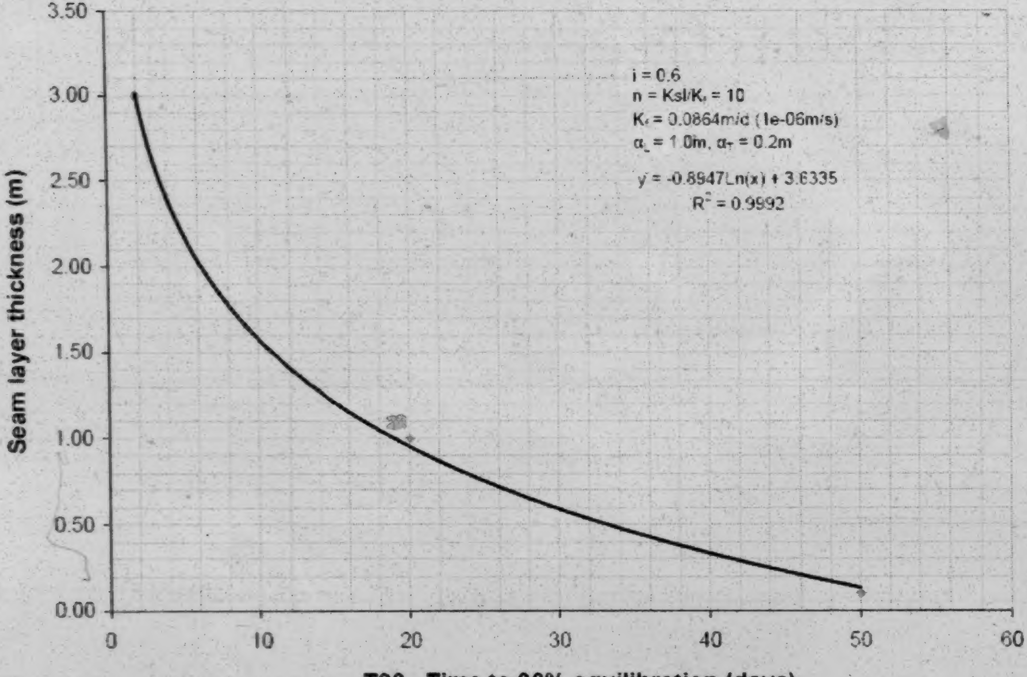

Figure3.15 Effects of seam layer thickness on equilibration time at the midpoint of the well for Case II-CHA (i.e. SL = 0.1m, V_{sl} = 473m/y, C_{sl} = 1mg/l, & C_f = 0).

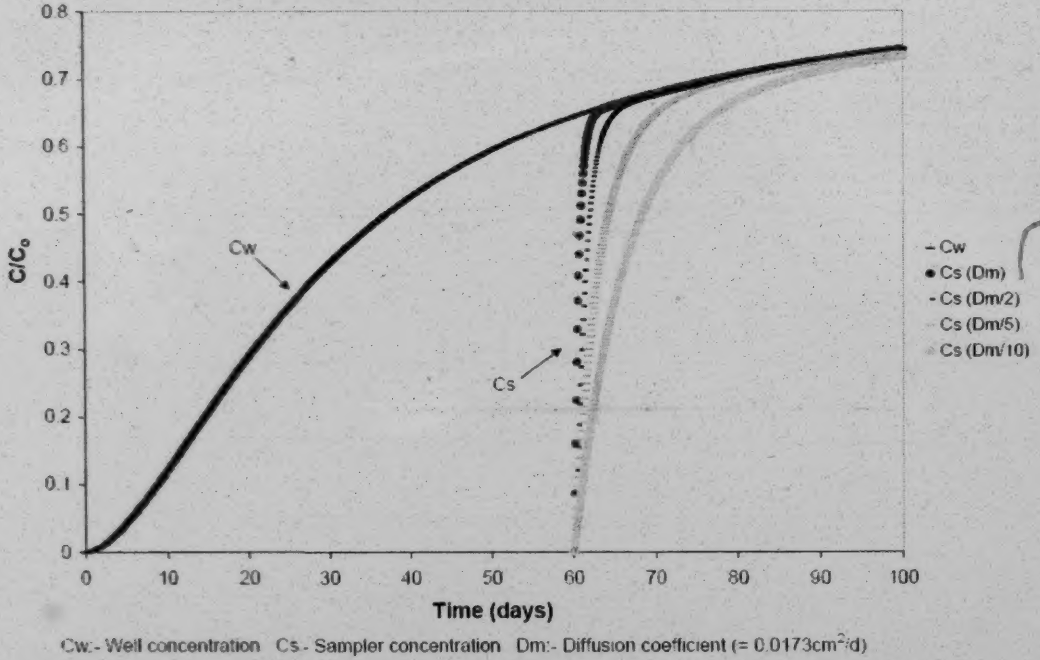

Figure 3.16 Diffusion sampler concentrations with time for the concentration profile at the middle of the well for Case I-Hn100-CHA (Figure 3.7).

3.8 Tables

Table 3.1 Basic Configuration

Domain	Dimension	Units
Model	2.0 × 2.0 × 8.5	m
Well radius	r = 0.025	m
Well screen thickness	t = 0.002	m
Sand pack thickness	t = 0.050	m
Well screen length	h = 3.00	m

Table 3.2 Properties of materials used for the simulation.

Material	Symbol	K_{sat} (m/s)	D* (m^2/s)	N	Comment
Well	Kw	3.30 E -04	3.00 E -08	1.00	Kept constant
Well Screen	Kws	3.30 E -04	3.00 E -08	0.90	"
Well Casing	Kwc	0	0	0	"
Sand Pack	Ksp_0	1.00 E -04	2.10 E -08	0.35	Varied from 100 to 0.1Ksp_0
Sand	K_f	1.00 E -06	1.50 E -08	0.33	Kept constant[8]
Clay	Kc	1.00 E -09	3.00 E -09	0.44	"
Seam Layer	Ksl_0	1.00 E -05	1.50 E –08	0.40	Varied from 100 to 0.1K_f

K_{sat}	Saturated hydraulic conductivity
D*	Effective diffusion coefficient
N	Porosity

---

[8] In some of the simulations with hydraulic gradient of 0.6 and 0.2, the conductivity of the sand was decreased by an order of magnitude to lower the velocity at such gradients.

Table 3.3 Sectional boundary conditions of the conceptual model

Case	Segment	SVFLUX (H) Boundary	CHEMFLUX Boundary (CH)			Comment
			A	B	C	
I	AB	No Boundary (NB)	No Boundary			The thickness of the seam layer (SL) adjacent to the well screen (WS) was 1m (segment BC) and its permeability ratio was varied from 1 to 100 times that of the sand layer (Kf) with a permeability of 1E-06m/s. The permeability of other layers were kept constant at their original values. For CHEMFLUX simulation, "No boundary" condition implies initial concentration of zero at the boundary
	BC	Head Expression =H_1	No Boundary			
	CD	Head Expression =H_1	No Boundary			
	DE	Head Expression = H_1	Conc. = 1			
	EF	Head Expression =H_1	No Boundary			
	FG	Head Expression =H_1	No Boundary			
	GH	Zero Flux	Zero Flux			
	HI	Head Expression =H_2	No Boundary			
	IJ	Head Expression =H_2	No Boundary			
	JK	Head Expression = H_2	No Boundary			
	KL	Head Expression =H_2	No Boundary			
	LM	Head Expression =H_2	No Boundary			
	MN	No Boundary	No Boundary			
	NA	Zero Flux	Zero Flux			
II	AB	No Boundary	No Boundary	No Boundary	No Boundary	This model is similar to Case I but SL was decreased to 0.1m. However, the dispersivity of the soils were varied from 1.0m to 0.2m for the longitudinal dispersivity and 1m to 0.02m for the transverse dispersivity for CHA boundary conditions with the permeability of the SL fixed at 1E-05m/s.
	BC	Head Expression =H_1	No Boundary	No Boundary	No Boundary	
	CD	Head Expression =H_1	No Boundary	Conc. = 1	Conc. = 1*(7-z)/3.45	
	DE	Head Expression = H_1	Conc. = 1	Conc. = 1	Conc. = 1	
	EF	Head Expression =H_1	No Boundary	Conc. = 1	Conc. = 1*(z/3.45)	
	FG	Head Expression =H_1	No Boundary	No Boundary	No Boundary	
	GH	Zero Flux	Zero Flux	Zero Flux	Zero Flux	
	HI	Head Expression =H_2	No Boundary	No Boundary	No Boundary	
	IJ	Head Expression =H_2	No Boundary	No Boundary	No Boundary	
	JK	Head Expression = H_2	No Boundary	No Boundary	No Boundary	
	KL	Head Expression =H_2	No Boundary	No Boundary	No Boundary	
	LM	Head Expression =H_2	No Boundary	No Boundary	No Boundary	
	MN	No Boundary	No Boundary	No Boundary	No Boundary	
	NA	Zero Flux	Zero Flux	Zero Flux	Zero Flux	
III	AB	No Boundary	No Boundary			The sand pack (SP) permeability was varied from 100 to 0.1K_f, assuming a SL thickness of 3m with the same properties as the sand formation (Table 3.2), when evaluating effects of SP permeability on free flow across the WS. In the CHEMFLUX analysis, the SL properties were set to its original values with permeability of 1E-05m/s to evaluate its thickness effects on contaminant flow.
	BC	Head Expression =H_1	No Boundary			
	CD	Head Expression =H_1	Conc. = 1			
	DE	Head Expression =H_1	No Boundary			
	EF	Zero Flux	Zero Flux			
	FG	Head Expression = H_2	No Boundary			
	GH	Head Expression = H_2	No Boundary			
	HI	Head Expression = H_2	No Boundary			
	IJ	No Boundary	No Boundary			
	JA	Zero Flux	Zero Flux			

Notes:

$$i = \frac{H_2 - H_1}{L} = \frac{H_2 - H_1}{2} = 0.6, 0.2, 0.003$$ [i= hydraulic gradient & L= length of domain]

An additional boundary condition termed "S" is further imposed on CHA and CHC indicated above as shown in Figure 3.3. The "S" indicates constant surface concentration boundary condition of 1mg/l at the seam layer interface.

References

Kearl, P.M., N.E. Korte, and T.A. Cronk (1992). Suggested modifications to ground water sampling procedures based on observations from the colloidal borescope. *Ground Water Monitoring Review*, vol 12, no 2, pp. 155–161.

Powell, R. M., and Puls, R. W. 1993. Passive sampling of groundwater monitoring wells without purging: Multilevel well chemistry and tracer disappearance. *Journal of Contaminant Hydrology*, vol. 12, pp. 51-77.

Robin, M. J. L. and Gilham, R. W. 1987. Field Evaluation of well purging procedures. *Ground Water Monitoring Review*. Vol. 7, no. 4, pp. 85-93.

Stianson, J. 2002. CHEMFLUX user's manual, first edition. SoilVision Systems Ltd, Saskatoon.

Stianson, J. 2002. SVFLUX user's manual, first edition. SoilVision Systems Ltd, Saskatoon.

Vroblesky, D.A., Petkewich, M.D. and Campbell, T.R., 2002, Field tests of diffusion samplers for inorganic constituents in wells and at a ground-water discharge zone: U.S. Geological Survey WRIR-02-4031, 24 p.

Vroblesky, D.A. (2001). User's Guide for Polyethylene-Based Passive Diffusion Bag Samplers to Obtain Volatile Organic Compound Concentrations in Wells. Part 1: Deployment, Recovery, Data Interpretation, and Quality Control and Assurance. U.S. Geological Survey, Water–Resources Investigations Report 01- 4060.

4 Conclusions and Recommendations

4.1 Conclusions

Diffusion samplers made from regenerated cellulose dialysis membrane showed promising results for long term monitoring associated with natural attenuation assessment. There was no significant difference in the response when using deoxygenated infill water in comparison to oxygenated infill water in the laboratory at the concentrations tested. The impacts may be more pronounced at very low BTEX concentrations near the regulatory limits of concern because it may take more than two weeks to achieve equilibrium with the surrounding water in a closed system when benzene oxidation is assumed within the samplers in the absence of oxidizeable ferrous ion. However, in the presence of sufficient oxidizeable iron, the impacts on BTEX concentration are significantly reduced due to faster depletion of the oxygen; and equilibration is achieved within a week of sampler deployment even at µg/l concentrations near the regulatory limits of concern. In an open system where BTEX is recharged from the formation, about 90% equilibration is achieved after three days at the µg/l range, implying the use of oxygenated infill-water in the sampler is acceptable within the limit of analytical variability. The experimental results conform to the analytical solution at elevated concentration but due to sensitivity of the experimental design, tests at low concentrations were not conducted. Thus, the presence of dissolved oxygen in the infill water of the sampler does not appear to significantly impact BTEX concentration for typical conditions in the field.

Throughout the six months deployment of the dialysis samplers in the field, no visible degradation of the membranes was noticed. The pressure and tensile strength test results are within 36% and 19% of the average strength of the new samplers. A major concern is the safe retrieval of the dialysis sampler from the well where abrasion may occur during installation or retrieval. Therefore, for petroleum contaminated sites similar to those tested (i.e. groundwater ambient temperature ≈ 2°C, free product either present or absent, complete submergence), dialysis membrane degradation does not appear to be a concern at times less than or equal to 180 days.

Any phenomenon that brings about decreases in the permeability of the sand pack will decrease the free flow exchange between the well and the formation on which the use of diffusion samplers are dependent on. A formation with variable permeability layers adjacent to the well open interval will lead to the development of concentration gradients within the well thereby necessitating the need for sampling at discrete depths within the well. If thin highly permeable seam layers intersect the well open interval, there will be adequate exchange between the well and the formation, thus, diffusion samplers are amenable for sampling in such cases. At bigger thickness of the seam layer with the same seepage velocity, more contaminant moves within the well, and time to achieving equilibration is shortened. Equilibration of dialysis samplers with water within the well should take place within three days of sampler deployment. Any processes such as precipitation or settling of colloidal substances on the membrane surface area will increase the time to achieve by reducing the surface area available for diffusive flux, however, this effect was not studied, so is not quantified.

4.2 Recommendations

The results obtained in this study on the use of dialysis samplers are promising and the following are recommended for future work:

- The permeability of dialysis membrane to microbes should be investigated as this will affect the integrity of samples obtained and the membrane itself over time.

- More field testing should be undertaken under different conditions including higher temperature, presence of chlorinated solvents, and other chemical conditions.
- More detailed experimental study should be undertaken to determine the effects of oxygenated infill water at very low BTEX concentration to verify the analytical results of the model.
- The laboratory set-up for the BTEX analysis should be optimized and modified to accurately sample the BTEX concentration in the reservoir before the start of the experiment and at each sampling interval. This may be achieved by using a rigid reservoir system with an embedded non-removable calibrated glass syringe with one inlet and discharge ends. The inlet end should penetrate about one-fourth the length of the reservoir. Each end should have a small micro-valve fitted to it so that with an upward stroke, fluid could be siphoned into the syringe's annulus while keeping the discharge end closed. Then, with a downward stroke the inlet valve is closed and the fluid will pass through the discharge end to the sampling vials.
- The change in permeability of sand pack with time should be investigated to determine how diffusion sampler may respond with age.
- A model incorporating biological and geochemical conditions for known field conditions should be simulated to improve understanding of well response with the surrounding formation for such conditions.

APPENDIX A: Results data on the impacts of oxygenation of infill water and the integrity of the dialysis samplers with time

APPENDIX A.1 Concentration profiles based on the analytical equations developed for the dialysis samplers

Symbols

Cbr_i^*	Benzene concentration in the reservoir/formation with no oxidation
Cbr_i	Benzene concentration in the reservoir/formation considering its oxidation
Cbr_{if}	Benzene concentration in the reservoir/formation considering its oxidation with an initial iron concentration of 5mg/L
Ca_i^*	Benzene concentration in the sampler with no oxidation
Cl_i	Benzene concentration in the sampler considering its oxidation
Cl_{if}	Benzene concentration in the sampler considering its oxidation in a system with initial iron concentration of 5mg/L
Cfr_i^*	Iron concentration in the reservoir/formation with no oxidation
Cfr_i	Iron concentration in the reservoir/formation considering its oxidation
Cg_i^*	iron concentration in the sampler with no oxidation
Ch_i	Iron concentration in the sampler considering its oxidation coupled with benzene oxidation
C_0	Initial concentration in the reservoir/formation
Y_i	Dissolved oxygen concentration in the sampler at ith period

Note:

The Cl_{if} profiles were not included in system with $C_0 > 5$mg/L because of the closeness of the profiles i.e. as the initial concentration increases, the effects of iron in the sampled concentration decreases.

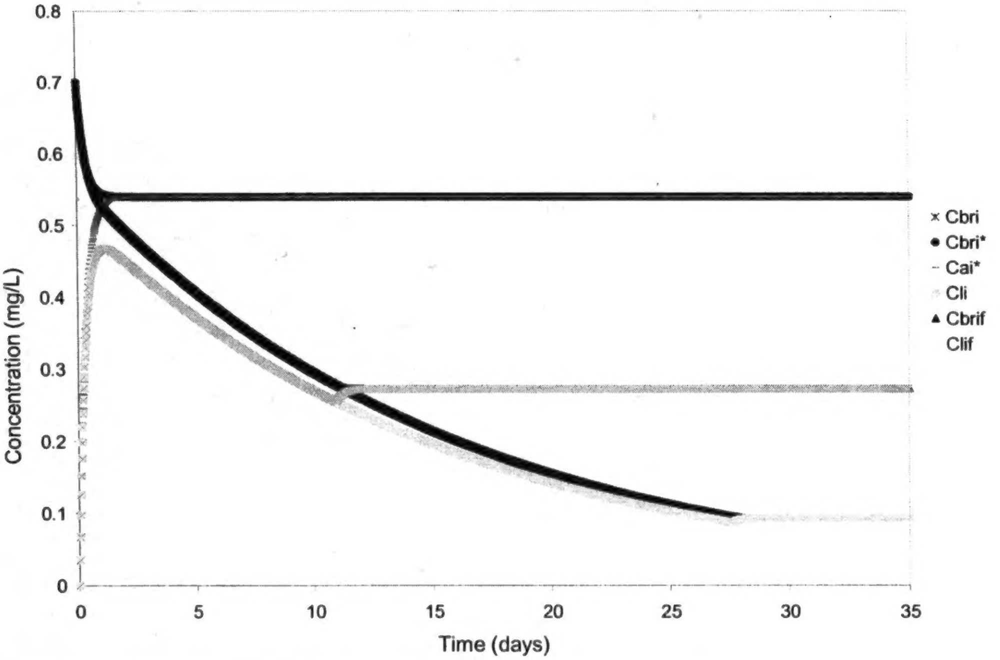

Figure A1.1 Analytical diffusion profile for initial benzene concentration "C_o" of 0.7mg/L for the experimental set-up (closed system).

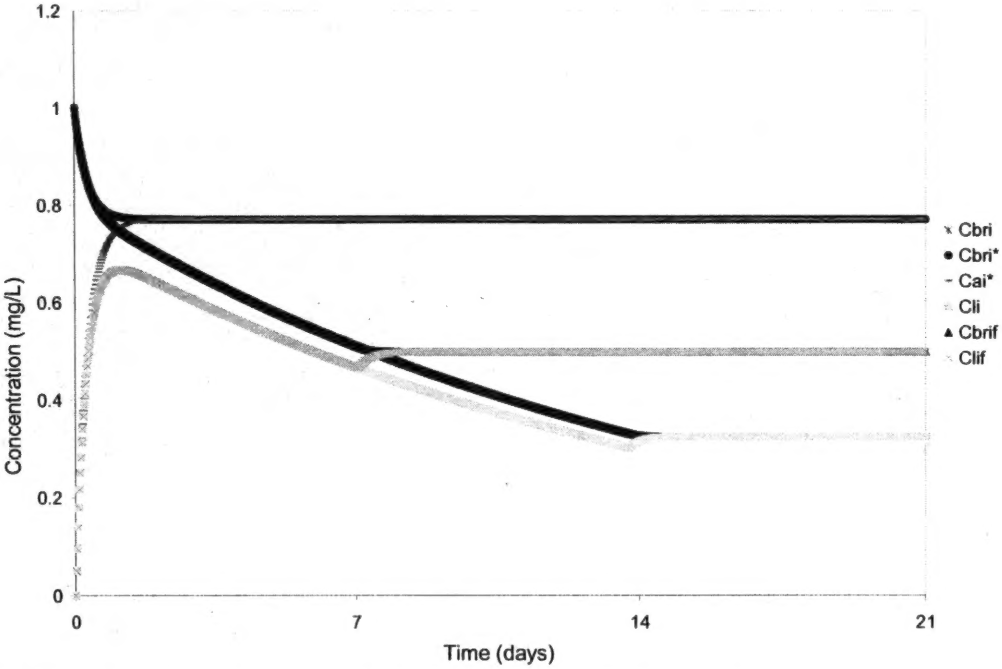

Figure A1.2 Analytical diffusion profile for 1mg/L benzene for the experimental set-up.

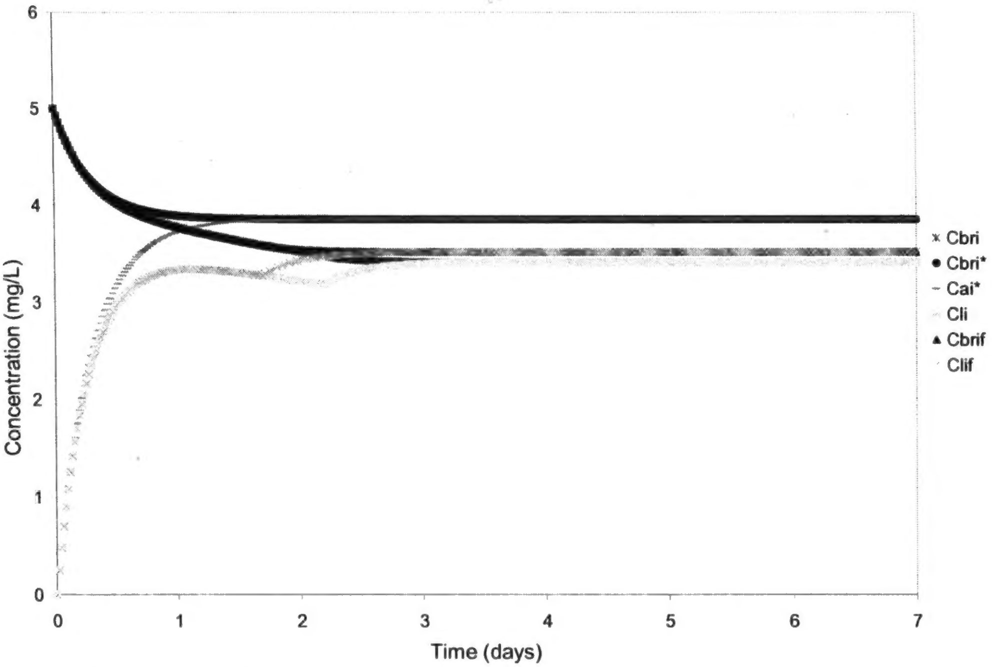

Figure A1.3 Analytical diffusion profile for 5mg/L benzene for the experimental set-up.

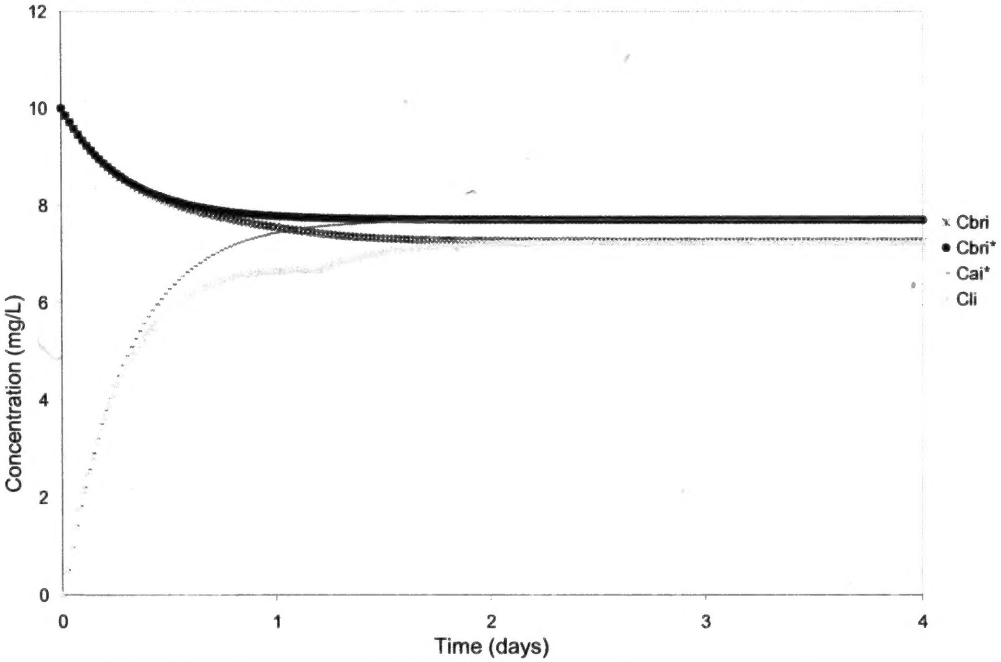

Figure A1.4 Analytical diffusion profile for 10mg/L benzene for the experimental set-up.

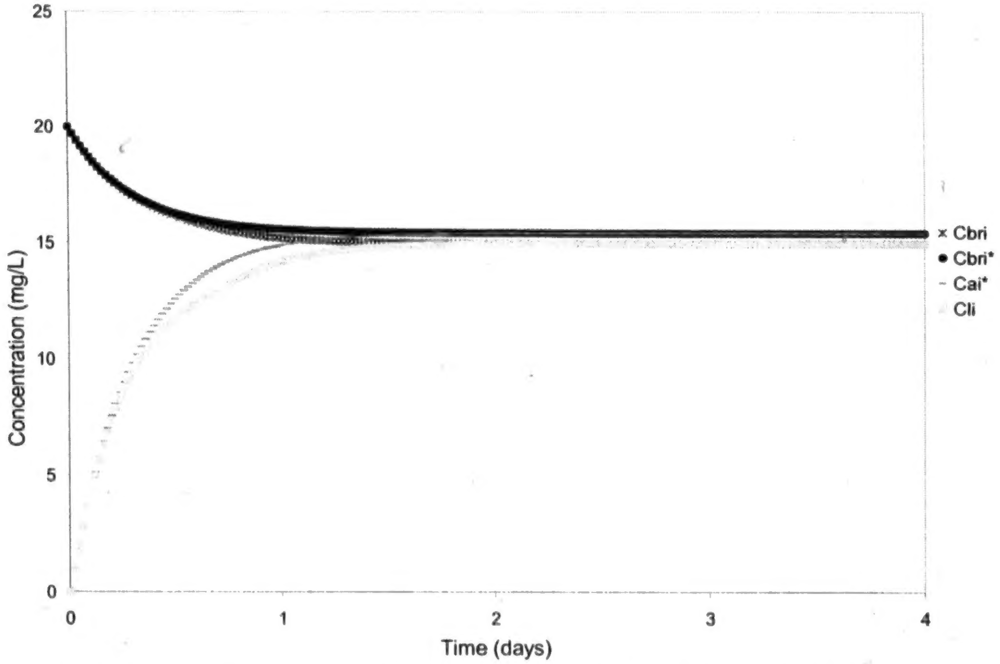

Figure A1.5 Analytical diffusion profile for 20mg/L benzene for the experimental set-up.

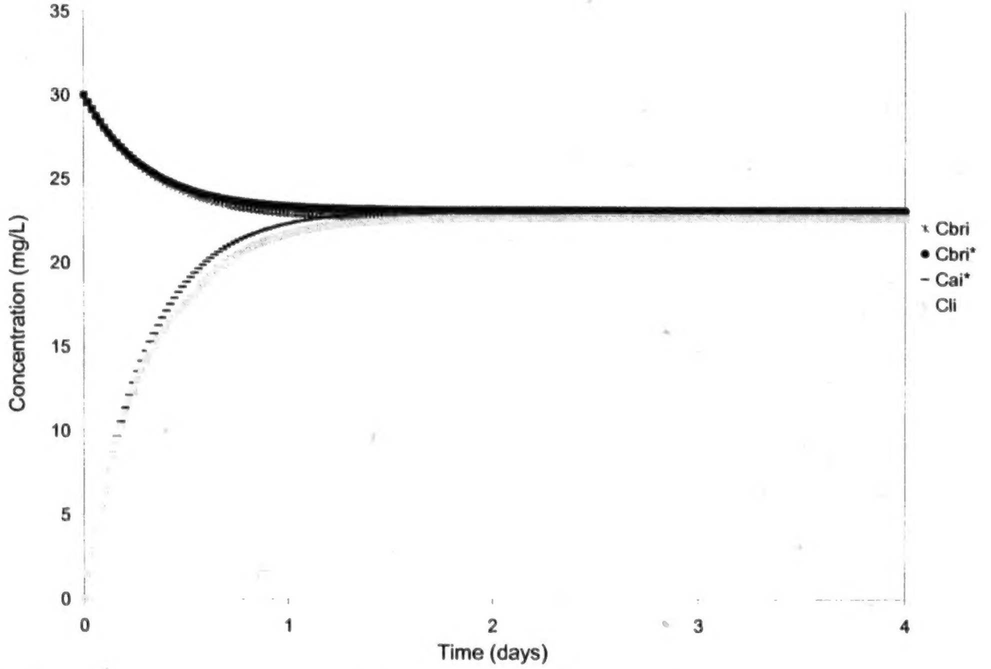

Figure A1.6 Analytical diffusion profile for 30mg/L benzene for the experimental set-up.

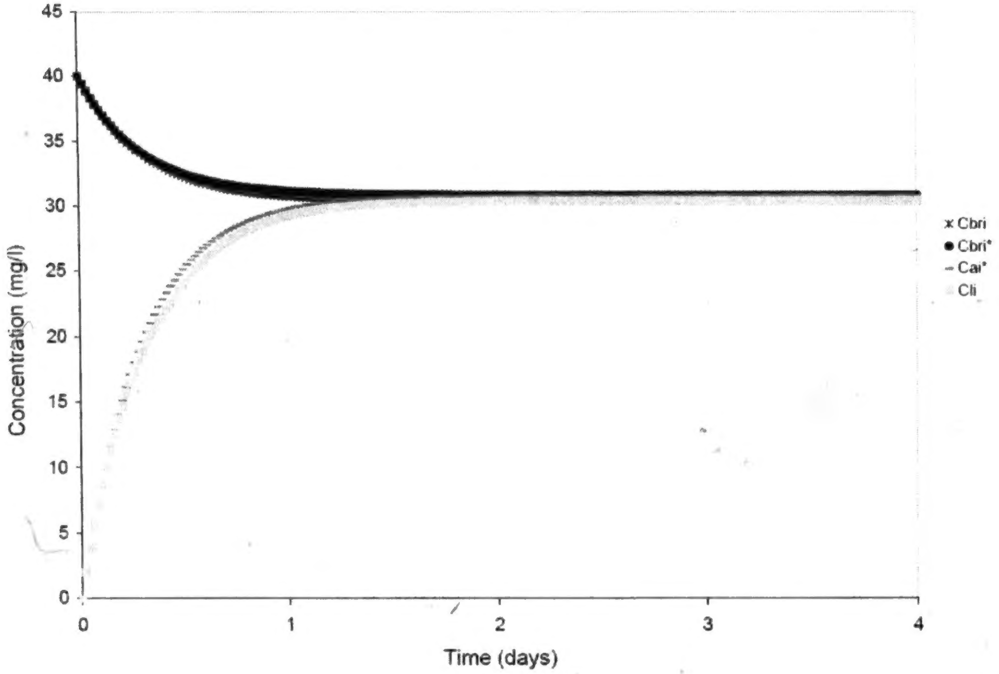

Figure A1.7 Analytical diffusion profile for 40mg/L benzene for the experimental set-up.

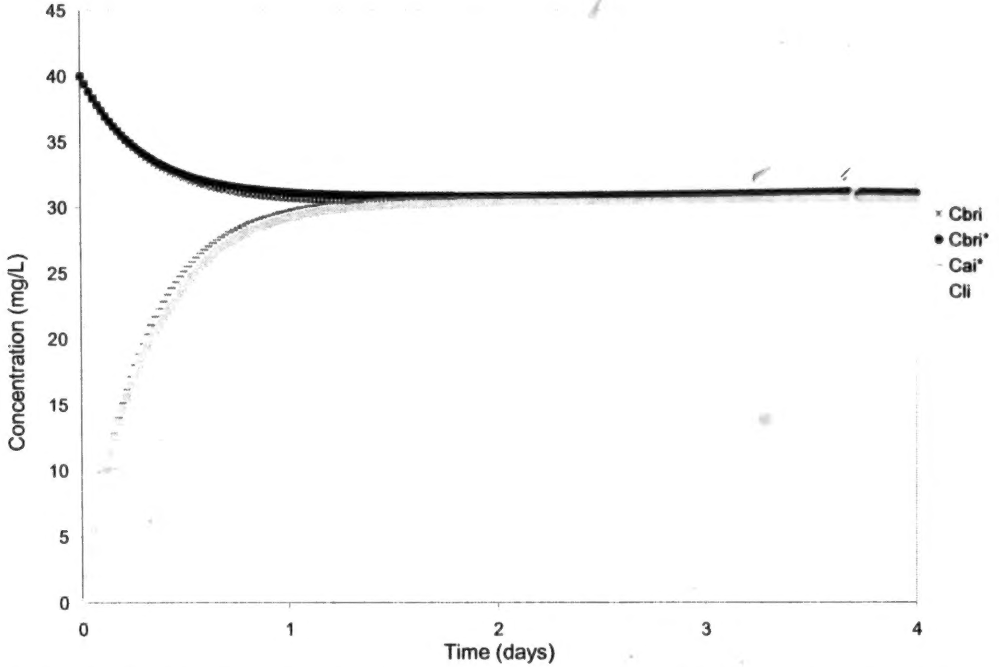

Figure A1.8 Analytical diffusion profile for 5mg/L iron concentration for the experimental set-up with coupled profile for 1mg/l of benzene concentration.

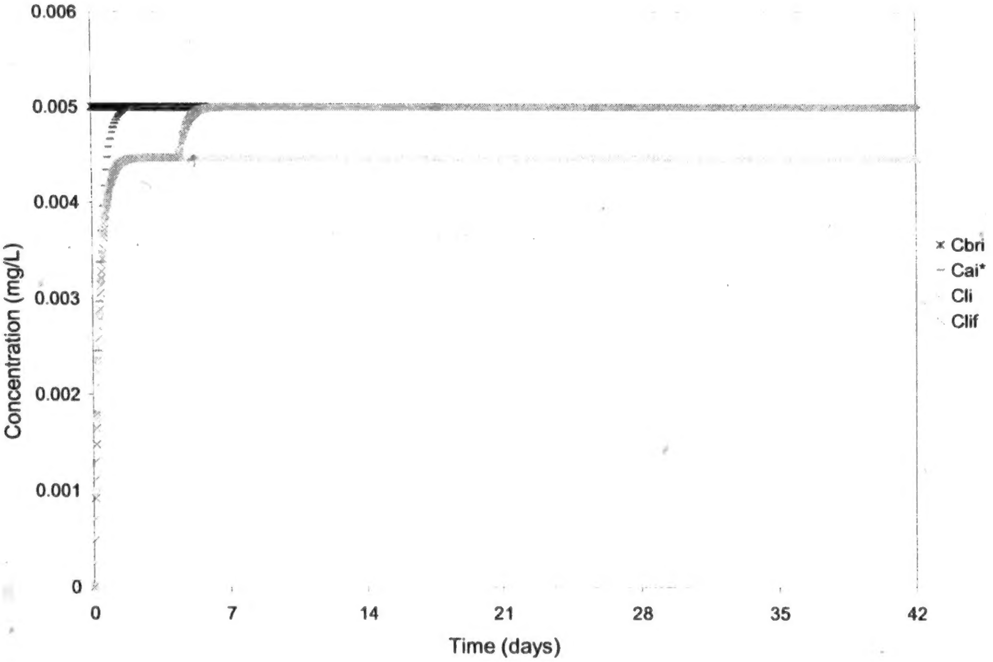

Figure A1.9 Analytical diffusion profile for constant 0.005mg/L benzene in a formation (open system).

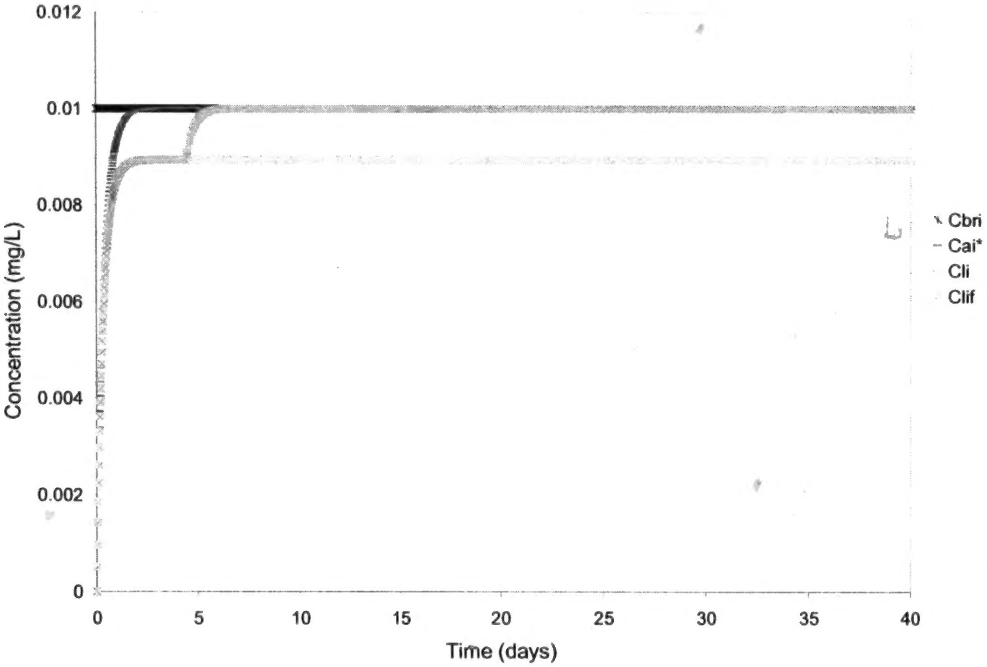

Figure A1.10 Analytical diffusion profile for constant 0.01mg/L benzene in a formation.

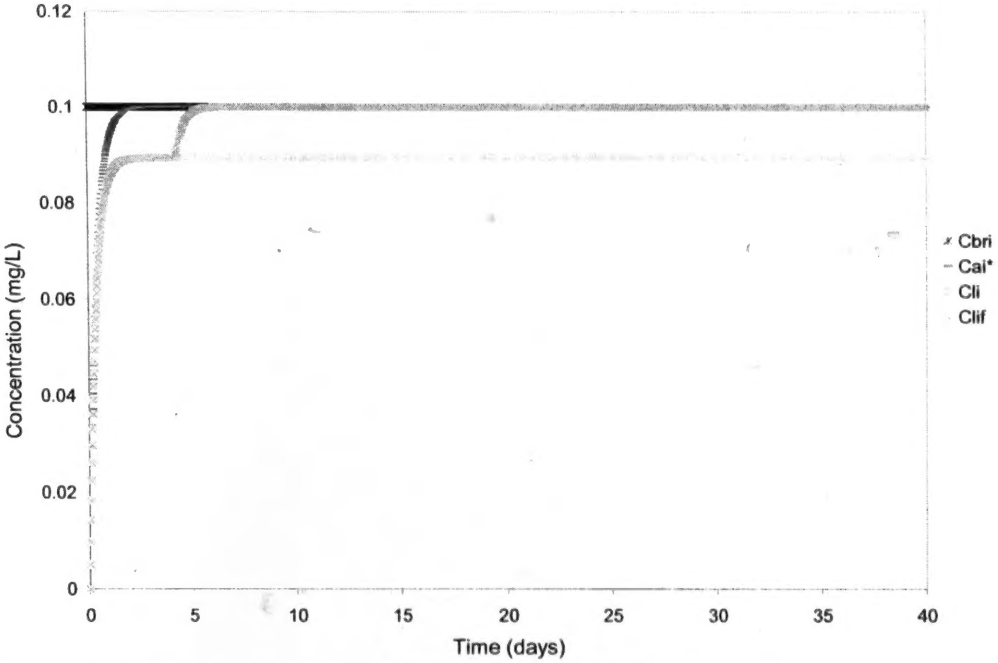

Figure A1.11 Analytical diffusion profile for constant 0.1mg/L benzene in a formation.

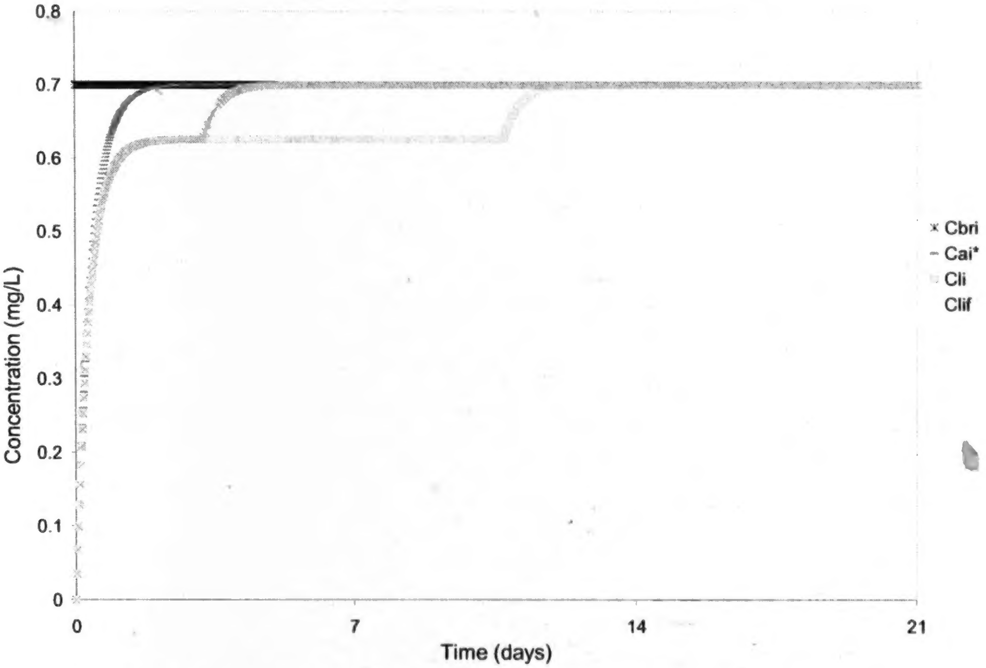

Figure A1.12 Analytical diffusion profile for constant 0.7mg/L benzene in a formation.

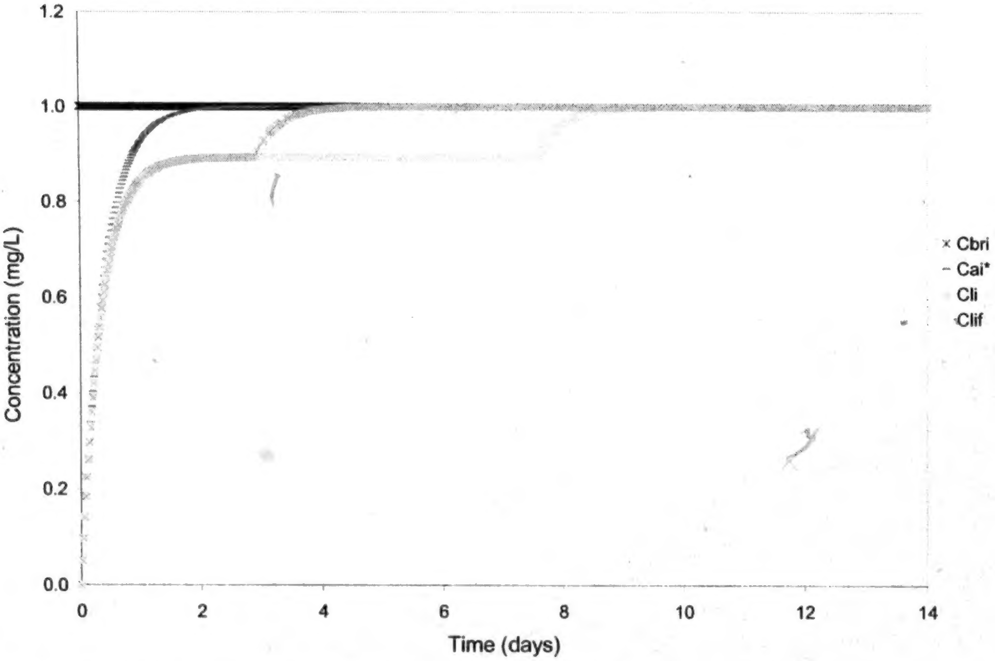

Figure A1.13 Analytical diffusion profile for constant 1mg/L benzene in a formation.

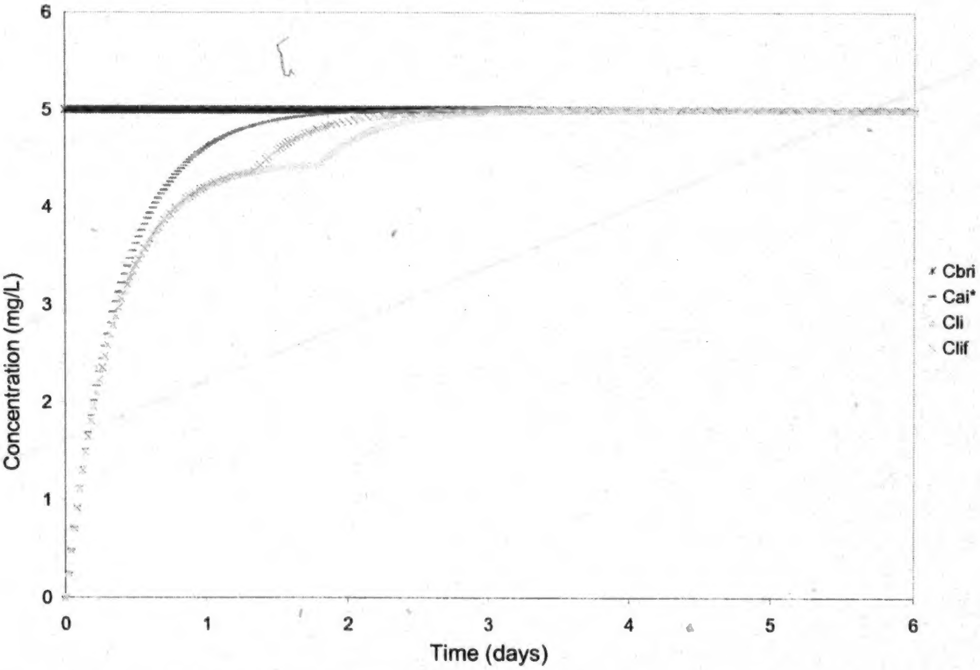

Figure A1.14 Analytical diffusion profile for constant 5mg/L benzene in a formation.

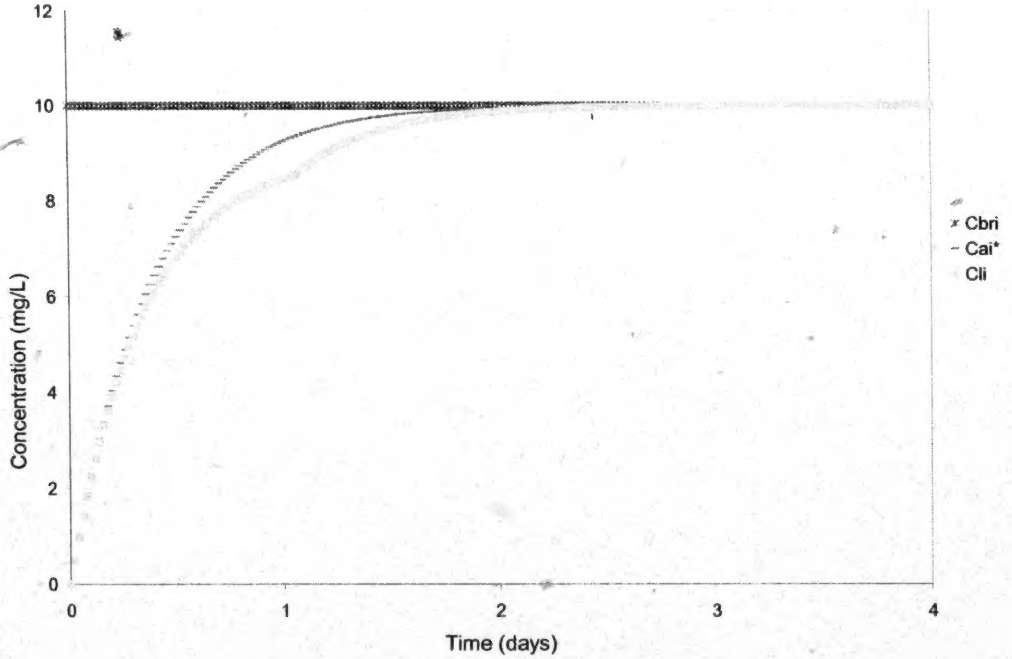

Figure A1.15 Analytical diffusion profile for constant 10mg/L benzene in a formation.

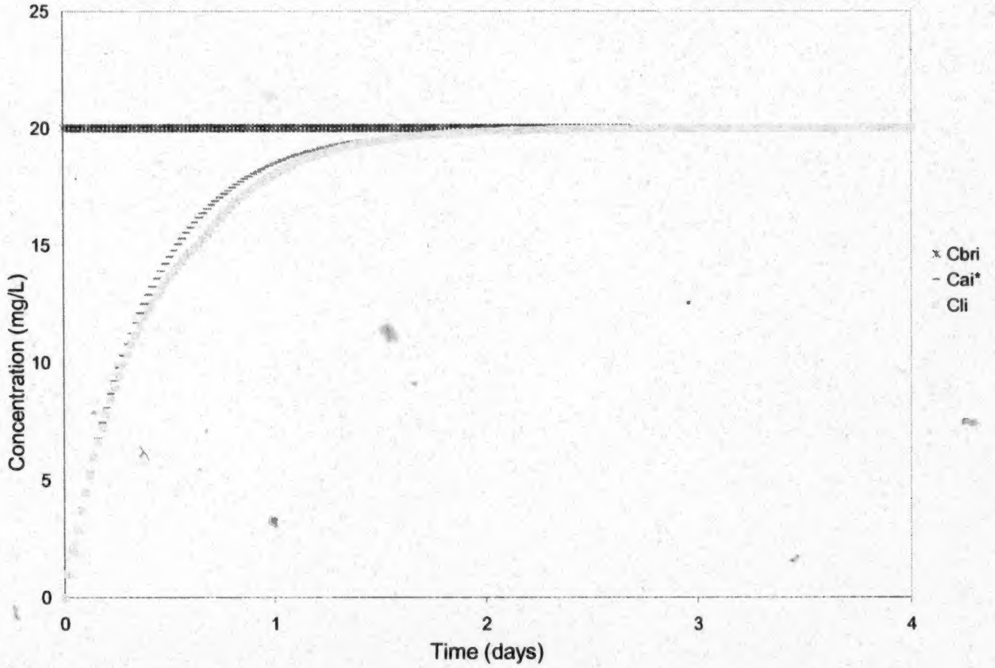

Figure A1.16 Analytical diffusion profile for constant 20mg/L benzene in a formation.

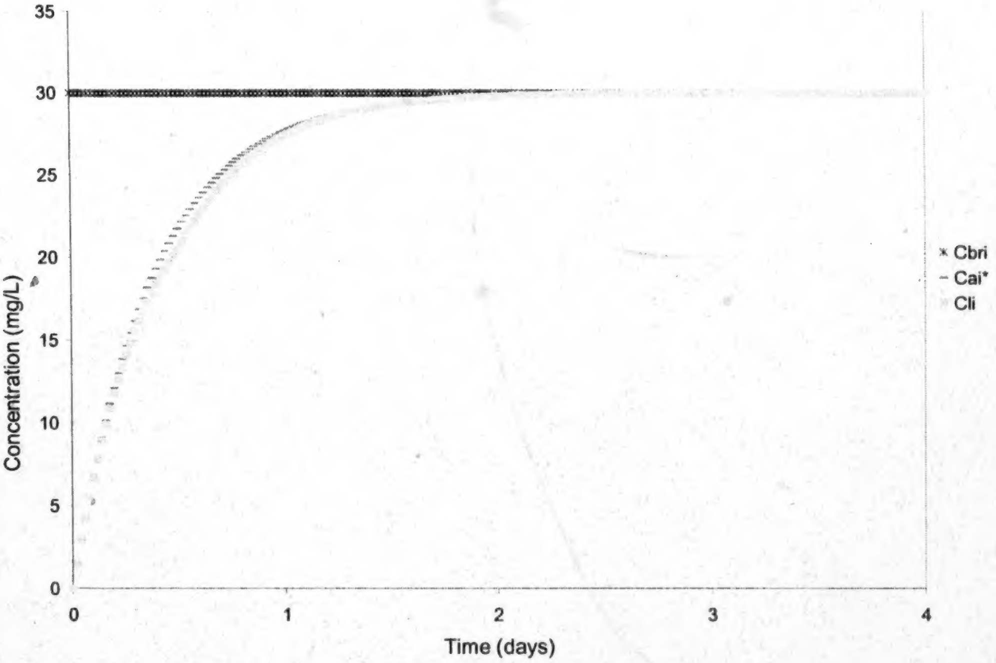

Figure A1.17 Analytical diffusion profile for constant 30mg/L benzene in a formation.

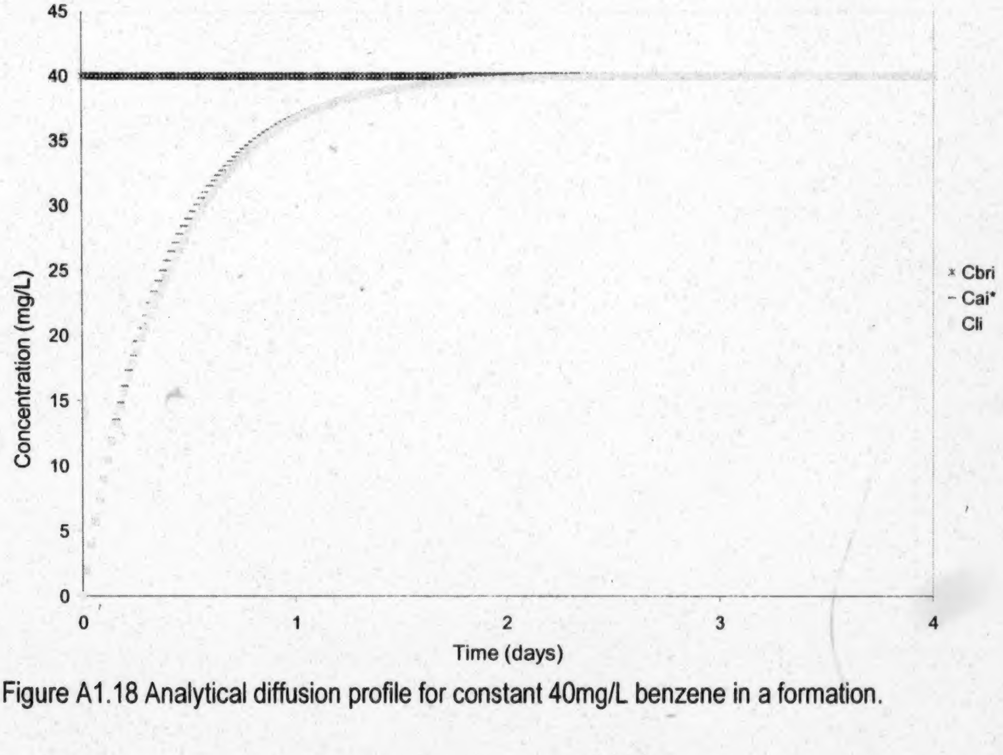

Figure A1.18 Analytical diffusion profile for constant 40mg/L benzene in a formation.

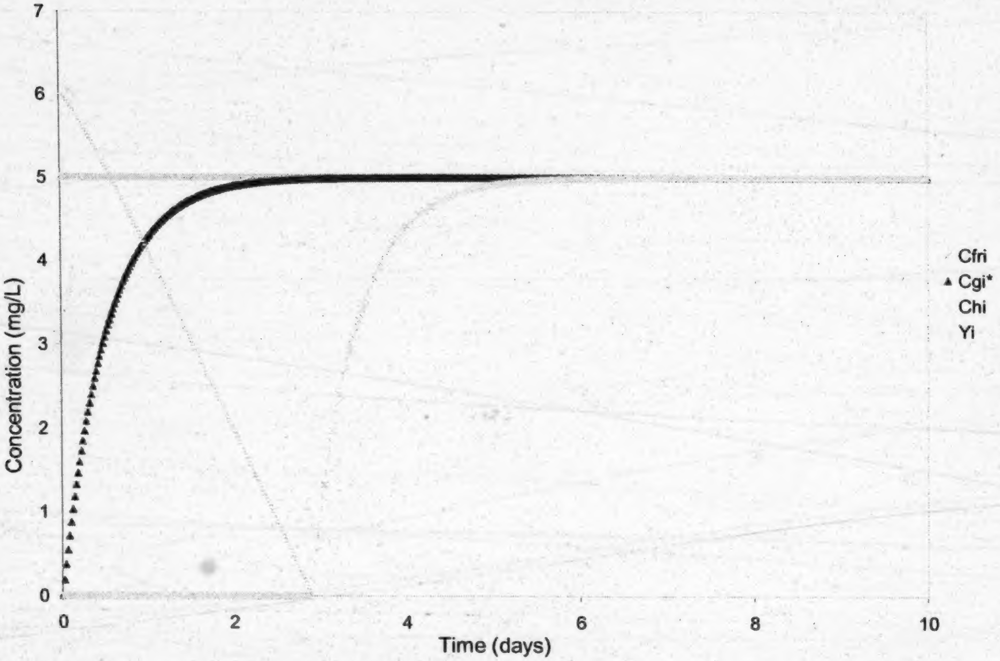

Figure A1.19 Analytical diffusion profile for constant 5mg/L iron concentration in a formation with coupled profile for constant 1mg/l of benzene concentration.

APPENDIX A.2 Results of laboratory experiments on the impacts of infill water oxygenation in the samplers

Symbols

C_r	Measured reservoir concentration
C_s	Measured sampler concentration
DeOx	Deoxygenated infill water
FW	Formation water
LW	Laboratory water
M_r	Mass of dissolved compound in the reservoir only ($=C_rV_r$)
M_s	Mass of dissolved compound in the sampler ($= C_sV_s$)
Ox	Oxygenated infill water
R	Reservoir
S	Sampler (If suffix T, M, or B are present, it means top, middle or bottom samplers respectively)
V_r	Volume of reservoir water (= 1.513litres)
V_s	Sampler volume (= 0.450litres)
V	Capacity of the reservoir unit (= 1.963litres)

Table A2.1 Summary of sampler results using laboratory water (LW)

Compound	Benzene				
Sample \ Time	0	3DeOx	3Ox	6DeOx	6Ox
ST (mg/L)	0.00	28.35	26.46	26.85	27.10
SM (mg/L)	0.00	24.92	24.49	25.13	25.41
SB (mg/L)	0.00	23.03	24.47	23.94	24.50
Average	0.00	25.44	25.14	25.31	25.67
Std. Deviation		2.70	1.15	1.46	1.32
Coeff. of Variance		10.60%	4.55%	5.78%	5.15%
Compound	Toulene				
Sample \ Time	0	3DeOx	3Ox	6DeOx	6Ox
ST (mg/L)	0.00	18.11	16.97	16.62	16.75
SM (mg/L)	0.00	16.01	15.98	16.15	16.21
SB (mg/L)	0.00	14.78	15.95	15.41	15.80
Average	0.00	16.30	16.30	16.06	16.25
Std. Deviation		1.68	0.58	0.61	0.48
Coeff. of Variance		10.33%	3.56%	3.81%	2.95%
Compound	Ethylbenzene				
Sample \ Time	0	3DeOx	3Ox	6DeOx	6Ox
ST (mg/L)	0.00	12.98	12.20	11.51	11.53
SM (mg/L)	0.00	11.62	11.74	11.81	11.67
SB (mg/L)	0.00	10.74	11.73	11.27	11.41
Average	0.00	11.78	11.89	11.53	11.54
Std. Deviation		1.13	0.27	0.27	0.13
Coeff. of Variance		9.56%	2.26%	2.35%	1.14%
Compound	M&p Xylene				
Sample \ Time	0	3DeOx	3Ox	6DeOx	6Ox
ST (mg/L)	0.00	7.44	7.01	6.67	6.64
SM (mg/L)	0.00	6.71	6.67	6.81	6.73
SB (mg/L)	0.00	6.25	6.68	6.53	6.59
Average	0.00	6.80	6.78	6.67	6.65
Std. Deviation		0.60	0.19	0.14	0.07
Coeff. of Variance		8.85%	2.85%	2.14%	1.04%
Compound	o-Xylene				
Sample \ Time	0	3DeOx	3Ox	6DeOx	6Ox
ST (mg/L)	0.00	3.25	3.07	2.96	2.94
SM (mg/L)	0.00	2.94	2.97	2.99	2.96
SB (mg/L)	0.00	2.75	2.97	2.87	2.90
Average	0.00	2.98	3.00	2.94	2.93
Std. Deviation		0.25	0.06	0.06	0.03
Coeff. of Variance		8.48%	2.01%	2.17%	1.18%

Table A2.2 Summary of experimental data using laboratory water (LW)

Summary of measured concentration				
Time (days)-ID	3-DeOx	3-Ox	6-DeOx	6-Ox
Compound	Average of measured concentrations (mg/l)			
R-Benzene (mg/L)	28.02	28.21	29.16	26.78
S-Benzene (mg/L)	25.44	25.14	25.31	25.67
R-Toluene (mg/L)	16.17	16.47	16.72	15.10
S-Toluene (mg/L)	16.30	16.30	16.06	16.25
R-EthylBenzene (mg/L)	10.03	10.54	10.06	9.05
S-Ethylbenzene (mg/L)	11.78	11.89	11.53	11.54
R-m&p Xylene (mg/L)	5.87	6.13	5.87	5.33
S-m&p Xylene (mg/L)	8.97	9.30	9.05	8.26
R-o Xylene (mg/L)	2.67	2.77	2.69	2.46
S-o Xylene (mg/L)	2.98	3.00	2.94	2.93
Total mass summary of the BTEX compounds				
Compound	Mass = CV (i.e. $M_r = C_rV_r$, $M_s = C_sV_s$)			
R-Benzene (mg)	42.39	42.68	44.12	40.51
S-Benzene (mg)	11.45	11.31	11.39	11.55
R-Toluene (mg)	24.47	24.91	25.30	22.85
S-Toluene (mg)	7.33	7.33	7.23	7.31
R-EthylBenzene (mg)	15.17	15.94	15.22	13.70
S-Ethylbenzene (mg)	5.30	5.35	5.19	5.19
R-m&p Xylene (mg)	8.89	9.27	8.88	8.06
S-m&p Xylene (mg)	3.06	3.05	3.00	2.99
R-o Xylene (mg)	4.04	4.18	4.07	3.72
S-o Xylene (mg)	1.34	1.35	1.32	1.32
Sum of total mass	123.43	125.39	125.73	117.21

Table A2.3 Summary of sampler results using formation water (FW)

Compound	Benzene				
Sample \ Time	0	5-DeOx	5-Ox	10-DeOx	10-Ox
ST (mg/L)	0.00	28.82	28.25	27.57	28.71
SM (mg/L)	0.00	24.65	26.97	26.17	27.81
SB (mg/L)	0.00	24.27	25.89	26.53	26.40
Average	0.00	25.92	27.04	26.76	27.64
Std. Deviation		2.53	1.18	0.73	1.16
Coeff. of Variance		9.75%	4.35%	2.71%	4.21%
Compound	**Toluene**				
Sample \ Time	0	5-DeOx	5-Ox	10-DeOx	10-Ox
ST (mg/L)	0.00	19.75	18.87	18.37	18.66
SM (mg/L)	0.00	17.43	19.20	18.45	19.61
SB (mg/L)	0.00	17.20	18.50	18.91	18.70
Average	0.00	18.13	18.85	18.58	18.99
Std. Deviation		1.41	0.35	0.29	0.54
Coeff. of Variance		7.78%	1.84%	1.55%	2.82%
Compound	**Ethylbenzene**				
Sample \ Time	0	5-DeOx	5-Ox	10-DeOx	10-Ox
ST (mg/L)	0.00	14.12	12.89	12.45	11.72
SM (mg/L)	0.00	12.96	14.28	13.51	14.03
SB (mg/L)	0.00	12.77	13.81	13.86	13.44
Average	0.00	13.28	13.66	13.27	13.06
Std. Deviation		0.73	0.71	0.73	1.20
Coeff. of Variance		5.49%	5.17%	5.52%	9.15%
Compound	**M&p Xylene**				
Sample \ Time	0	5-DeOx	5-Ox	10-DeOx	10-Ox
ST (mg/L)	0.00	8.04	7.55	7.19	6.89
SM (mg/L)	0.00	7.50	8.26	7.74	8.08
SB (mg/L)	0.00	7.39	8.02	7.93	7.77
Average	0.00	7.64	7.94	7.62	7.58
Std. Deviation		0.35	0.36	0.39	0.62
Coeff. of Variance		4.54%	4.58%	5.10%	8.16%
Compound	**o-Xylene**				
Sample \ Time	0	5-DeOx	5-Ox	10-DeOx	10-Ox
ST (mg/L)	0.00	3.43	3.23	3.09	3.00
SM (mg/L)	0.00	3.17	3.45	3.27	3.41
SB (mg/L)	0.00	3.13	3.40	3.33	3.29
Average	0.00	3.24	3.36	3.23	3.24
Std. Deviation		0.16	0.12	0.12	0.21
Coeff. of Variance		5.05%	3.55%	3.78%	6.48%

Table A2.4 Summary of experimental data using formation water (LW)

Summary of measured concentration				
Time (days)-ID	5-DeOx	5-Ox	10-DeOx	10-Ox
Compound	Average of measured concentrations (mg/l)			
R-Benzene (mg/L)	32.16	29.89	29.71	28.94
S-Benzene (mg/L)	25.92	27.04	26.76	27.64
R-Toluene (mg/L)	20.69	18.44	17.86	17.66
S-Toluene (mg/L)	18.13	18.85	18.58	18.99
R-EthylBenzene (mg/L)	12.74	8.54	9.77	9.21
S-Ethylbenzene (mg/L)	13.28	13.66	13.27	13.06
R-m&p Xylene (mg/L)	7.40	6.53	5.84	5.97
S-m&p Xylene (mg/L)	10.88	9.75	8.98	9.04
R-o Xylene (mg/L)	3.24	2.90	2.67	2.69
S-o Xylene (mg/L)	3.24	3.36	3.23	3.24
Total mass summary of the BTEX compounds				
Compound	Mass = CV (i.e. $M_r = C_rV_r$, $M_s = C_sV_s$)			
R-Benzene (mg)	48.66	45.22	44.95	43.78
S-Benzene (mg)	11.66	12.17	12.04	12.44
R-Toluene (mg)	31.31	27.90	27.02	26.73
S-Toluene (mg)	8.16	8.48	8.36	8.54
R-EthylBenzene (mg)	19.28	12.92	14.78	13.93
S-Ethylbenzene (mg)	5.98	6.15	5.97	5.88
R-m&p Xylene (mg)	11.19	9.89	8.83	9.03
S-m&p Xylene (mg)	3.44	3.57	3.43	3.41
R-o Xylene (mg)	4.90	4.39	4.04	4.07
S-o Xylene (mg)	1.46	1.51	1.45	1.46
Sum of total mass	146.03	132.19	130.88	129.27

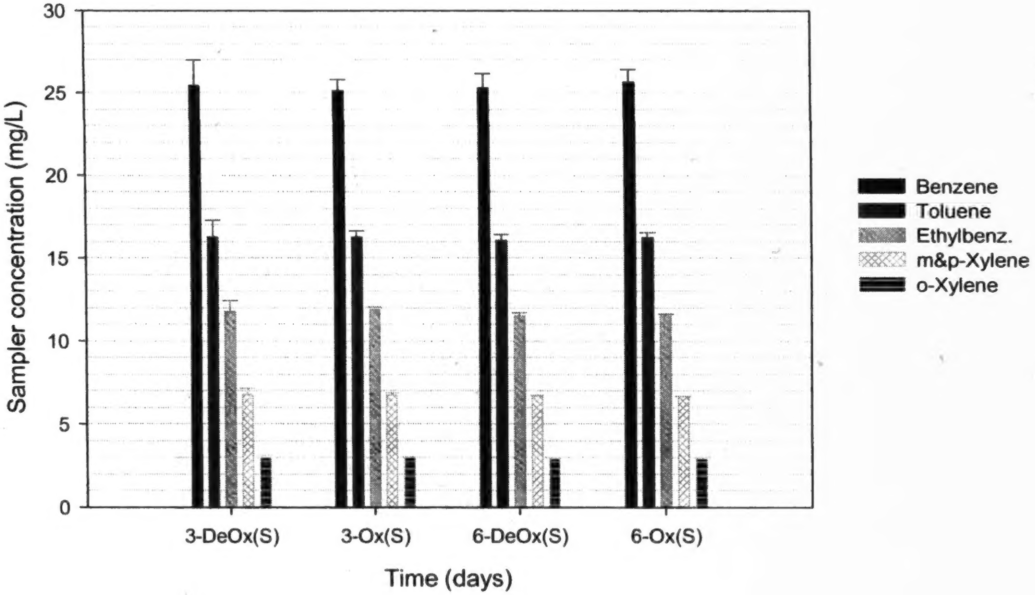

Figure A2.1 Equilibrium concentration using laboratory water.

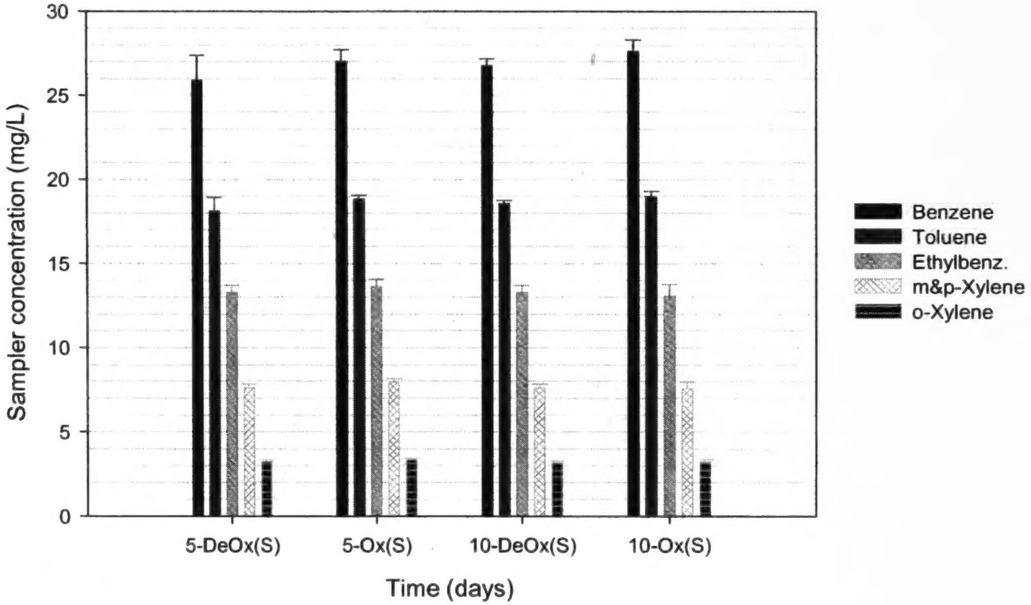

Figure A2.2 Equilibrium concentration using field formation water.

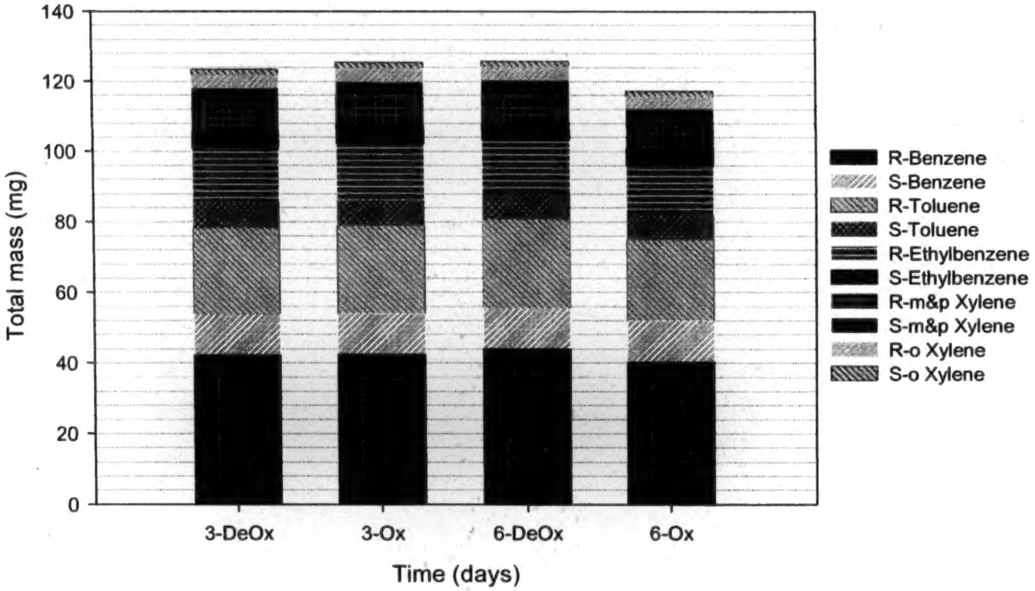

Figure A2.3 BTEX mass balance comparison for experimental run using laboratory water.

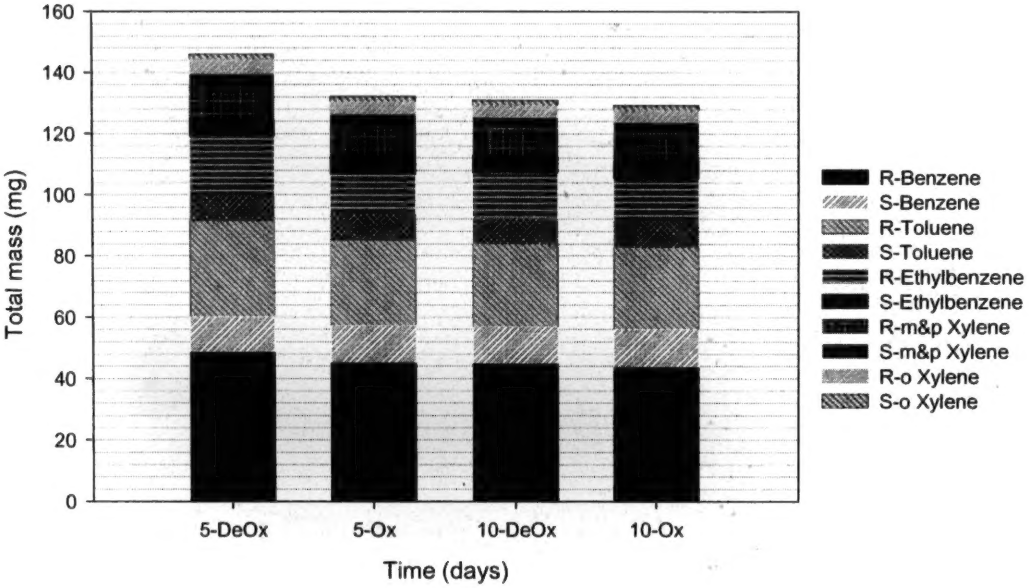

Figure A2.4 BTEX mass balance comparison for experimental run using formation water.

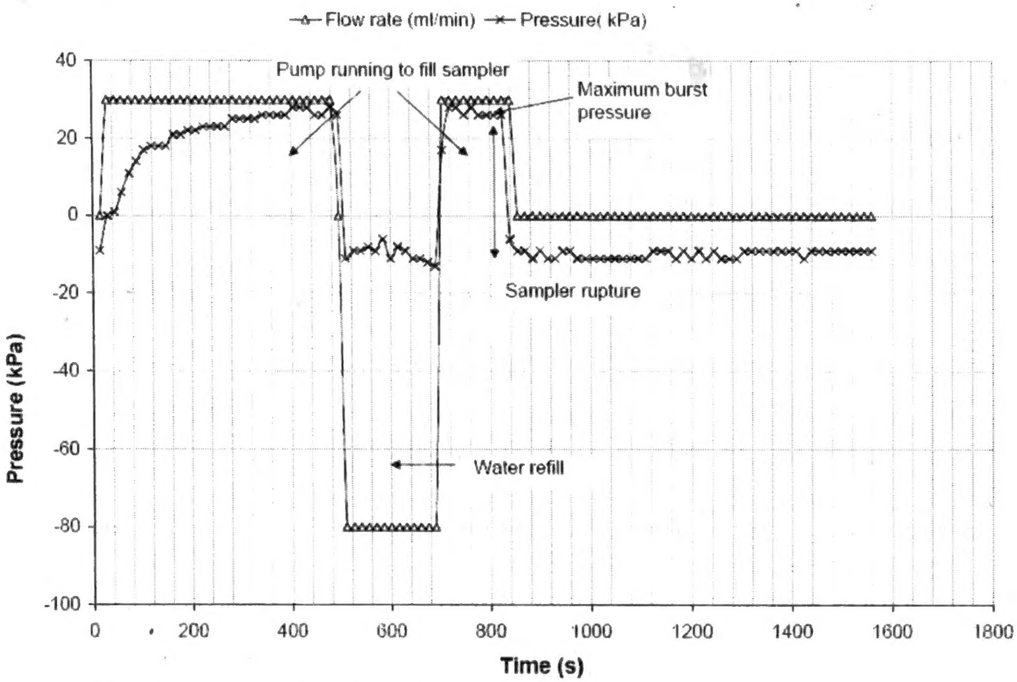

Figure A2.5 Typical pressure test response for the dialysis samplers.

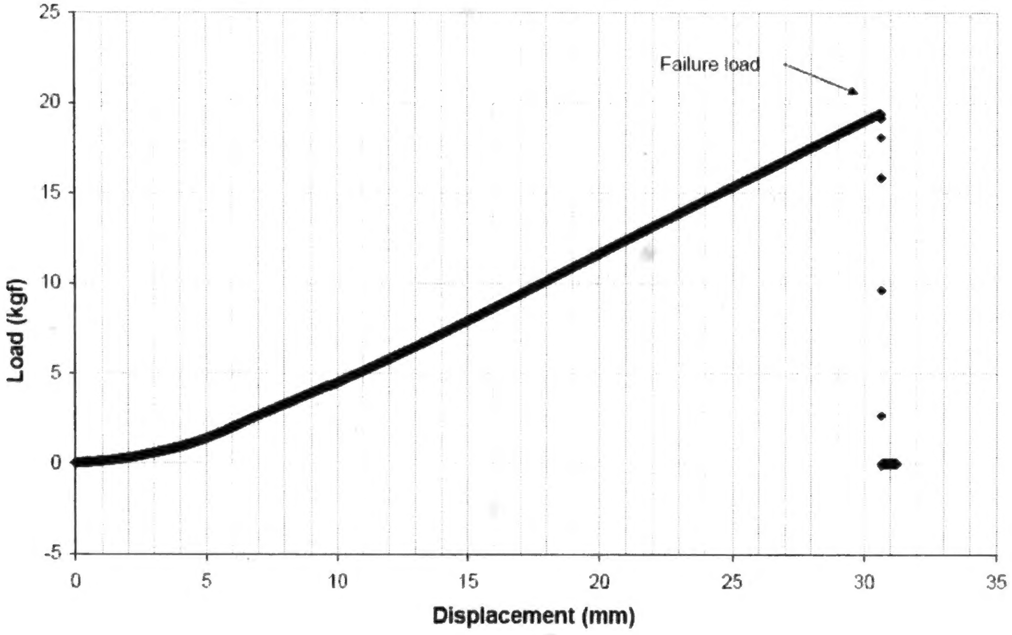

Figure A2.6 Typical grab-tensile strength results on the dialysis membrane.

APPENDIX A.3 *Sorption Batch test results for dialysis membrane analyzed based on Langmuir adsorption isotherm*

Equation:

$$C_s = \frac{\alpha \beta_{\max}}{1 + \alpha C} C$$

C_s	Adsorbed concentration ratio (mg/g/cm^2)
β_{max}	Maximum C_s concentration (i.e. site limited sorption)
C	Equilibrium concentration (mg/l)
α	Constant

Table A3.1 Summary of Parameters for BTEX compounds using SIGMAPLOT 8.0[9]

Compound	β (mg/g/cm^2)	α	R^2
Benzene	0.0014	0.6005	0.7622
Toluene	0.0017	0.4690	0.8461
Ethylbenzene	0.0018	0.5467	0.8355
M & P Xylene	0.0032	0.3661	0.8057
O Xylene	0.0015	0.6376	0.8579

---

[9] SigmaPlot 2002 for Windows Version 8.02 by SPSS Inc

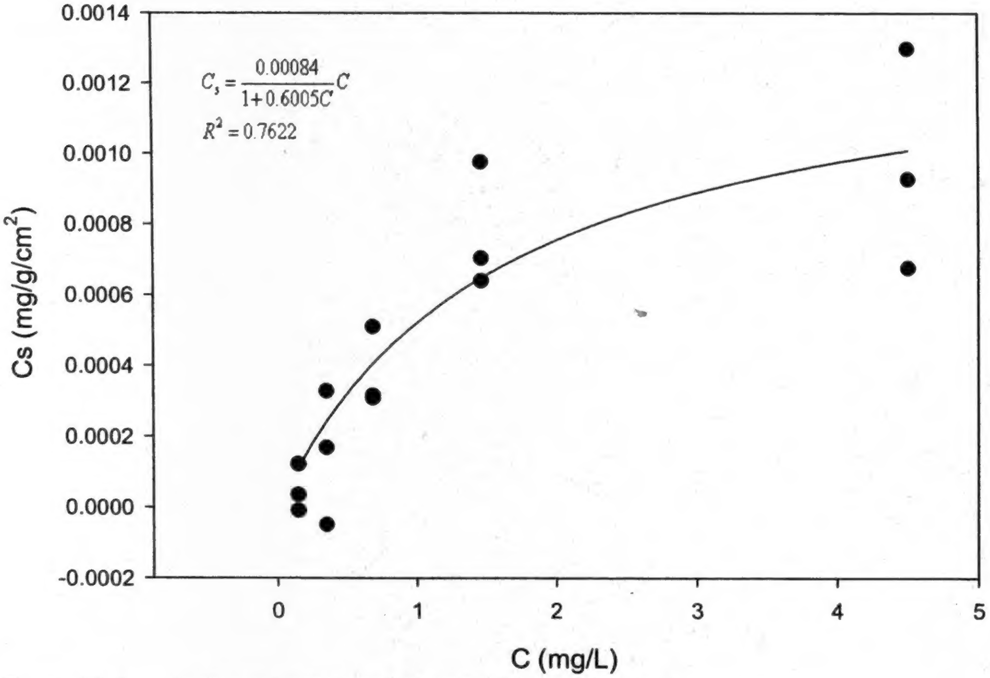

Figure A3.1 Isotherm for benzene with dialysis membrane

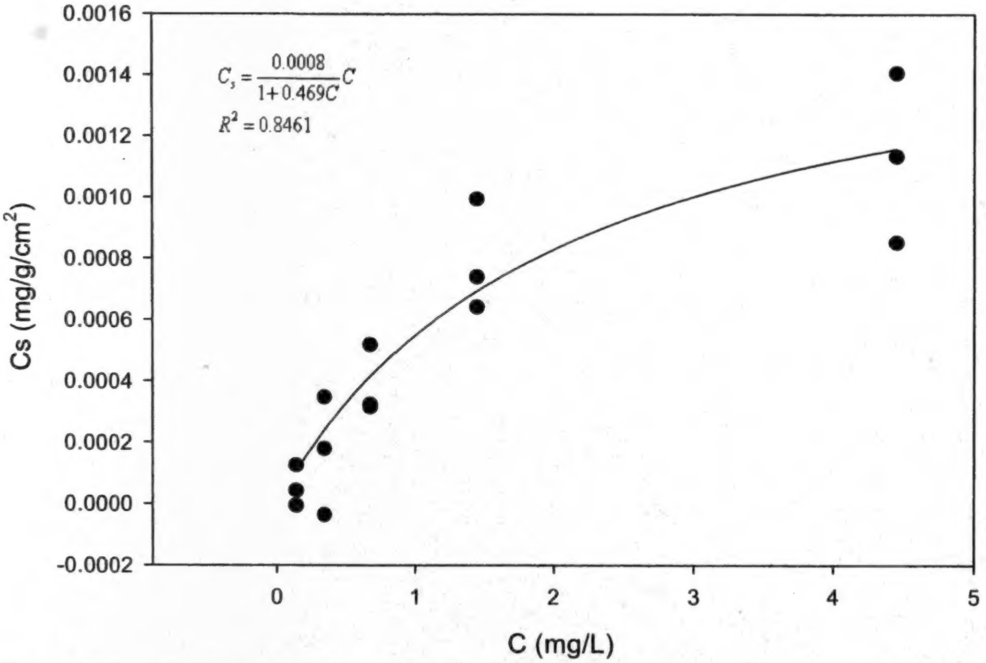

Figure A3.2 Isotherm for Toluene with dialysis membrane

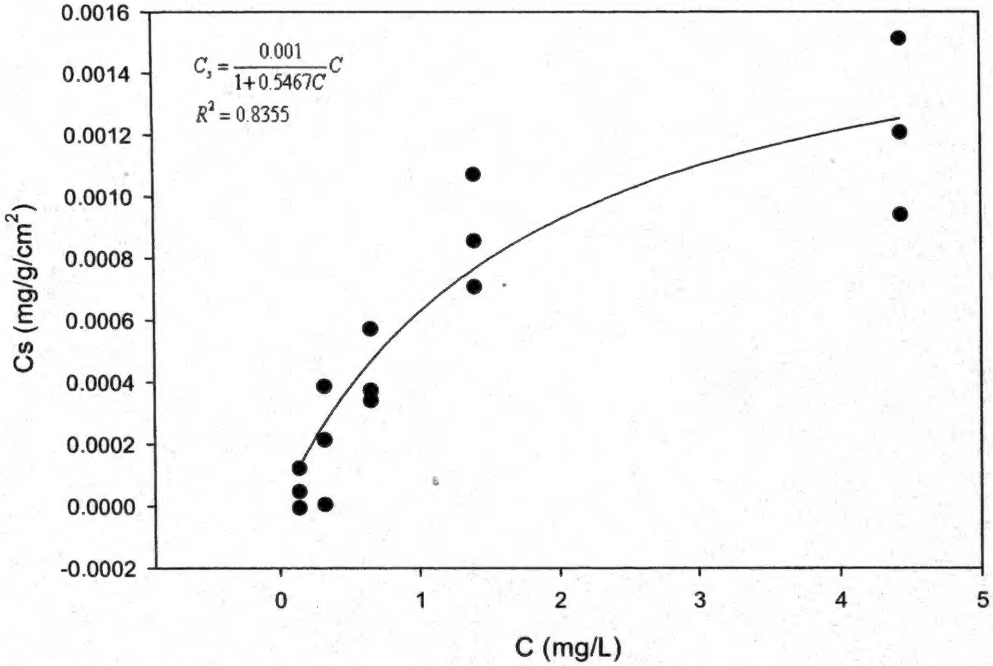

Figure A3.3 Isotherm for Ethylbenzene with dialysis sampler

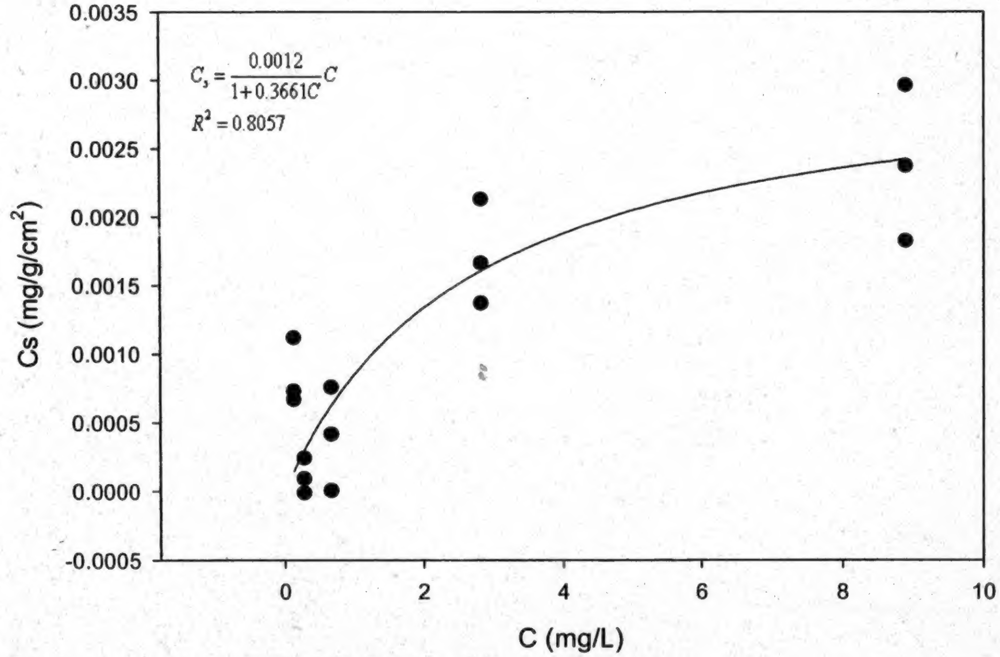

Figure A3.4 Isotherm for M & P Xylene with dialysis sampler

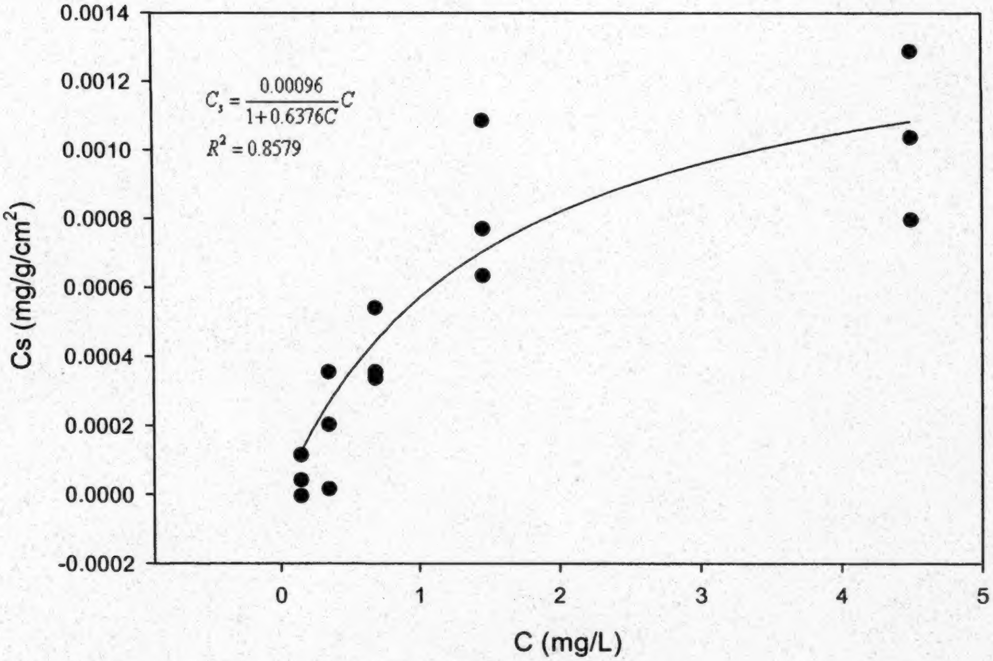

Figure A3.5 Isotherm for O - Xylene with dialysis sampler

APPENDIX A.4 Analyses of BTEX Data

A statistical student-t test was performed on the measured BTEX results from the laboratory experiment to determine if the difference in the means of the data obtained for both deoxygenated (D_eO_x) and O_x systems with time were significant. The dilution equation for the experiment assuming no degradation is given below:

$$C_iV = C_sV_s + C_rV_r$$

Where,

C_i	Measured initial concentration in the reservoir (mg/L)
C_s	Measured sampler concentration after "N" days
C_r	Measured reservoir concentration after "N" days
V_s	Volume of samplers in each reservoir (150*3 = 450mL)
V_r	Volume of each reservoir excluding sampler (1513mL)
$V = V_s + V_r$	Volume of reservoir including samplers (1513+450 = 1913mL)
$C_{ip} = \frac{C_sV}{V_r}$	Projected initial concentration

Since each concentration values in the equation above was measured at each time step, there should be no significant difference between the sampler concentrations in the D_eO_x and that in the O_x system (i.e. Cs-ND_eO_x ≈ Cs-NO_x) if they have the same population variance, but significant if they are not of the same population variance in statistical terms. At equilibrium, the measured sampler concentration "C_s" should be equal to the equilibrium concentration "C_{eq}" (i.e. $C_s = C_{eq}$), and the measured reservoir concentration "C_r" should also be equal to that of the sampler (i.e. $C_r = C_s$). If there is no mass loss in the system, the measured initial concentration "C_i" should be equal to the projected initial concentration "C_{ip}" (i.e. $C_i = C_{ip}$). Therefore, given the above sets of conditions, student t-test was used to test if there is a significant difference in the mean values obtained for each set of measured concentration values given in Table A4.1 and A4.2. The tested conditions are summarized in Table A4.3.

Student t-test

The student t-test is used to evaluate the null hypothesis whether the difference of the mean values between two data sets are significant or not. Two types of t-tests are used, which are: Paired and Unpaired t-tests. Paired t-test is used when the number of samples (n) for each of the two sets under consideration is equal (i.e. $n_1 = n_2$, where the subscripts 1 and 2 stands for data set 1 $\{x_1, x_2, \ldots. x_{n_1}\}$ and data set 2 $\{y_1, y_2, \ldots y_{n_2}\}$). The unpaired t-test is used when the number of samples for each set is different (i.e. $n_1 \neq n_2$).

Depending on the nature of the problem, two-sided or one-sided t-test can be performed. A two-sided test is used when consideration is given to the absolute difference in the mean values, it does not matter whether the mean value of one is greater or smaller than the other. However, a one-sided test is used when consideration is given to the mean difference in a particular direction only. The two-sided test is used for the data analyses in this report because the objective is to test whether the difference of the mean is significant or not.

The unpaired t-test is adopted for these analyses for consistency because the numbers of samples in some of the experimental data sets compared are not equal.

Nevertheless, a concise summary of t-tests and the equations used for the calculation of t-values for each data set are presented below:

Paired t-Test

$$t = \frac{\overline{D}}{S_D}$$

Where,

$$\overline{D} = \overline{x} - \overline{y}$$

and

$$S_{\overline{D}} = \sqrt{\frac{\sum_1^n D_i^2 - \frac{\left(\sum_1^n D_i\right)^2}{n}}{n(n-1)}}$$

$$D_i = x_i - y_i$$

The degree of freedom for paired data is given by:

$$D_f = n - 1$$

Unpaired t-Test

$$t = \frac{\overline{D}}{\sqrt{\frac{1}{n_1} + \frac{1}{n_2}} \sqrt{\frac{\sum_1^{n_1} x_i^2 - n_1 \overline{x}^2 + \sum_1^{n_2} y_i^2 - n_2 \overline{y}^2}{n_1 + n_2 - 2}}}$$

Where,

$$\overline{x} = \frac{\sum_1^{n_1} x_i}{n_1}$$

$$\overline{y} = \frac{\sum_1^{n_2} y_1}{n_2}$$

The degree of freedom for unpaired data is given by:

$$D_f = n_1 + n_2 - 1$$

The equations used for estimating the probability that difference of the mean occur by chance and not real cause at the calculated t-values is given by:

$$P(t) = 2\left(0.5 - \frac{1}{\sqrt{2\pi}} \int_0^t e^{-t^2/2} dt\right) = 1 - Erf\left(\frac{t}{\sqrt{2}}\right)$$

The calculated probability is then compared to the significant level "α" of interest as shown below:

If $P(t) < \alpha$, the null hypothesis is rejected, meaning the difference between the two data sets of interest is significant due to real causes and not by chance. Otherwise, when $P(t) \geq \alpha$, the null hypothesis is rejected, meaning the difference between the two data sets is not significant at that level of significance, and may be due to chance rather than real causes.

The analytical solution to the probability equation above is not usually given but the tabulated estimated solution using numerical methods are mostly employed. When performing the t-test using tables, the calculated t-value is compared with tabulated t-value (TableA4.4) corresponding to the specific level of significance "α" of interest at the calculated degree of freedom for the data sets (i.e. if $t_{calculated} > t_{tabulated}$, the null hypothesis is rejected and if $t_{calculated} \leq t_{tabulated}$, the null hypothesis is accepted).

Sample Calculation

From Table A4.1, sample calculations for t-test on benzene ($Cs\text{-}3D_eO_x$ vs. $Cs\text{-}3O_x$) are given below:

Sample calculation for benzene concentration in sampler

S/N	Cs-3D$_e$O$_x$	Cs-3O$_x$	Conditions	
n$_i$	x	y	x^2	y^2
1	26.9130	27.0497	724.3096	731.6863
2	30.9194	26.1797	956.0093	685.3767
3	27.2194	26.1592	740.8957	684.3037
4	24.9682	25.3799	623.4110	644.1393
5	24.8867	24.3344	619.3478	592.1630
6	24.9152	23.7535	620.7672	564.2288
7	23.1356	25.0361	535.2560	626.8063
8	23.3735	24.4819	546.3205	599.3634
9	22.5870	23.8926	510.1726	570.8563
$\sum_1^n$	228.9180	226.2670	5876.4897	5698.9239

$$\bar{x} = \frac{228.9180}{9} = 25.4353$$

$$\bar{y} = \frac{226.2670}{9} = 25.1408$$

$$\bar{D} = \bar{x} - \bar{y} = 25.4353 - 25.1408 = 0.2945$$

$$t = \frac{\bar{D}}{\sqrt{\frac{1}{n_1}+\frac{1}{n_2}}\sqrt{\frac{\sum_1^{n_1} x_i^2 - n_1\bar{x}^2 + \sum_1^{n_2} y_i^2 - n_2\bar{y}^2}{n_1+n_2-2}}} = \frac{0.2945}{\sqrt{\frac{1}{9}+\frac{1}{9}}\sqrt{\frac{5876.49 - 9\times 25.44 + 5698.92 - 9\times 25.14}{9+9-2}}}$$

$$= \frac{0.2945}{0.4714\times 2.004} = 0.31174$$

$$P(t) = 1 - Erf\left(\frac{t}{\sqrt{2}}\right) = 1 - Erf\left(\frac{0.31174}{\sqrt{2}}\right) \approx 0.76$$

Using 5% significant level, $P(t) > \alpha$ (i.e. 0.76>0.05), therefore, the null hypothesis is accepted; meaning the difference in the observed means is due to chance and not real causes. Alternatively, from TableA4.4, the tabulated t-value at 5% level of significance corresponding to D_f of 16 is 2.120. Since this value is greater than the calculated value, the null hypothesis is accepted.

Results and Discussion

The results of the t-test analyses are given in Table A4.5 and A4.6 respectively. SIGMAPLOT software was used for the t-test analysis. The results showed that there is no significant difference in using deoxygenated to oxygenated infill water for the dialysis samplers. There are no significant differences at each time step for the samplers as well, indicating equilibration occurred in about three days. A comparison of the measured initial reservoir concentration with the projected values showed the difference is significant due to real causes and not by chance. The real cause of this difference may be volatilization of the BTEX compounds during sampling. It should be recalled that the initial reservoir was sampled using glass syringe at the valve outlet; the siphoned water at this outlet is not under full flow due to low infill rate (13mL/min) of the reservoir.

Comparison of the measured sampler concentration with that of the reservoir at each sampling interval showed varied results. Benzene and toluene tend to fall within the same population variance but ethylene and Xylene differences are consistently significant. These observed differences may also be attributed to the way the reservoir samples were taken. After each sampling interval, the lid of each reservoir column was removed and there is interaction between air and water at the top of the reservoir where the samples were taken. The dimensionless Henry constant for toluene, ethylbenzene and Xylene are higher than that of benzene, which may account for rapid volatilizations of these compounds. Buoyancy of these compounds may also play a role in the observed differences.

Conclusions

In conclusion, no significant difference was observed in using deoxygenated water over oxygenated infill water for the dialysis samplers at the concentrations tested, and equilibration at the tested concentrations occurred in three days, which is welcoming news for the use of the dialysis samplers in practice. The laboratory reservoir system will have to be optimized to be able to accurately sample initial concentration in the reservoir, its concentration at each time step, and at lower concentration.

Table A4.1 Experimental data using laboratory water

Time	Compound	Ci (mg/L)	Cs (mg/L)	Cr (mg/L)	Cip (mg/L)	Time	Compound	Ci (mg/L)	Cs (mg/L)	Cr (mg/L)	Cip (mg/L)
3 - DeOx	Benzene	23.10	26.91	28.53	34.92	6 - DeOx	Benzene	23.10	26.86	28.85	34.85
		24.17	30.92	27.60	40.12			24.17	27.32	29.69	35.45
		26.00	27.22	27.88	35.32			26.00	26.37	28.92	34.22
		27.51	24.97		32.39			27.51	24.96		32.38
		28.94	24.89		32.29			28.94	25.33		32.86
		28.15	24.92		32.33			28.15	25.09		32.56
		24.42	23.14		30.02			24.42	24.09		31.26
		29.32	23.37		30.33			29.32	24.12		31.30
			22.59		29.30				23.61		30.64
	Tolune	14.19	17.00	16.54	22.06		Tolune	14.19	16.52	16.64	21.43
		14.92	19.99	15.92	25.94			14.92	17.00	16.96	22.05
		15.91	17.32	16.05	22.48			15.91	16.36	16.56	21.22
		16.90	16.02		20.78			16.90	16.02		20.78
		17.91	15.98		20.73			17.91	16.33		21.18
		17.27	16.03		20.79			17.27	16.09		20.88
		11.59	14.84		19.25			11.59	15.50		20.11
		17.86	15.02		19.49			17.86	15.53		20.15
			14.47		18.78				15.19		19.71
	Ethylbenzene	9.39	12.15	10.31	15.76		Ethylbenzene	9.39	11.34	10.10	14.71
		10.74	14.30	9.89	18.55			10.74	11.77	10.17	15.26
		11.36	12.48	9.88	16.19			11.36	11.42	9.91	14.82
		11.85	11.63		15.08			11.85	11.71		15.20
		12.95	11.60		15.05			12.95	11.96		15.51
		12.27	11.62		15.08			12.27	11.77		15.27
		6.29	10.76		13.97			6.29	11.33		14.70
		11.15	10.94		14.19			11.15	11.37		14.75
			10.52		13.65				11.12		14.43
	m&p xylene	5.94	7.01	6.02	9.09		m&p xylene	5.94	6.58	5.87	8.54
		6.24	8.14	5.80	10.56			6.24	6.80	5.93	8.82
		6.55	7.18	5.80	9.31			6.55	6.62	5.79	8.58
		6.91	6.72		8.72			6.91	6.76		8.77
		7.32	6.70		8.70			7.32	6.89		8.94
		7.07	6.71		8.71			7.07	6.79		8.81
		4.16	6.26		8.12			4.16	6.56		8.51
		7.26	6.35		8.24			7.26	6.58		8.53
			6.13		7.96				6.45		8.37
	o-xylene	2.77	3.08	2.73	3.99		o-xylene	2.77	2.93	2.69	3.80
		2.89	3.53	2.62	4.58			2.89	3.01	2.73	3.91
		2.97	3.13	2.65	4.06			2.97	2.94	2.65	3.81
		3.12	2.94		3.82			3.12	2.97		3.85
		3.22	2.94		3.81			3.22	3.01		3.91
		3.14	2.94		3.81			3.14	2.98		3.87
		2.21	2.75		3.57			2.21	2.88		3.73
		3.22	2.79		3.62			3.22	2.89		3.74
			2.70		3.50				2.83		3.67

Legend

Ci	Measured initial concentration in the reservoir (mg/L)
C_{ip}	Projected initial concentration from the measured sampler concentration
C_r	Measured concentration in the reservoir after "N" days
C_s	Measured sampler concentration after "N" days
D_eO_x	Deoxygenated sampler/reservoir system
O_x	Oxygenated sampler/reservoir system

Table A4.1 Experimental data using laboratory water (contd)

Time	Compound	Ci (mg/L)	Cs (mg/L)	Cr (mg/L)	Cip (mg/L)	Time	Compound	Ci (mg/L)	Cs (mg/L)	Cr (mg/L)	Cip (mg/L)
3 - Ox	Benzene	23.10	27.05	27.72	35.09	6 - Ox	Benzene	23.10	27.59	26.03	35.79
		24.17	26.18	28.77	33.97			24.17	26.62	26.86	34.54
		26.00	26.16	28.12	33.94			26.00	27.10	27.42	35.16
		27.51	25.38		32.93			27.51	25.61		33.22
		28.94	24.33		31.57			28.94	25.52		33.11
		28.15	23.75		30.82			28.15	25.10		32.57
		24.42	25.04		32.48			24.42	24.38		31.64
		29.32	24.48		31.76			29.32	27.32		35.45
			23.89		31.00				21.78		28.25
	Tolune	14.19	17.28	16.13	22.42		Tolune	14.19	17.03	14.46	22.10
		14.92	16.81	16.77	21.81			14.92	16.43	14.94	21.32
		15.91	16.81	16.49	21.81			15.91	16.79	15.89	21.79
		16.90	16.51		21.42			16.90	16.30		21.15
		17.91	15.87		20.59			17.91	16.30		21.14
		17.27	15.55		20.17			17.27	16.04		20.80
		11.59	16.32		21.18			11.59	15.61		20.25
		17.86	15.95		20.69			17.86	17.86		23.17
			15.59		20.22				13.92		18.06
	Ethylbenzene	9.39	12.38	10.31	16.06		Ethylbenzene	9.39	11.67	8.74	15.14
		10.74	12.11	10.70	15.71			10.74	11.33	8.74	14.69
		11.36	12.12	10.59	15.72			11.36	11.60	9.98	15.05
		11.85	12.09		15.69			11.85	11.70		15.18
		12.95	11.68		15.16			12.95	11.75		15.24
		12.27	11.46		14.86			12.27	11.58		15.02
		6.29	11.98		15.54			6.29	11.26		14.61
		11.15	11.73		15.22			11.15	12.91		16.75
			11.48		14.89				10.06		13.05
	m&p xylene	5.94	7.10	6.01	9.21		m&p xylene	5.94	6.72	5.00	8.72
		6.24	6.96	6.20	9.03			6.24	6.54	5.16	8.48
		6.55	6.96	6.15	9.04			6.55	6.68	5.82	8.66
		6.91	6.95		9.02			6.91	6.74		8.74
		7.32	6.74		8.75			7.32	6.77		8.78
		7.07	6.31		8.19			7.07	6.68		8.66
		4.16	6.90		8.95			4.16	6.51		8.44
		7.26	6.77		8.78			7.26	7.39		9.58
			6.37		8.26				5.87		7.62
	o-xylene	2.77	3.11	2.72	4.04		o-xylene	2.77	2.97	2.33	3.86
		2.89	3.05	2.80	3.96			2.89	2.90	2.40	3.77
		2.97	3.05	2.77	3.96			2.97	2.95	2.64	3.83
		3.12	3.04		3.95			3.12	2.97		3.85
		3.22	2.95		3.83			3.22	2.98		3.87
		3.14	2.91		3.78			3.14	2.94		3.81
		2.21	3.02		3.92			2.21	2.87		3.73
		3.22	2.97		3.85			3.22	3.21		4.17
			2.92		3.78				2.60		3.38

Legend

C_i	Measured initial concentration in the reservoir (mg/L)
C_{ip}	Projected initial concentration from the measured sampler concentration
C_r	Measured concentration in the reservoir after "N" days
C_s	Measured sampler concentration after "N" days
D_eO_x	Deoxygenated sampler/reservoir system
O_x	Oxygenated sampler/reservoir system

Table A4.2 Experimental data using formation water

Time	Compound	Ci (mg/L)	Cs (mg/L)	Cr (mg/L)	Cip (mg/L)	Time	Compound	Ci (mg/L)	Cs (mg/L)	Cr (mg/L)	Cip (mg/L)
5 - DeOx	Benzene	30.08	28.14	28.53	36.51	10 - DeOx	Benzene	30.08	27.61	28.49	35.82
		30.54	27.96	27.60	36.28			30.54	27.12	28.86	35.19
		28.30	30.37	27.88	39.40			28.30	27.99	31.75	36.31
		28.82	25.05		32.50			28.82	26.41		34.26
		30.37	24.81		32.19			30.37	26.21		34.01
		32.53	24.11		31.28			32.53	25.90		33.60
		30.88	24.74		32.09			30.88	26.21		34.01
		31.20	24.19		31.39			31.20	25.70		33.34
			23.87		30.97				27.69		35.93
	Toluene	20.46	19.16	19.92	24.86		Toluene	20.46	18.30	16.88	23.74
		20.81	19.19	19.12	24.90			20.81	18.05	17.27	23.41
		19.36	20.90	23.01	27.11			19.36	18.77	19.41	24.35
		19.64	17.69		22.95			19.64	18.59		24.12
		20.46	17.52		22.73			20.46	18.48		23.98
		22.32	17.09		22.17			22.32	18.28		23.72
		21.04	17.54		22.75			21.04	18.58		24.10
		21.18	17.17		22.27			21.18	18.13		23.53
			16.89		21.91				20.01		25.96
	Ethylbenzene	15.61	13.62	12.33	17.67		Ethylbenzene	15.61	12.32	8.99	15.98
		15.91	13.78	11.77	17.88			15.91	12.21	9.56	15.84
		14.94	14.96	14.11	19.40			14.94	12.82	10.74	16.64
		15.10	13.14		17.05			15.10	13.61		17.66
		15.47	13.01		16.89			15.47	13.53		17.56
		16.82	12.73		16.52			16.82	13.40		17.38
		16.18	13.01		16.88			16.18	13.62		17.67
		15.99	12.75		16.54			15.99	13.23		17.16
			12.54		16.27				14.72		19.10
	m&p xylene	8.84	7.85	7.15	10.18		m&p xylene	8.84	7.12	5.48	9.24
		9.00	7.91	6.88	10.26			9.00	7.05	5.66	9.15
		8.51	8.36	8.15	10.84			8.51	7.38	6.36	9.58
		8.59	7.59		9.85			8.59	7.79		10.11
		8.76	7.52		9.76			8.76	7.76		10.07
		9.47	7.38		9.57			9.47	7.69		9.97
		9.06	7.52		9.76			9.06	7.80		10.12
		9.02	7.39		9.58			9.02	7.60		9.86
			7.27		9.43				8.40		10.90
	o-xylene	3.68	3.33	3.14	4.32		o-xylene	3.68	3.07	2.54	3.99
		3.74	3.35	3.02	4.34			3.74	3.05	2.60	3.95
		3.55	3.61	3.54	4.68			3.55	3.16	2.87	4.10
		3.58	3.21		4.16			3.58	3.29		4.27
		3.66	3.18		4.13			3.66	3.27		4.24
		3.91	3.12		4.05			3.91	3.25		4.21
		3.76	3.18		4.12			3.76	3.28		4.26
		3.77	3.12		4.05			3.77	3.21		4.16
			3.08		4.00				3.49		4.53

Legend

C_i	Measured initial concentration in the reservoir (mg/L)
C_{ip}	Projected initial concentration from the measured sampler concentration
C_r	Measured concentration in the reservoir after "N" days
C_s	Measured sampler concentration after "N" days
D_eO_x	Deoxygenated sampler/reservoir system
O_x	Oxygenated sampler/reservoir system

Table A4.2 Experimental data using formation water (contd)

Time	Compound	Ci (mg/L)	Cs (mg/L)	Cr (mg/L)	Cip (mg/L)	Time	Compound	Ci (mg/L)	Cs (mg/L)	Cr (mg/L)	Cip (mg/L)
5- Ox	Benzene	30.08	28.26	28.35	36.66	10 - Ox	Benzene	30.08	28.22	28.29	36.62
		30.54	28.40	32.64	36.85			30.54	28.73	28.97	37.27
		28.30	28.08	28.65	36.43			28.30	29.17	29.53	37.84
		28.82	27.62		35.84			28.82	27.38		35.52
		30.37	26.64		34.57			30.37	28.08		36.43
		32.53	26.63		34.56			32.53	27.98		36.30
		30.88	25.82		33.50			30.88	26.58		34.48
		31.20	25.99		33.72			31.20	26.33		34.16
			25.87		33.56				26.29		34.11
	Toluene	20.46	18.68	17.80	24.23		Toluene	20.46	17.48	16.96	22.68
		20.81	18.86	20.05	24.47			20.81	18.91	17.75	24.53
		19.36	19.06	17.45	24.73			19.36	19.58	18.26	25.41
		19.64	19.66		25.51			19.64	19.33		25.08
		20.46	18.94		24.58			20.46	19.77		25.64
		22.32	18.98		24.63			22.32	19.72		25.59
		21.04	18.44		23.92			21.04	18.82		24.42
		21.18	18.61		24.15			21.18	18.66		24.21
			18.46		23.95				18.63		24.17
	Ethylbenzene	15.61	12.57	5.87	16.31		Ethylbenzene	15.61	10.07	9.76	13.07
		15.91	12.75	10.42	16.55			15.91	12.12	9.76	15.72
		14.94	13.34	9.33	17.31			14.94	12.99	10.22	16.85
		15.10	14.59		18.93			15.10	13.82		17.93
		15.47	14.13		18.33			15.47	14.15		18.35
		16.82	14.11		18.31			16.82	14.11		18.31
		16.18	13.75		17.85			16.18	13.48		17.49
		15.99	13.90		18.04			15.99	13.45		17.45
			13.76		17.86				13.39		17.37
	m&p xylene	8.84	7.36	6.71	9.55		m&p xylene	8.84	5.99	5.63	7.78
		9.00	7.49	6.79	9.71			9.00	7.10	6.02	9.21
		8.51	7.79	6.10	10.11			8.51	7.57	6.24	9.82
		8.59	8.43		10.93			8.59	7.97		10.35
		8.76	8.18		10.62			8.76	8.14		10.57
		9.47	8.18		10.61			9.47	8.12		10.54
		9.06	7.99		10.36			9.06	7.80		10.12
		9.02	8.07		10.47			9.02	7.76		10.07
			7.99		10.37				7.75		10.06
	o-xylene	3.68	3.16	2.93	4.10		o-xylene	3.68	2.69	2.57	3.49
		3.74	3.20	3.02	4.16			3.74	3.08	2.71	4.00
		3.55	3.31	2.74	4.29			3.55	3.24	2.79	4.21
		3.58	3.52		4.56			3.58	3.37		4.37
		3.66	3.42		4.44			3.66	3.44		4.46
		3.91	3.42		4.43			3.91	3.43		4.45
		3.76	3.48		4.52			3.76	3.31		4.29
		3.77	3.38		4.38			3.77	3.29		4.27
			3.35		4.35				3.28		4.26

Legend

C_i	Measured initial concentration in the reservoir (mg/L)
C_{ip}	Projected initial concentration from the measured sampler concentration
C_r	Measured concentration in the reservoir after "N" days
C_s	Measured sampler concentration after "N" days
D_eO_x	Deoxygenated sampler/reservoir system
O_x	Oxygenated sampler/reservoir system

Table A4.3 Conditions tested

1. Conditions tested when laboratory water was used	
Tested Condition	Comment
Cs-3D_eO_x vs. Cs-3O_x	Measured sampler concentration at the end of three days in the D_eO_x and O_x reservoir systems.
Cs-6D_eO_x vs. Cs-6O_x	Measured sampler concentration at the end of six days in the D_eO_x and O_x reservoir systems.
Cs-3D_eO_x vs. Cs-6D_eO_x	Measured sampler concentration at the end of three and six days in the D_eO_x reservoir systems.
Cs-3O_x vs. Cs-6O_x	Measured sampler concentration at the end of three and six days in the O_x reservoir systems.
Cs-3 vs. Cs-6	Measured sampler concentration at the end of three and six days combined for the reservoir systems.
Cs vs. Cr	Measured sampler concentration vs. that in the reservoir at each time step in the reservoir systems
C_i vs. C_{ip}	Measured initial concentration vs. that projected in the reservoir systems.
2. Conditions tested when site (formation) water was used	
Cs-5D_eO_x vs. Cs-5O_x	Measured sampler concentration at the end of five days in the D_eO_x and O_x reservoir systems.
Cs-10D_eO_x vs. Cs-10O_x	Measured sampler concentration at the end of ten days in the D_eO_x and O_x reservoir systems.
Cs-5D_eO_x vs. Cs-10D_eO_x	Measured sampler concentration at the end of five and ten days in the D_eO_x reservoir systems.
Cs-5O_x vs. Cs-10O_x	Measured sampler concentration at the end of five and ten days in the O_x reservoir systems.
Cs-5 vs. Cs-10	Measured sampler concentration at the end of five and ten days combined for the reservoir systems.
Cs vs. Cr	Measured sampler concentration vs. that in the reservoir at each time step in the reservoir systems
C_i vs. C_{ip}	Measured initial concentration vs. that projected in the reservoir systems.

Table A4.4 Statistical table of t-distribution

t-distribution graph

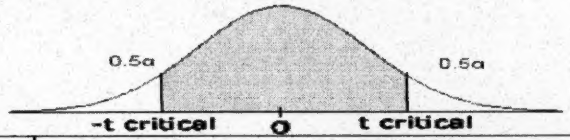

Degree of freedom	Probability α (level of significance)			
D_f	*0.10*	*0.05*	*0.01*	*0.001*
1	6.314	12.706	63.657	636.619
2	2.920	4.303	9.925	31.598
3	2.353	3.182	5.841	12.941
4	2.132	2.176	4.604	8.610
5	2.015	2.571	4.032	6.859
6	1.943	2.447	3.707	5.959
7	1.895	2.365	3.499	5.405
8	1.860	2.306	3.355	5.041
9	1.833	2.262	3.250	4.781
10	1.812	2.228	3.169	4.587
11	1.796	2.201	3.106	4.437
12	1.782	2.179	3.055	4.318
13	1.171	2.160	3.012	4.221
14	1. 761	2.145	2.977	4,140
15	1.753	2.131	2.947	4.073
16	1.746	2.120	2.921	4.015
17	1.740	2.110	2.898	3.965
18	1.734	2.101	2.878	3.922
19	1. 729	2.093	2.861	3.883
20	1. 725	2.086	2.845	3.850
21	1.721	2.080	2.831	3.819
22	1.717	2.074	2.8]9	3.792
23	1.714	2.069	2.807	3.767
24	1.711	2.064	2.797	3.745
25	1.708	2.060	2.787	3.725
26	1.706	2.056	2.779	.1.707
27	1.703	2.052	2.711	3.690
28	1.701	2.048	2. 763	3.674
29	1.699	2.045	2.756	3.659
30	1.697	2.042	2.750	3.646
40	1.684	2.021	2. 704	3.551
60	1.671	2.000	2.660	.1.460
120	1.658	1.980	2.617	*3.313*
?	1.645	1.960	2.576	3.291

This table gives the value of t corresponding to various values of of the probability α (level of significance) of a random variable falling inside the shaded areas in the figure, for a given number of degrees of freedom D_f available for the estimation of error. For one-sided test, the confidence are obtained for α/2.

Table A4.5 T-test results from comparing means of experimental data using laboratory water (assuming 5% level of significance)

Condition		Cs-3DeOx vs Cs-3Ox				Cs-6DeOx vs Cs-6Ox			
	Compound	t	P(t)	D_f	Comment	t	P(t)	D_f	Comment
	Benzene	0.3117	0.7593	16	Accept the null hypothesis	0.4855	0.6339	16	Accept the null hypothesis
	Toluene	0.0031	0.9976	16	Accept	0.4757	0.6407	16	Accept
	Ethylbenz.	0.2876	0.7773	16	Accept	0.0294	0.9769	16	Accept
	m&p Xyl.	0.0699	0.9451	16	Accept	0.1171	0.9082	16	Accept
	o-Xyl.	0.3051	0.7642	16	Accept	0.0601	0.9528	16	Accept
Condition		Cs-3DeOx vs Cs-6DeOx				Cs-3Ox vs Cs-6Ox			
	Compound	t	P(t)	D_f	Comment	t	P(t)	D_f	Comment
	Benzene	0.1326	0.8961	16	Accept the null hypothesis	0.7379	0.4712	16	Accept the null hypothesis
	Toluene	0.4013	0.6935	16	Accept	0.1079	0.9154	16	Accept
	Ethylbenz.	0.6320	0.5363	16	Accept	1.3220	0.2048	16	Accept
	m&p Xyl.	0.6294	0.5380	16	Accept	0.8300	0.4188	16	Accept
	o-Xyl.	0.4500	0.6588	16	Accept	1.2003	0.2475	16	Accept
Condition		Cs-3 vs Cs-6							
	Compound	t	P(t)	D_f	Comment				
	Benzene	0.3409	0.7353	34	Accept the null hypothesis				
	Toluene	0.4017	0.6904	34	Accept				
	Ethylbenz.	1.3041	0.2010	34	Accept				
	m&p Xyl.	1.0343	0.3083	34	Accept				
	o-Xyl.	1.0683	0.2929	34	Accept				
Condition		Cs vs Cr				Ci vs Cip			
Time	Compound	t	P(t)	D_f	Comment	t	P(t)	D_f	Comment
3-DeOx	Benzene	1.6544	0.1291	10	Accept the null hypothesis	6.1564	0.0000	15	Reject the null hypothesis
	Toluene	0.1281	0.9006	10	Accept	6.4368	0.0000	15	Reject
	Ethylbenz.	2.5698	0.0279	10	Reject the null hypothesis	6.1097	0.0000	15	Reject
	m&p Xyl.	2.5506	0.0288	10	Reject	6.3103	0.0000	15	Reject
	o-Xyl.	2.0536	0.0671	10	Accept the null hypothesis	7.4919	0.0000	15	Reject
3-Ox	Benzene	4.3863	0.0014	10	Reject the null hypothesis				
	Toluene	0.4353	0.6726	10	Accept the null hypothesis				
	Ethylbenz.	6.8093	0.0000	10	Reject the null hypothesis				
	m&p Xyl.	3.9770	0.0026	10	Reject				
	o-Xyl.	5.5137	0.0003	10	Reject				
6-DeOx	Benzene	4.8819	0.0006	10	Reject				
	Toluene	1.9092	0.0853	10	Accept the null hypothesis				
	Ethylbenz.	8.7058	0.0000	10	Reject the null hypothesis				
	m&p Xyl.	9.0185	0.0000	10	Reject				
	o-Xyl.	6.3292	0.0001	10	Reject				
6-Ox	Benzene	0.9932	0.3440	10	Accept the null hypothesis				
	Toluene	1.6971	0.1205	10	Accept				
	Ethylbenz.	4.8995	0.0006	10	Reject the null hypothesis				
	m&p Xyl.	4.9896	0.0005	10	Reject				
	o-Xyl.	4.4875	0.0012	10	Reject				

Legend

D_f	Degree of freedom
P(t)	Probability that such a difference may occur by chance and not due to real causes
t	Calculated unpaired T-value

Table A4.6 T-test results from comparing means of experimental data using laboratory water (assuming 5% level of significance)

Condition	Cs-5DeOx vs Cs-5Ox					Cs-10DeOx vs Cs-10Ox			
	Compound	t	P(t)	D_f	Comment	t	P(t)	D_f	Comment
	Benzene	1.3207	0.2052	16	Accept the null hypothesis	1.9453	0.0695	16	Accept the null hypothesis
	Toluene	1.5716	0.1356	16	Accept	1.3327	0.2013	16	Accept
	Ethylbenz.	1.1309	0.2747	16	Accept	0.4239	0.6773	16	Accept
	m&p Xyl.	1.8541	0.0822	16	Accept	0.1536	0.8798	16	Accept
	o-Xyl.	1.7668	0.0963	16	Accept	0.0742	0.9418	16	Accept
Condition	Cs-5DeOx vs Cs-10DeOx					Cs-5Ox vs Cs-10Ox			
	Compound	t	P(t)	D_f	Comment	t	P(t)	D_f	Comment
	Benzene	1.0264	0.3200	16	Accept the null hypothesis	1.2080	0.2446	16	Accept the null hypothesis
	Toluene	0.9241	0.3691	16	Accept	0.4944	0.6278	16	Accept
	Ethylbenz.	0.0255	0.9800	16	Accept	1.2393	0.2331	16	Accept
	m&p Xyl.	0.1269	0.9006	16	Accept	1.4355	0.1704	16	Accept
	o-Xyl.	0.1504	0.8824	16	Accept	1.4269	0.1728	16	Accept
Condition	Cs-5 vs Cs-10								
	Compound	t	P(t)	D_f	Comment				
	Benzene	1.4541	0.1551	34	Accept the null hypothesis				
	Toluene	1.0112	0.3191	34	Accept				
	Ethylbenz.	1.0255	0.3124	34	Accept				
	m&p Xyl.	1.2491	0.2202	34	Accept				
	o-Xyl.	1.1960	0.2400	34	Accept				
Condition	Cs vs Cr					Ci vs Cip			
Time	Compound	t	P(t)	D_f	Comment	t	P(t)	D_f	Comment
5-DeOx	Benzene	1.5086	0.1623	10	Accept the null hypothesis	6.3571	0.0000	15	Reject the null hypothesis
	Toluene	2.5448	0.0291	10	Reject the null hypothesis	9.7322	0.0000	15	Reject
	Ethylbenz.	0.9487	0.3651	10	Accept the null hypothesis	4.7778	0.0002	15	Reject
	m&p Xyl.	0.8772	0.4010	10	Accept	6.5610	0.0000	15	Reject
	o-Xyl.	0.0468	0.9636	10	Accept	9.2113	0.0000	15	Reject
5-Ox	Benzene	2.9757	0.0139	10	Reject the null hypothesis				
	Toluene	0.8881	0.3953	10	Accept the null hypothesis				
	Ethylbenz.	6.3196	0.0001	10	Reject the null hypothesis				
	m&p Xyl.	6.0492	0.0001	10	Reject				
	o-Xyl.	5.5969	0.0002	10	Reject				
10-DeOx	Benzene	3.9988	0.0025	10	Reject				
	Toluene	1.3531	0.2058	10	Accept the null hypothesis				
	Ethylbenz.	6.6558	0.0001	10	Reject the null hypothesis				
	m&p Xyl.	6.4022	0.0001	10	Reject				
	o-Xyl.	5.8654	0.0002	10	Reject				
10-Ox	Benzene	1.9673	0.0775	10	Accept the null hypothesis				
	Toluene	2.8195	0.0182	10	Reject the null hypothesis				
	Ethylbenz.	4.0985	0.0021	10	Reject				
	m&p Xyl.	3.9198	0.0029	10	Reject				
	o-Xyl.	3.8699	0.0031	10	Reject				

Legend

D_f	Degree of freedom
P(t)	Probability that such a difference may occur by chance and not due to real causes
t	Calculated unpaired T-value

Gas Chromatography (GC/FID) Method

Scope and application

- This gas chromatography with flame ionization detector can be used for both qualitative and quantitative determination of BTEX compounds, and other fractions of petroleum hydrocarbon including volatile organic compounds.
- The method detection limit is 0.05mg/L.

Summary of method

- EPA method 8015D was used for the analysis. Check and water samples from dialysis samplers were analyzed using GC/FID. The setting for the method is given in Table A5.1. The check samples were prepared by diluting standard solution of BTEX to desired concentration in 44mL glass-vials. The dialysis water samples were pipetted by glass syringe from the samplers and diluted into 44mL glass-vials with no head space. Deionized water from the laboratory was used for the dilution.

Interferences

- No interferences were observed for this method and all necessary precautions were taken to prevent cross contamination of the samples by analyzing and placing blank samples between each set of dialysis samples.

Sample collection, preservation and handling

- Refer to section 2.3 of Chapter 2 for reservoir sampling protocol.
- Samples were analyzed immediately after sampling. The standard procedure is to analyze the samples within four hours of preparation when preservatives are not used.

- No preservatives were used for the laboratory experiment because the samples were not stored.

Safety

- Gloves were used during the course of sample preparations to prevent direct contact with the samples. Lab coat with goggle was also worn.
- The dilution and preparation of the samples were done in fume hooded area to minimize exposure to benzene and methanol.
- The experimental set-up area was secluded from area frequented by people and appropriate warning signs were provided.

Apparatus

- Glass GC-gas tight micro syringe ranging from 10µL to 5mL
- 50mL beakers and 10mL volumetric flasks
- 44mL glass vials and 2mL vials with Teflon lined septa
- HP 6890 GCFID system with a Purge and Trap (P & T) concentrator (Aqua Tek 70 liquid autosampler)

Materials and reagents

- Deionised distilled (DI) organic free water from the laboratory (18.2MΩ-cm)
- Distilled Methanol (99.99% HPLC grade)
- BTEX standard solution (containing 2000µg/mL in methanol) from SUPELCO

Calibration

- A working BTEX concentration of 200mg/L in a 2mL vial was prepared from a standard solution of BTEX containing 2000µg/mL (From SUPELCO). This was done by pipetting 200µL from the standard solution into the 2mL vial containing 1.8ml of methanol.

- Five different calibrated solutions of BTEX ranging from 0.1mg/L to 5mg/L in 44mL vial were prepared from the 200mg/L working solution by pipetting the required volume to make up the intended concentration into vials which were partially filled with DI water. More DI water was added to each vial to make up the 44mL capacity with no head space.
- The vials were covered with Teflon septa laid cover, and mixed in a sonicator for 2min.
- The solution vials were then placed in the GC rack for analysis.

Calculations

- The GC determines the area under the chromatogram of each compound using embedded software in the system. The calculated area is then tabulated with the prepared. concentration to determine the response factor (which is the slope of the straight line graph obtained from the calibration plot of each compound). The response factors obtained from the sets of calibration plots for each compound are used in determining the concentration of the unknown samples. This is achieved by multiplying the response factor with the area under the chromatogram with the same retention time with that calibrated to obtain the concentration of the compound in the water sample.
- The GC system was calibrated for every sampling sequence event; check standards and blanks were included with each set of samples tested.
- The calibration range was typically 0.1mg/L to 5mg/L but the tested linear range was 0.05mg/L to 10mg/L for the HP 6890 GC/FID system.

Gas Chromatography

- The operating condition for the GC and the auto sampler used for the analysis are given in Table A5.1 and A5.2.

- If the response of any of the BTEX compounds is outside the calibrated linear range discussed earlier, the sample may be diluted or the system recalibrated.

Quality assurance and control

- Blank deionised water samples were analyzed prior to analyzing the main samples to ensure that glassware and reagents are free of interferences.
- Blanks were also placed in-between each set of samples to prevent cross contamination.
- Triplicate samples were prepared to determine potential bias and precision in the analytical procedures.
- Check standards were interspersed within the samples to ensure precision of results obtained.
- The vials were properly washed, oven dried, cleaned with methanol and dried after each usage and new sets of septa were used for each run.
- The system was recalibrated for each sampling event and the results compared with earlier calibration to make sure the system is working properly.

Table A5.1 GC/FID Analytical Parameters

Parameters	Description
Carrier Gas	Helium
FID parameters	Hydrogen and air flow rates of 35 and 350mL/min respectively. Helium make-up gas flow rate: 35mL/min
Injector	Mode: Split, Initial temp: 200°C, Pressure: 5psi Split ratio: 50:1, Split flow: 369.1mL/min, Total flow: 379.8mL/min, Gas type: Helium
Injector Temperature	200°C
Detector Temperature	250°C
Temperature Program of Oven	Initial temp: 36°C Maximum temp: 320°C Initial time: 4.00min Equilibration time: 3.00min Ramps # Rate (°C/min) Final temp (°C) Final time (min) 1 5 150 0 2 15 240 6 Post temp: 50°C Post time: 0.00min Run time: 38.80min
Column	Type: Capilary Column Model number: DB-1 O.T.S, (J & W Scientific), HP-1 Methyl Siloxane Nominal length: 30.0m Nominal diameter: 530μm Nominal thickness: 1.5μm Mode: Constant flow Initial flow: 7.4mL/min Nominal initial pressure: 5.00psi Average velocity: 0.5m/s
Auto sampler	See Table A5.2 for the autosampler settings

Table A5.2 Purge and Trap (Aqua Tek 70 autosampler) settings (TEKLINK 4000J method version 1.02)

Parameter	Value	Parameter	Value
Line Temp	180°C	Sample Drain	On
Valve Temp	180°C	Bake Time	10 Minutes
Mount Temp	30°C	Bake Temp	225°C
MCS Line Temp	40°C	Bake Gas Bypass	Off
Purge Ready Temp	36°C	Bypass Delay Time	2 Minutes
Purge Temp	0°C	MCS Bake Temp	300°C
Turbo Cool Temp	-20°C	AquateK 70	on
Sample Heater	Off	Pressurize Time	0.25 Minutes
Prepurge Time	3 Minutes	Fill IS	Off
Sample Preheat Time	5 Minutes	Xfer Sample	0.50 Minutes
Sample Preheat Temp	40°C	Rinse Lines	0.25 Minutes
Purge Time	11 Minutes	Purge Lines	0.50 Minutes
Drypurge Time	0 Minutes	Bake Rinse	0.75 Minutes
GC Start Option	Start of Desorb	Bake Tranfer	0.75 Minutes
GC Cycle Time	0 Minutes	Rinse Cycles	1
Cryo Focuser	Off		
Desorb Preheat Temp	220°C		
Desorb Time	4 Minutes		
Desorb Temp	225°C		

Ion Chromatography (IC) Method

Scope and application

- This ion chromatography is used for the determination of cations and anions in a water sample. Initial filtering of the sample is required to prevent ferrous ion and dirt clogs in the system.
- The method detection limit is 1mg/L for the anion and 0.5mg/L for the cation.

Summary of method

- EPA method 300.1 was used for the analysis.

Interferences

- No interferences were observed for this method. However, iron build-up within the IC system may stall its proper functioning and the system must be devoid of oxygen to prevent sample bias.

Sample collection, preservation and handling

- Samples are collected in clean containers.
- If samples will not be analyzed on the day they were collected, they should be filtered as soon as possible (ASAP) otherwise; bacteria in the sample may cause concentration bias.
- The sample should be refrigerated at temperature below 4°C to decrease biological activity in the sample. The samples may be preserved for at least a week by refrigerating.
- Samples containing nitrites (NO_2^{-1}) and sulphites (SO_3^{-2}) should be analyzed as soon as possible to prevent oxidation to nitrates (NO_3^{-1}) and sulphates (SO_4^{-2}) respectively.

- For this study, the black precipitates from one of the samplers deployed in the field was filtered out of solution and dissolved with nitric acid to keep it in solution.
- No other preservatives were used for the laboratory experiment.

Safety

- Gloves were used during the course of sample preparations to prevent direct contact with the samples. Lab coat with goggle was also worn.
- The dilution and preparation of the samples were done in fume hooded area to minimize exposure to acid fumes.
- The experimental set-up area was secluded from area frequented by people and appropriate warning signs were provided.

Apparatus

- Eppendorf glass pipettes ranging from 0.1μL to 10μL
- Filtering apparatus with 0.2μm paper filters
- 50mL beakers and 10mL volumetric flasks
- 10mL glass vials with Teflon lined septa
- DIONEX ICS-2500 system with analytical columns of CS12A and AS14A for cations and anions analyses respectively

Materials and reagents

- Deionised distilled (DI) organic free water from the laboratory (18.2MΩ-cm)
- Six Cation standard II from DIONEX
- Seven Anion standard II from DIONEX

Calibration

- 2 to 20 times dilution of stock solutions were prepared for the seven anion standards (F^{-1}, Cl^{-1}, NO_2^{-1}, NO_3^{-1}, Br^{-1}, PO_4^{-2}, and $S0_4^{-2}$) with minimum concentration ranging from 1mg/l for Fluoride ion to 10mg/l for phosphate.
- 2 to 100 times dilution stock solutions were prepared for the six cation standards (Li^{+1}, Na^{+1}, NH_4^{+1}, K^{+1}, Mg^{+2}, and Ca^{+2}) with minimum concentration ranging from 0.5mg/L for Lithium ion to 5mg/L for both Calcium and Potassium ions.
- The prepared solutions were made into 10mL volumetric flasks and transferred into 10Ml vials covered with Teflon septa-laid cover, and analyzed with the IC system.

Calculations

- The IC system determines the area under the chromatogram of each ion using embedded software in the system based on their retention times. The calculated area is then tabulated with the prepared concentration to determine the response factor (which is the slope of the straight line graph obtained from the calibration). The response factor obtained from the sets of calibration plots for each ion is used in determining the concentration of the unknown ion in the sample. This is achieved by multiplying the response factor with the area under the chromatogram with the same retention time with that calibrated to obtain the concentration of the ion in the water sample.
- The IC system was calibrated for every sampling event and check standards were included with each set of samples tested.
- The calibration range was typically 0.5mg/L to 250mg/L for the tested linear range with the exception of Ammonium and Magnesium ions which tend to quadratic at high concentrations for the ICS – 2500 Ion Chromatography system.

Ion Chromatography System

- The operating condition for the IC and the auto sampler used for the analysis are given in Table A5.3.
- If the response of any of the ions is outside the calibrated linear range discussed earlier, the sample may be diluted or the system recalibrated.

Quality assurance and control

- Blank deionized water samples were analyzed prior to analyzing the main samples to ensure that glassware and reagents are free of interferences.
- Blanks were also placed in-between each set of samples to prevent cross contamination
- Triplicate samples were prepared to determine potential bias and precision in the analytical procedures.
- Check standards were interspersed within the samples to ensure precision of results.
- New vials were used always for new sets of samples.
- The system was recalibrated for each sampling even and the results compared with earlier calibration to make sure the system is working properly.

Table A5.3 ICS settings used for the analysis

Specification	EPA Method 300.1			
Column Type	Anions	Size	Cations	Size
Analytical	IonPa AS14A	4 X 250mm	CS12A	4 X 250mm
Inorganic guard	AG14A	4 X 50mm	CG12A	4 X 50mm
Organic guard	NG1	4 X 35mm	NG1	4 X 35mm
Eluent	8mM Na_2CO_3/1.0mM $NaHCO_3$		22mN H_2SO_4	
Injection loop volume	25μL		25μL	
Eluent flow rate	1mL/min		1mL/min	
Detector used	Conductivity (mS) with SRS Ultra II suppressor			

APPENDIX B: Data from the SVFLUX and CHEMFLUX models on the movement of contaminant across the well open interval

APPENDIX B.1 Flow field around the well by varying sand pack permeability

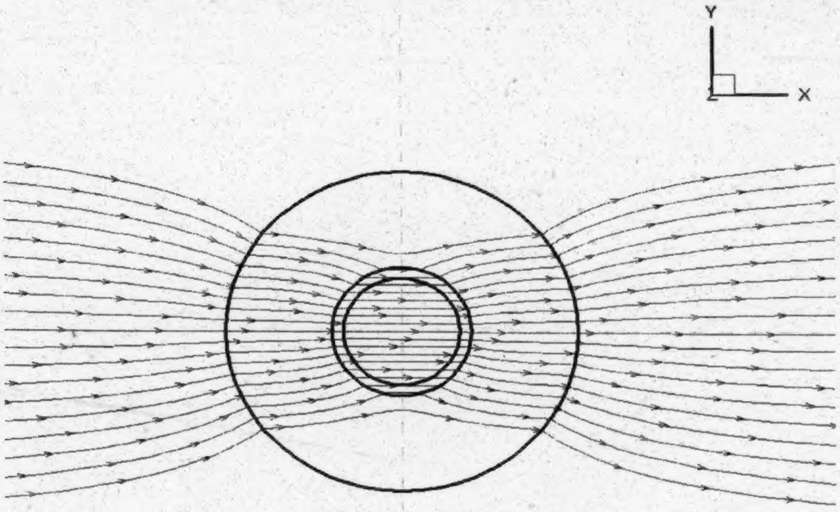

Figure B1.1 Flow field around the well at "q" (Ksp/K_f) = 100 (The streamlines are placed at 0.01m equidistant from the centre of the well from (4.91, 5, 3.5) to (5.09, 5, 3.5)

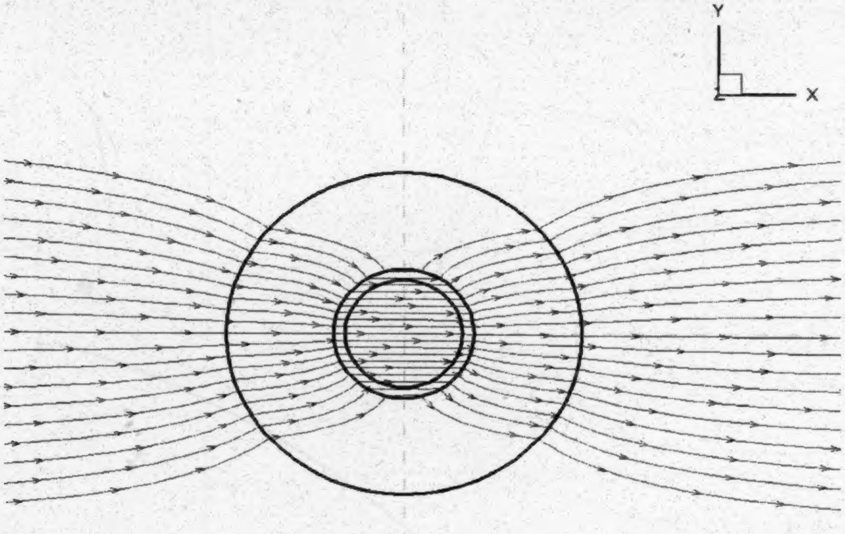

Figure B1.2 Flow field around the well at "q" (Ksp/K_f) = 10

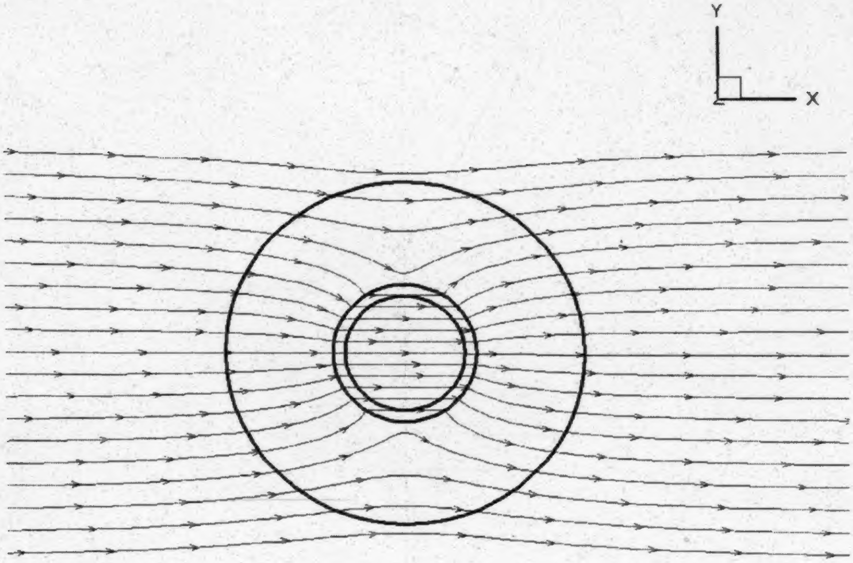

Figure B1.3 flow field around the well at “q” (Ksp/K_f) = 1

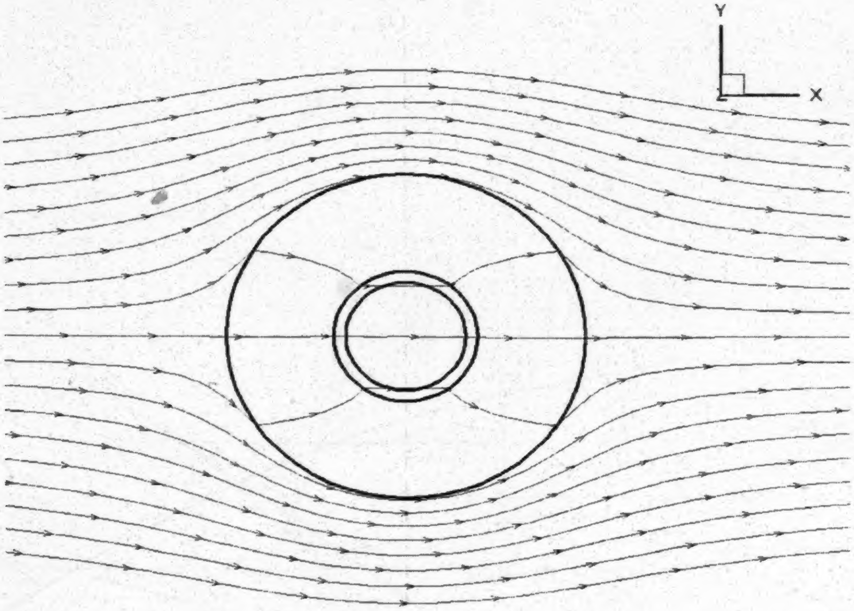

Figure B1.4 Flow field around the well at “q” (Ksp/K_f) = 0.1

APPENDIX B.2 Concentration Profiles for all the Case models

Acronyms

C_f	Formation constant boundary concentration
C_{SL}	Seam layer constant boundary concentration
$C_{sl\text{-}S}$	Seam layer constant surface concentration
C_{wf}	Initial finite concentration within formation
C_{wsl}	Initial finite concentration within seam layer
F	Sand formation
K_f	Permeability of sand formation
Ksl	Permeability of seam layer
Ksp	Permeability of sand pack
i	Hydraulic gradient
M	Concentration gradient ranging from 1 at SL intrerface to 0 at formation boundary
SL	Seam layer
SP	Sand Pack
α_L	Longitudinal dispersivity
α_T	Transverse dispersivity

Appendix B.2.1 CHA concentration profiles at different seepage velocities

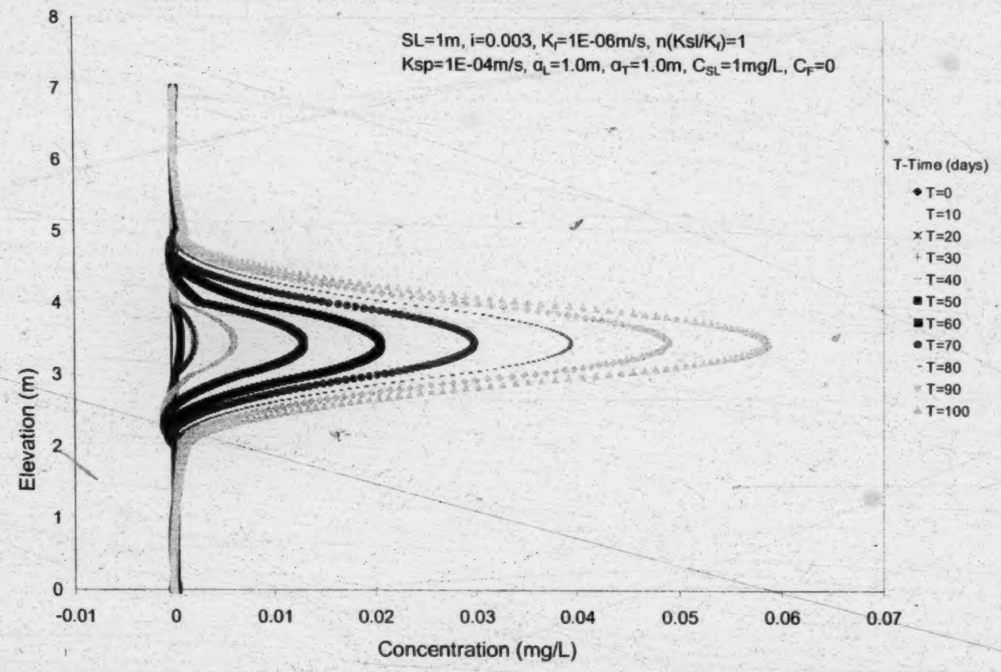

Figure B2.1 Case I-Hn1-CHA (V_{sl} = 0.237m/y, V_f = 0.287m/y: - less due to porosity "N")

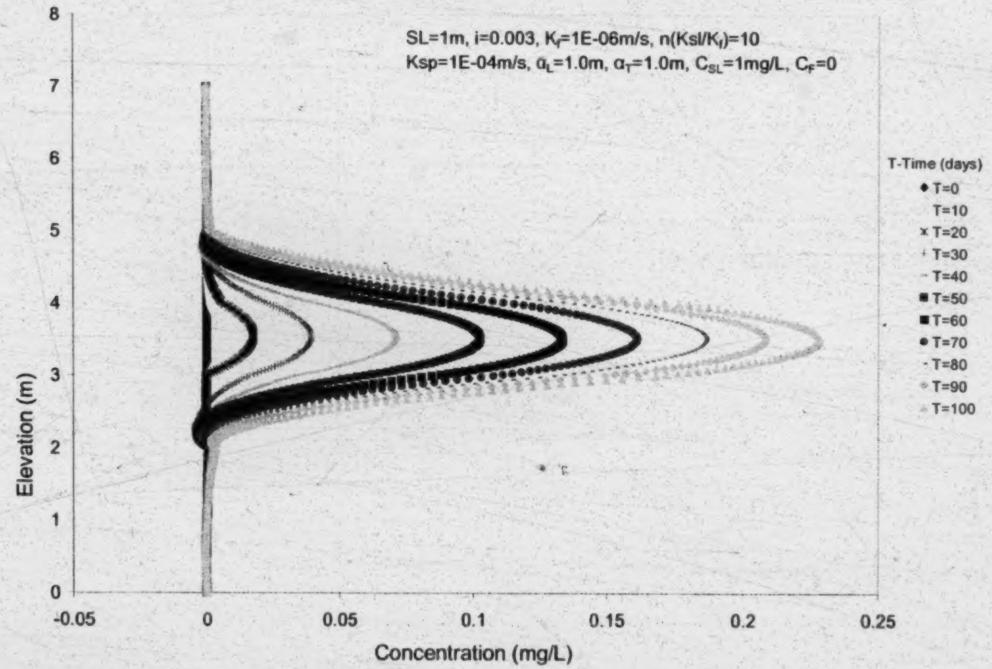

Figure B2.2 Case I-Hn10-CHA (V_{sl} = 2.37m/y, V_f = 0.287m/y)

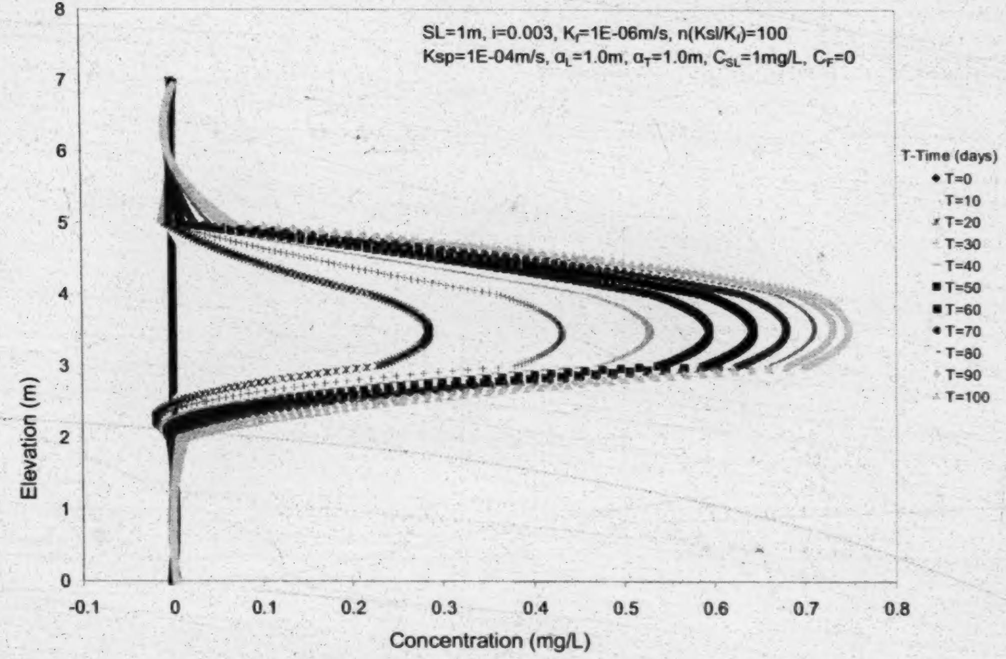

Figure B2.3 Case I-Hn100-CHA (V_{sl} = 23.7m/y, V_f = 0.287m/y)

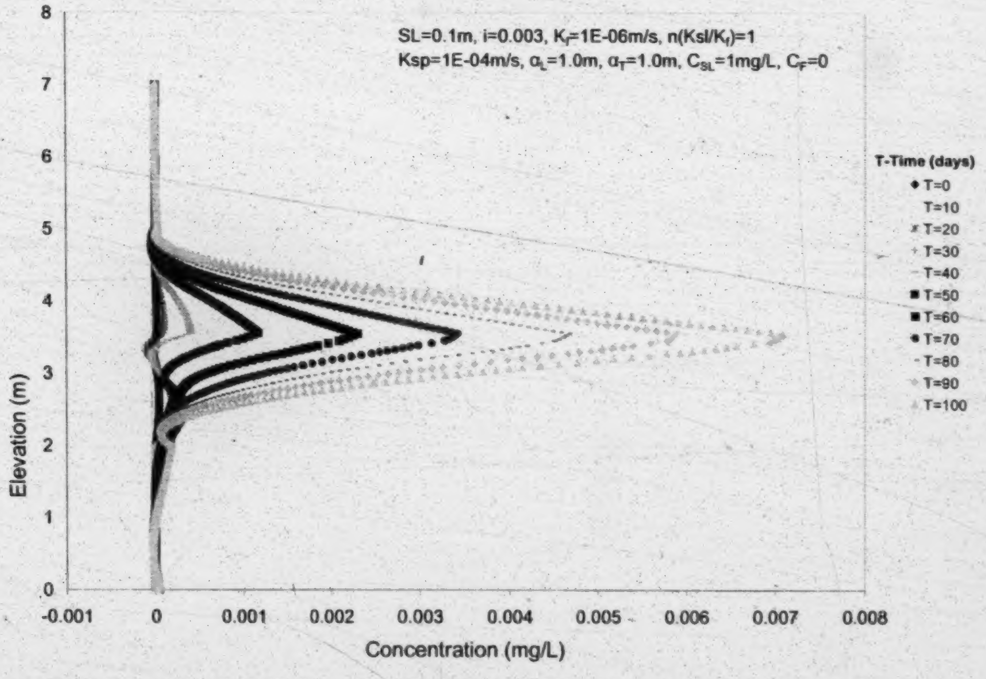

Figure B2.4 Case II-Hn1-CHA (V_{sl} = 0.237m/y, V_f = 0.287m/y)

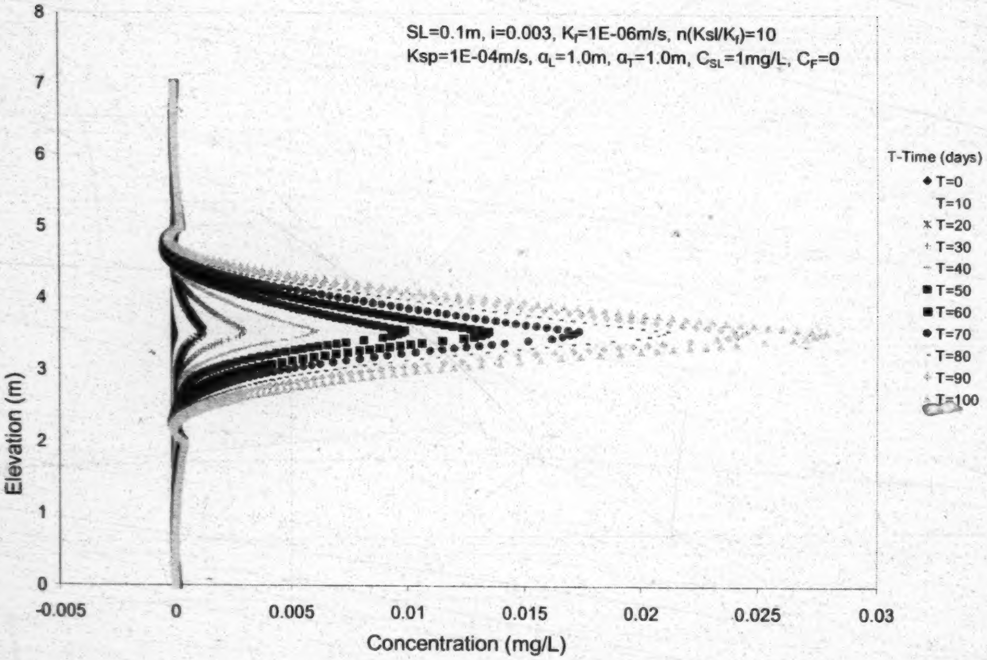

Figure B2.5 Case II-Hn10-CHA (V_{sl} = 2.37m/y, V_f = 0.287m/y)

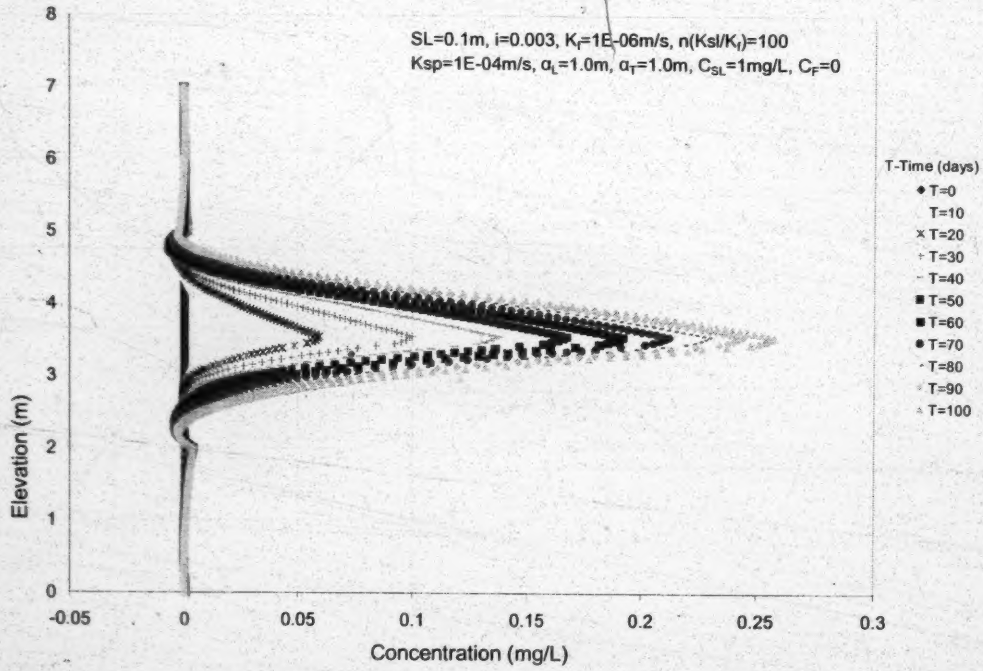

Figure B2.6 Case II-Hn100-CHA (V_{sl} = 23.7m/y, V_f = 0.287m/y)

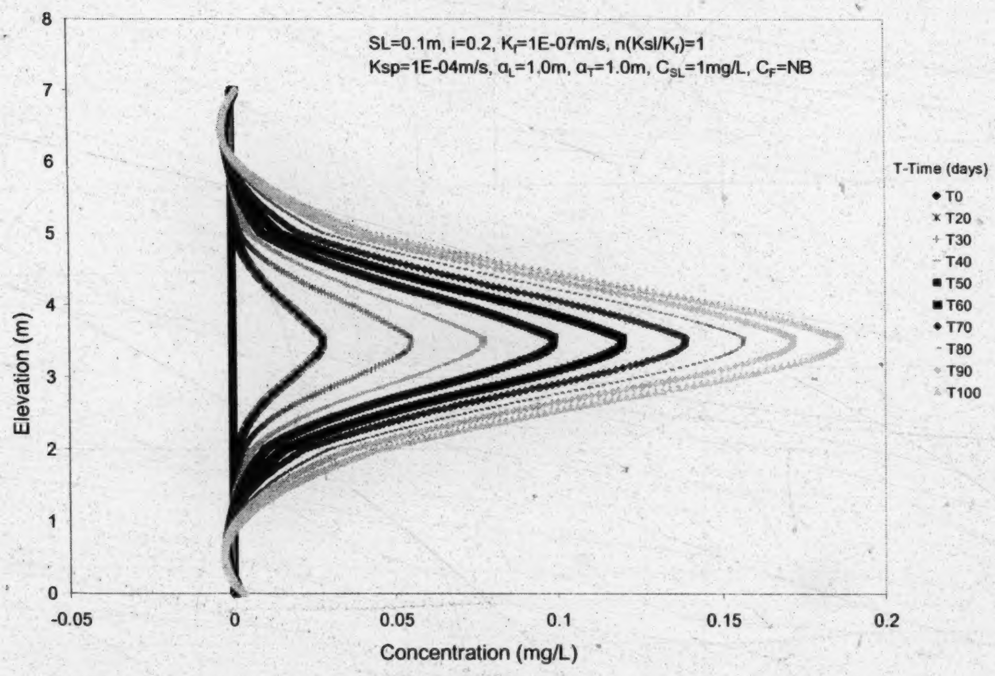

Figure B2.7 Case II-Hn1-CHA (V_{sl} = 1.58m/y, V_f = 1.91m/y)

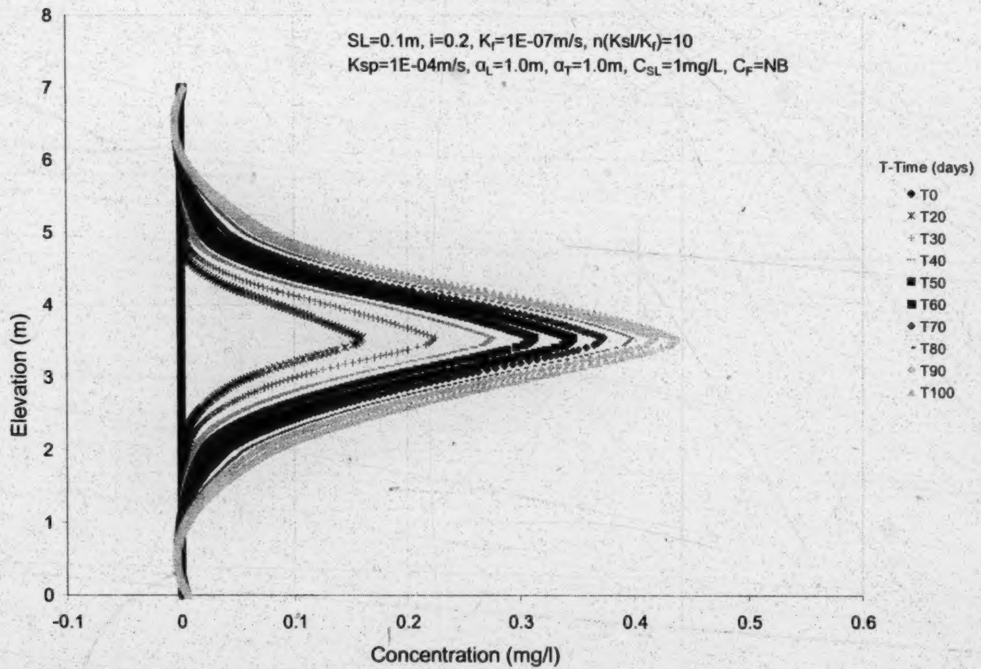

Figure B2.8 Case II-Hn10-CHA (V_{sl} = 15.8m/y, V_f = 1.91m/y)

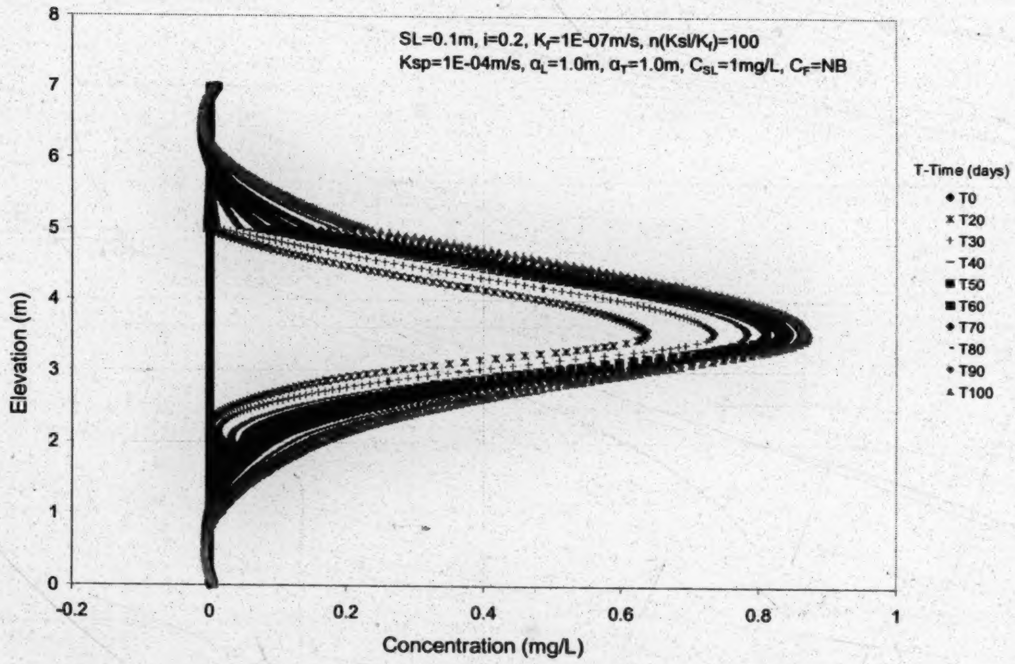

Figure B2.9 Case II-Hn100-CHA (V_{sl} = 158m/y, V_f = 1.91m/y)

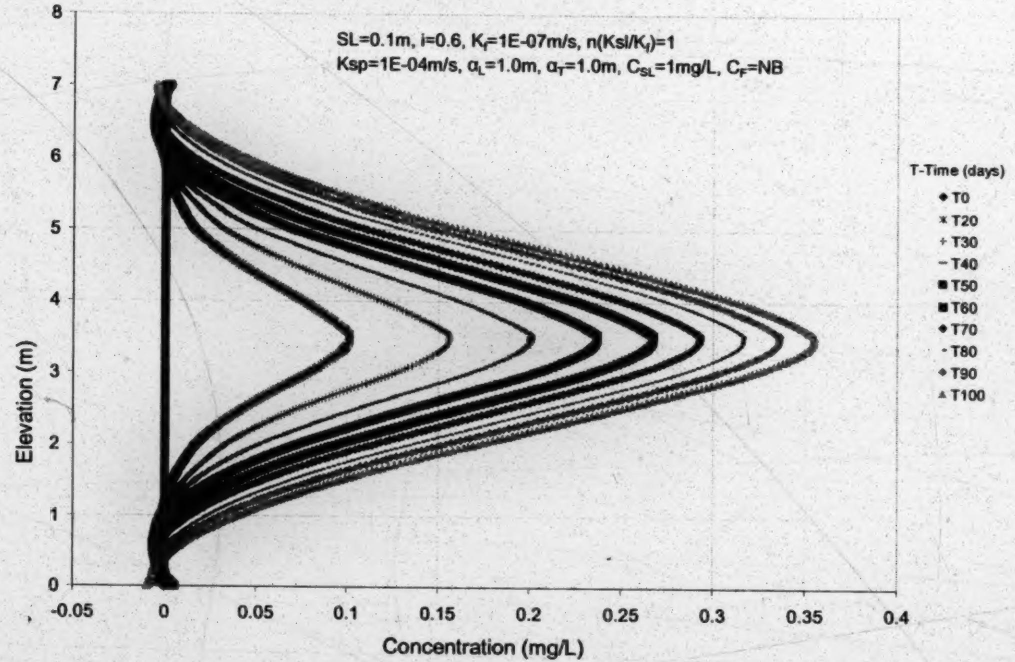

Figure B2.10 Case II-Hn1-CHA (V_{sl} = 4.73m/y, V_f = 5.73m/y)

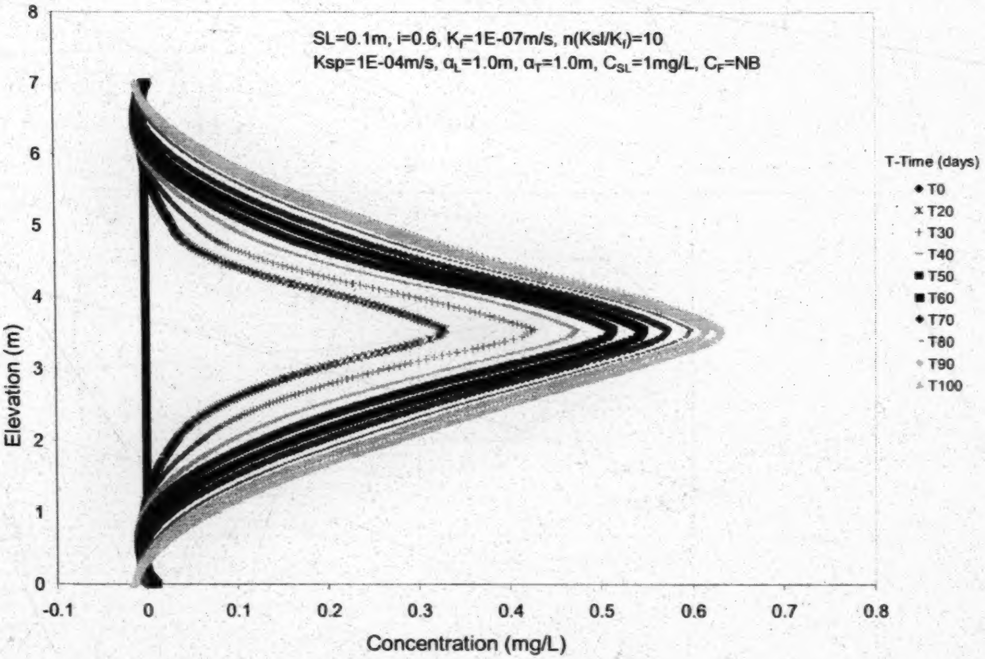

Figure B2.11 Case II-Hn10-CHA (V_{sl} = 47.3m/y, V_f = 5.73m/y)

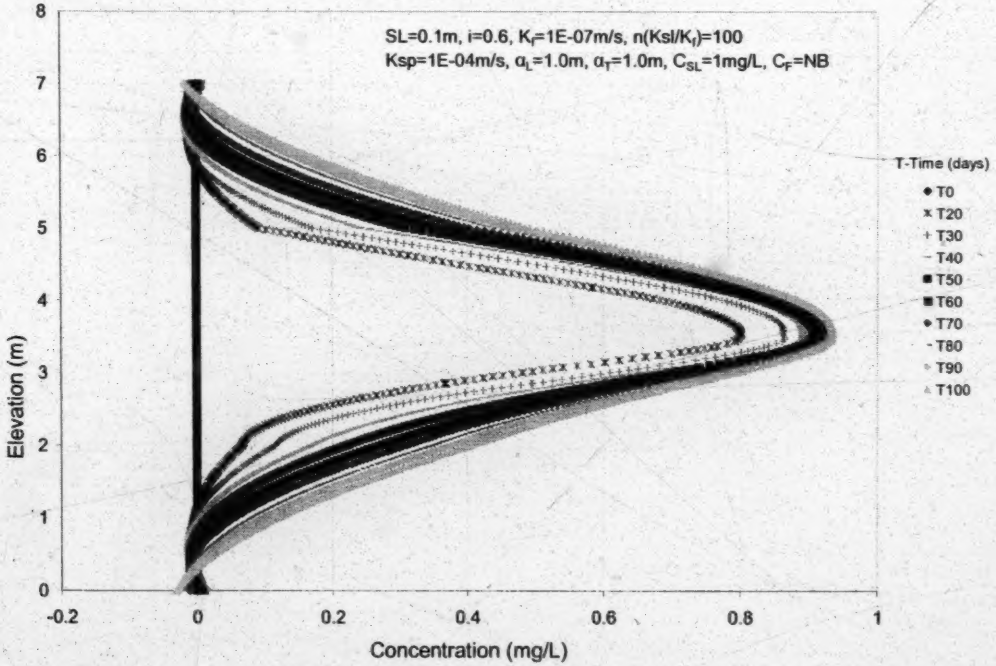

Figure B2.12 Case II-Hn100-CHA (V_{sl} = 473m/y, V_f = 5.73m/y)

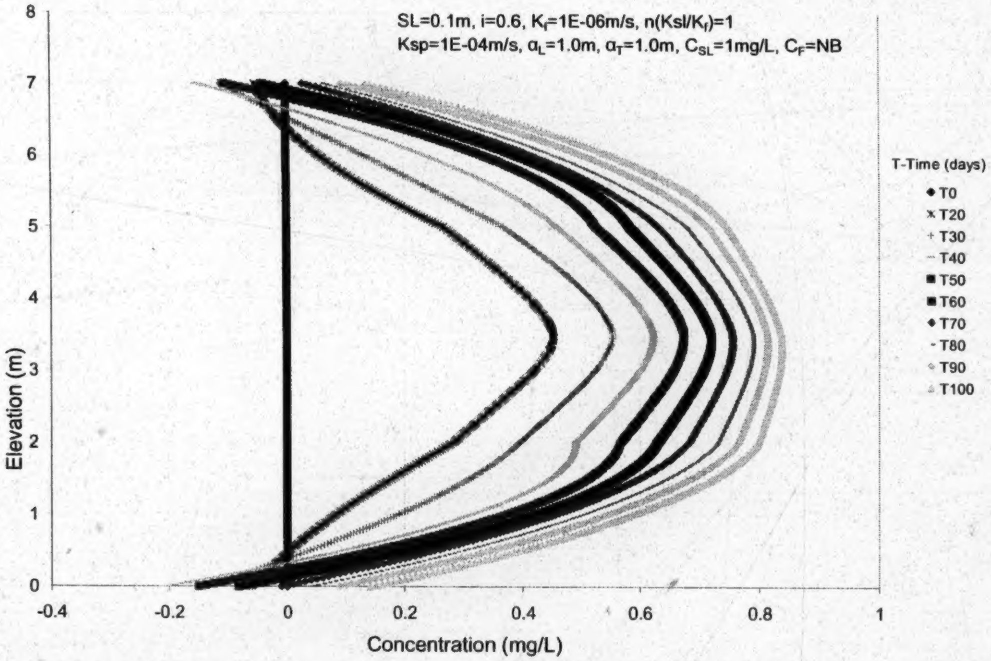

Figure B2.13 Case II-Hn1-CHA (V_{sl} = 47.3m/y, V_f = 57.3m/y)

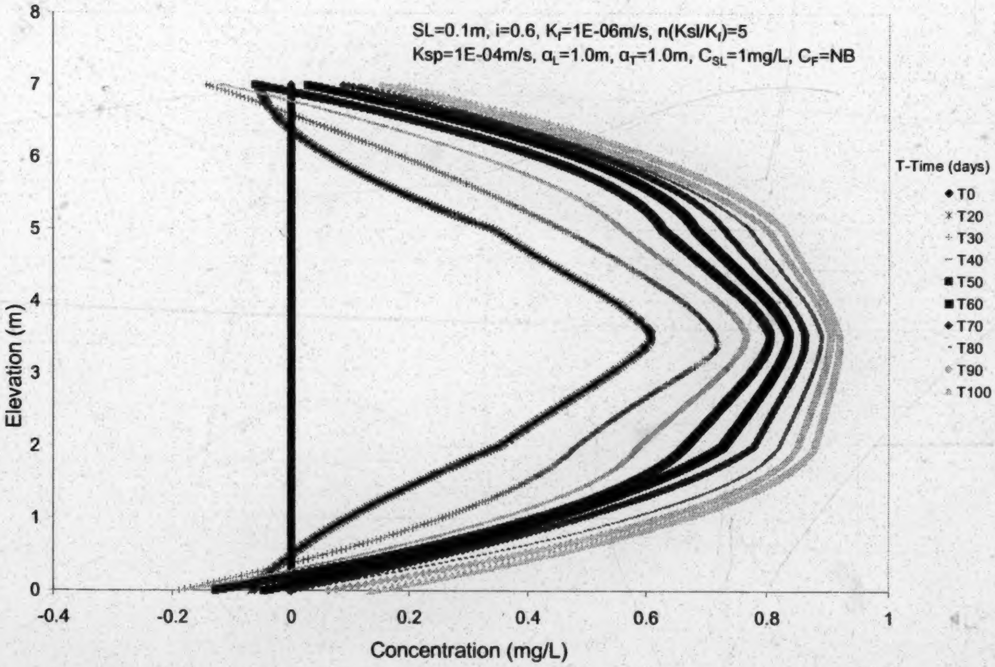

Figure B2.14 Case II-Hn5-CHA (V_{sl} = 237m/y, V_f = 57.3m/y)

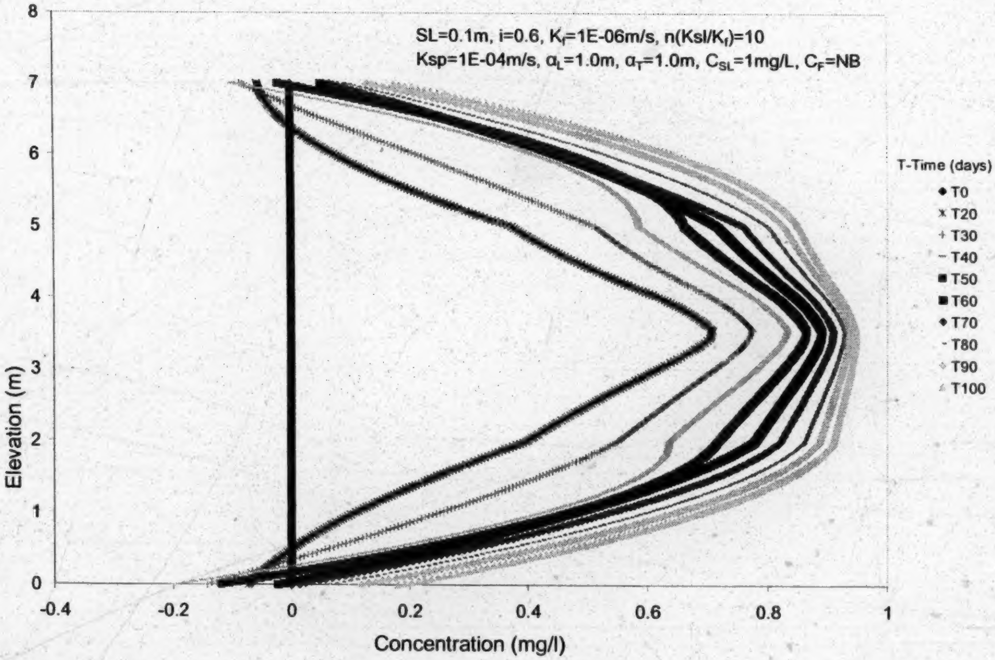

Figure B2.15 Case II-Hn10-CHA (V_{sl} = 473m/y, V_f = 57.3m/y)

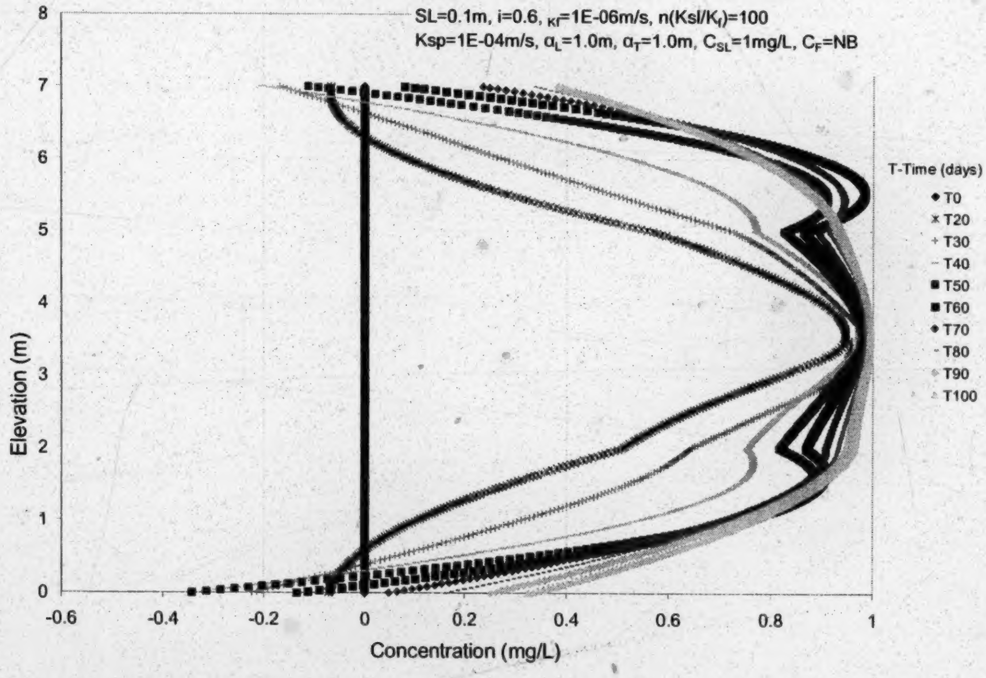

Figure B2.16 Case II-Hn100-CHA (V_{sl} = 4730m/y, V_f = 57.3m/y)

Appendix B.2.2 Results of varying seam layer thickness

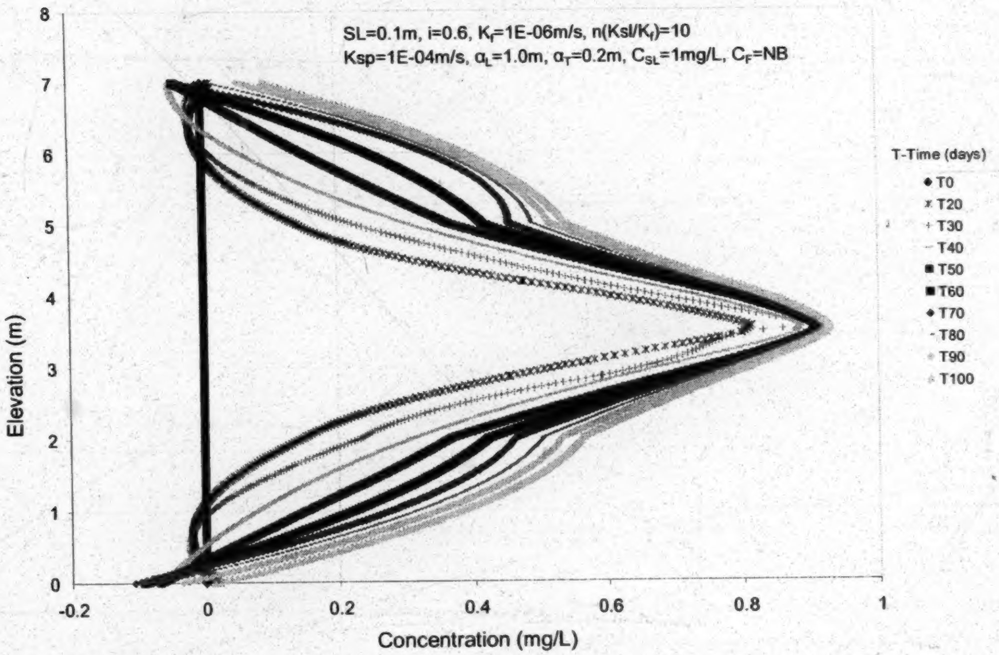

Figure B2.17 Case II-Hn10-CHA (V_{sl} = 473m/y, V_f = 57.3m/y)

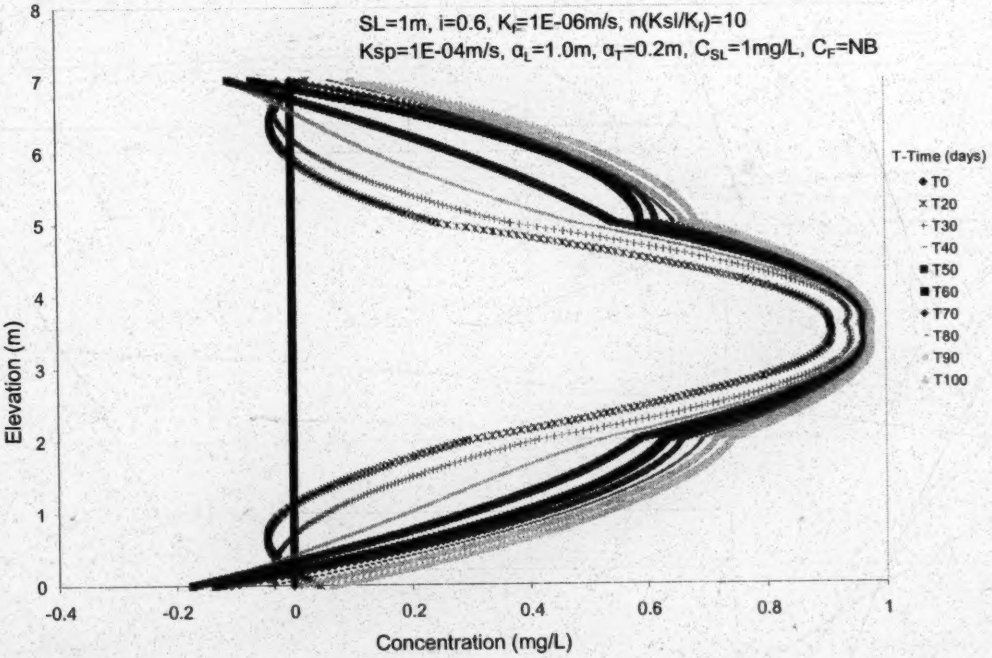

Figure B2.18 Case II-Hn10-CHA (V_{sl} = 473m/y, V_f = 57.3m/y)

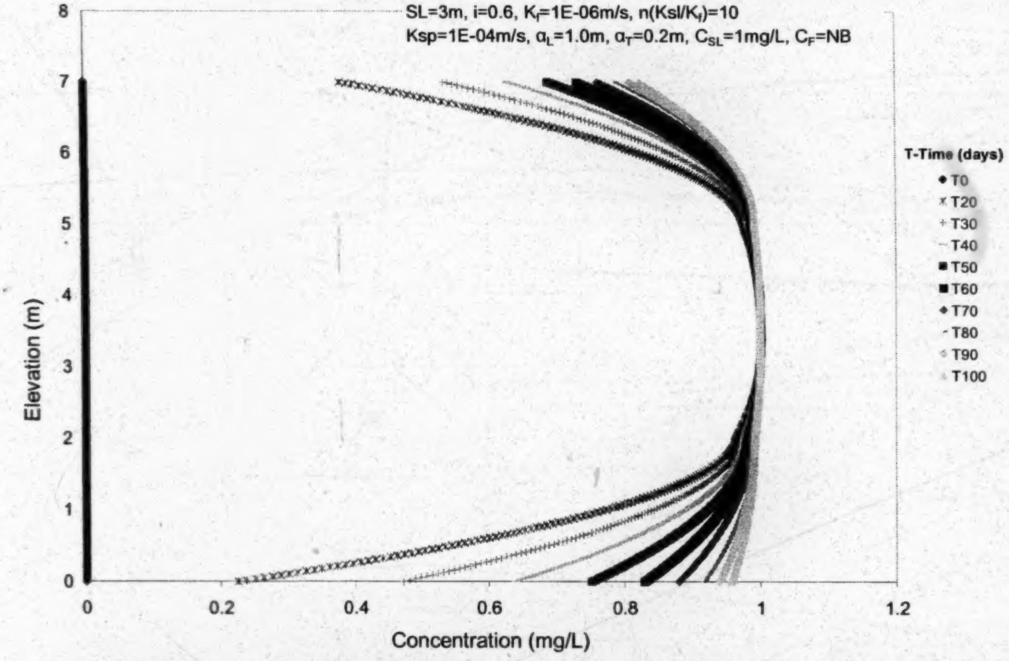

Figure B2.19 Case II-Hn10-CHA (V_{sl} = 473m/y, V_f = 57.3m/y)

Appendix B.2.3 Results of varying contaminant distribution in the formation

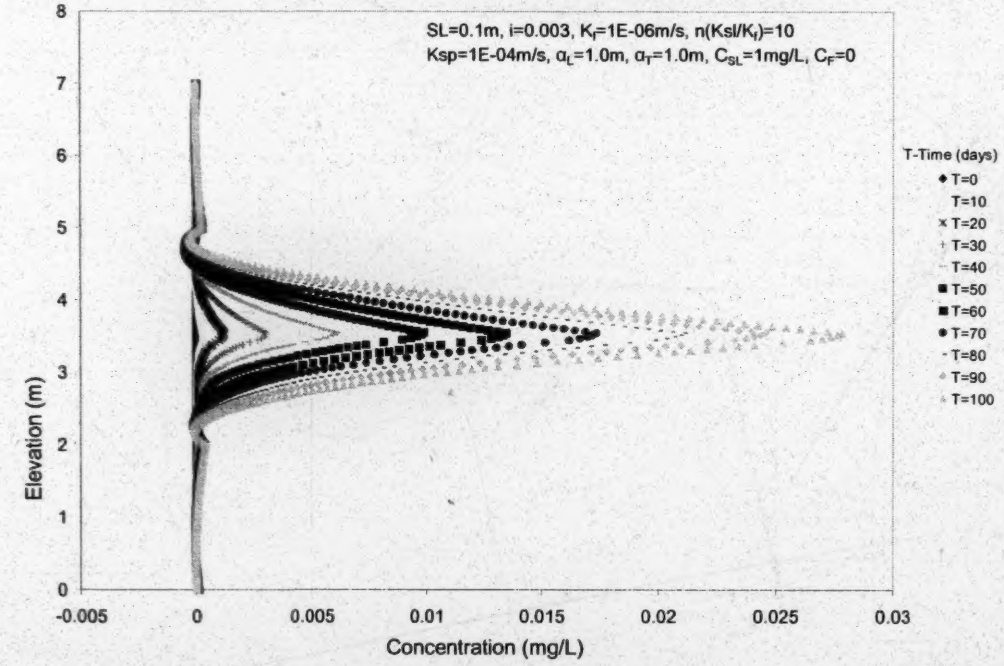

Figure B2.20 Case I-Hn10-CHA (V_{sl} = 2.37m/y, V_f = 0.287m/y)

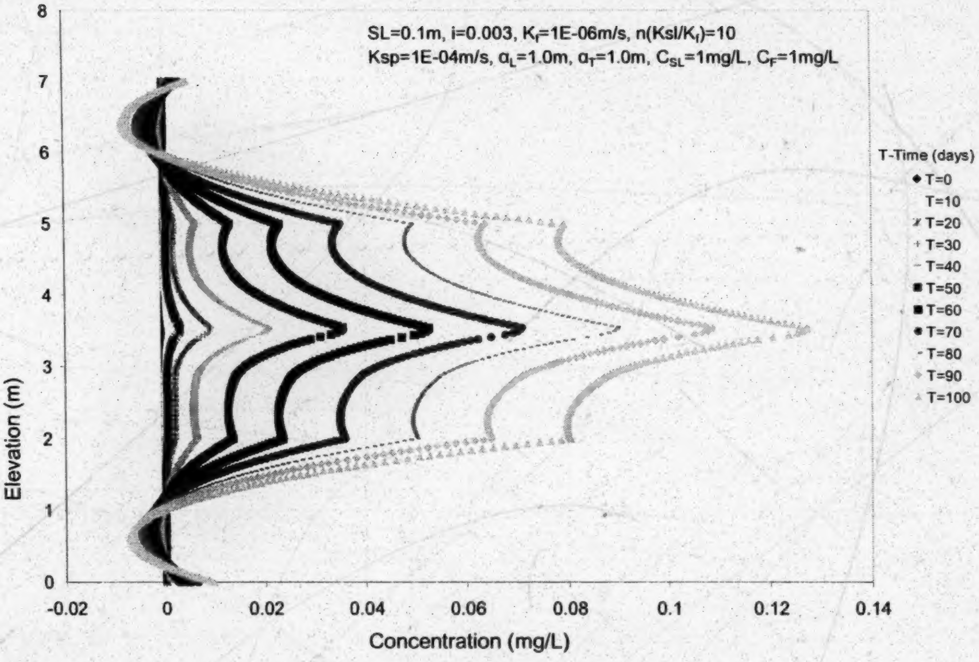

Figure B2.21 Case II-Hn10-CHB (V_{sl} = 2.37m/y, V_f = 0.287m/y)

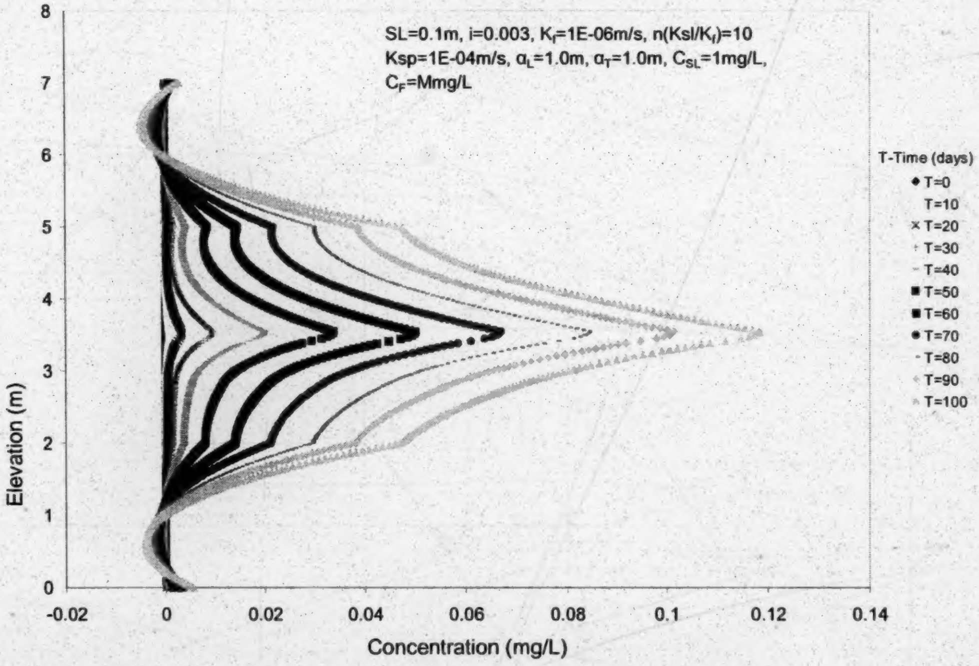

Figure B2.22 Case II-Hn10-CHC (V_{sl} = 2.37m/y, V_f = 0.287m/y)

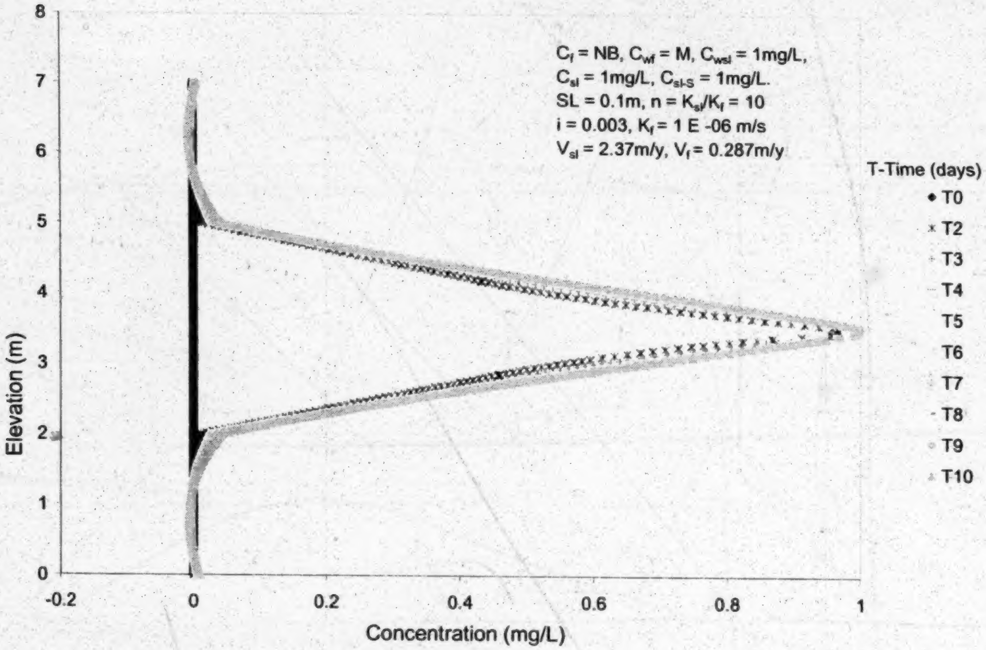

Figure B2.23 Case II-Hn10-CHAS with formation gradient (V_{sl} = 2.37m/y, V_f = 0.287m/y)

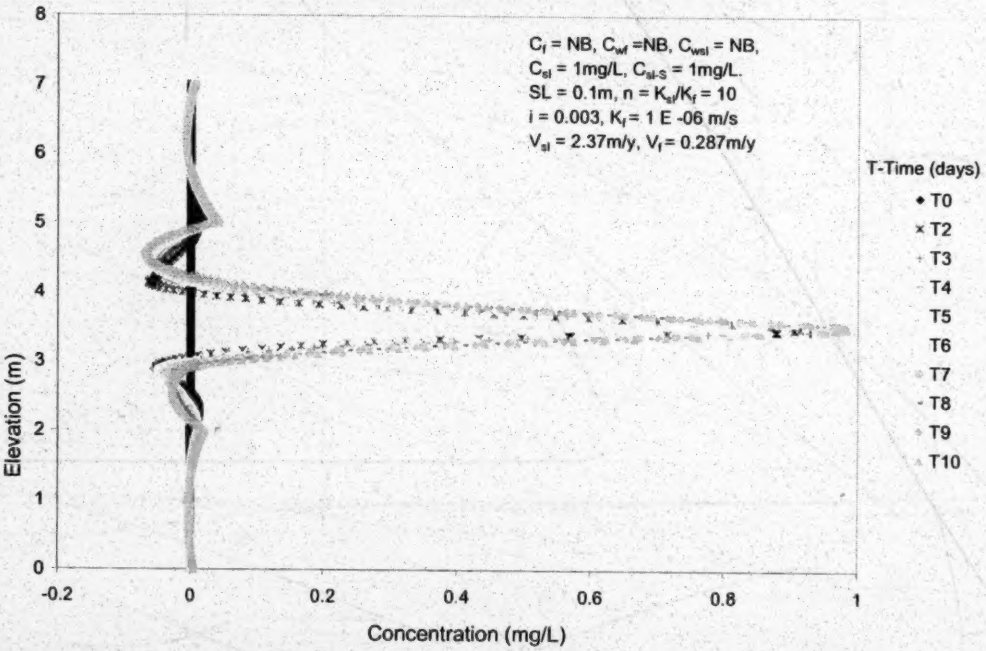

Figure B2.24 Case II-Hn10-CHAS without formation gradient (V_{sl} = 2.37m/y, V_f = 0.287m/y)

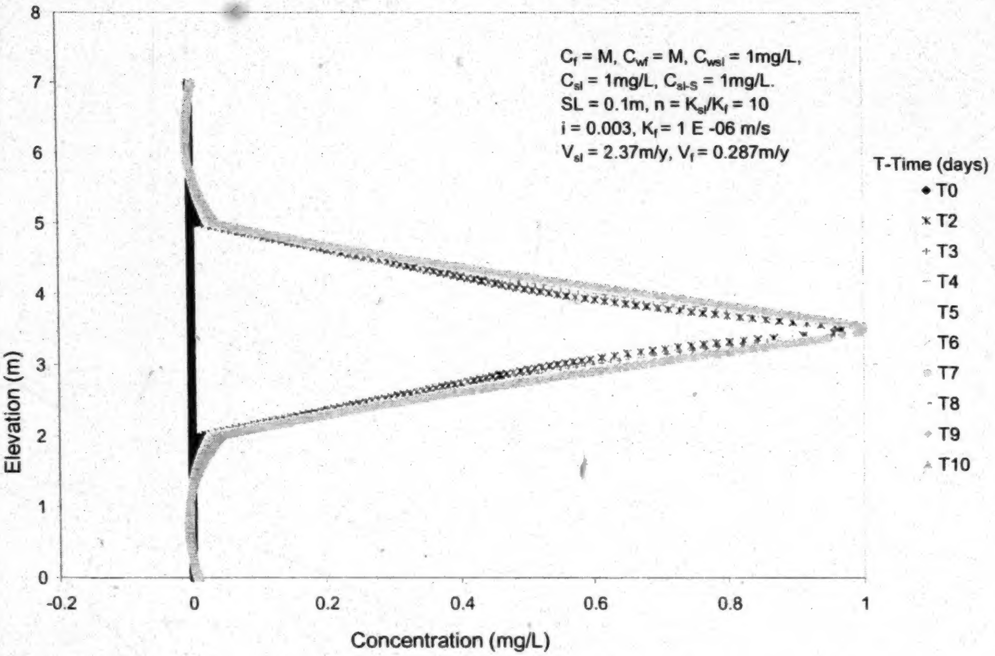

Figure B2.25 Case II-Hn10-CHCS with formation gradient (V_{sl} = 2.37m/y, V_f = 0.287m/y)

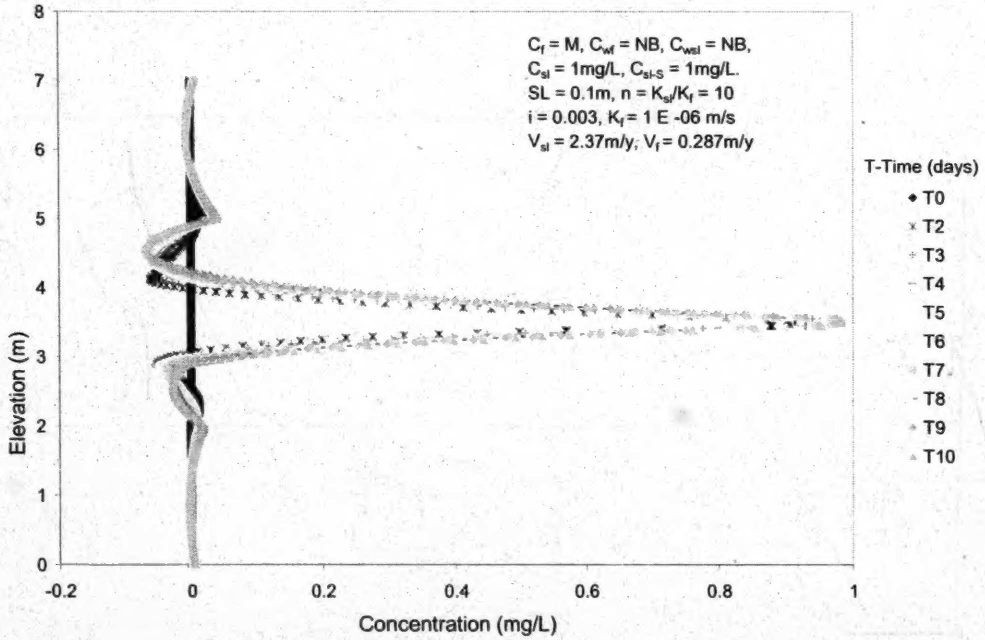

Figure B2.26 Case II-Hn10-CHCS without formation gradient (V_{sl} = 2.37m/y, V_f = 0.287m/y)

Appendix B.2.4 Results of varying dispersivity

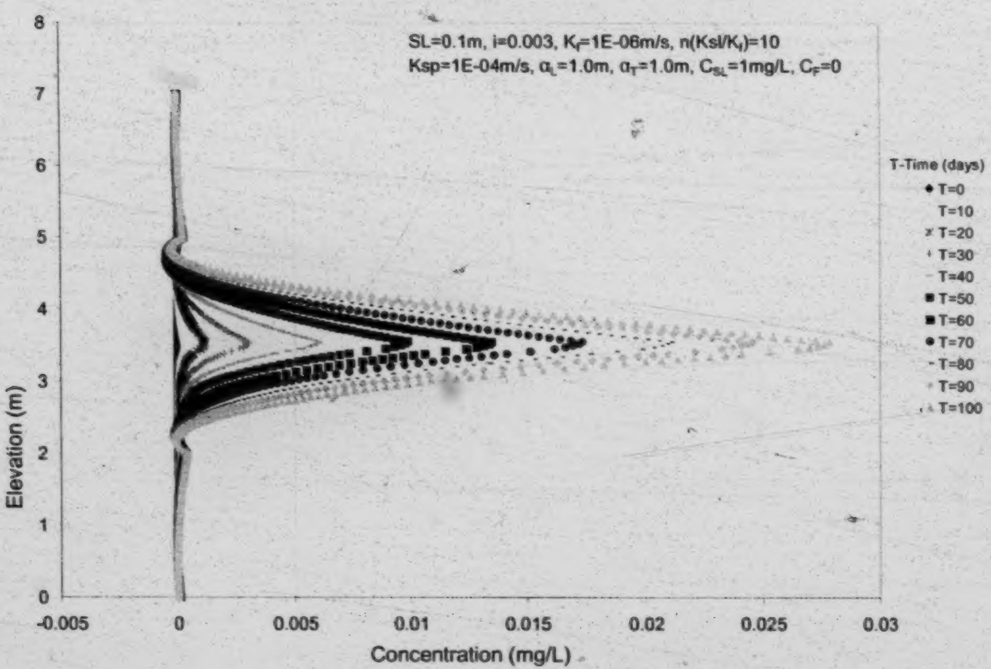

Figure B2.27 Case II-Hn10-CHA (α_L = 1.0m, α_T = 1.0m, Vs_l = 2.37m/y, V_f = 0.287m/y)

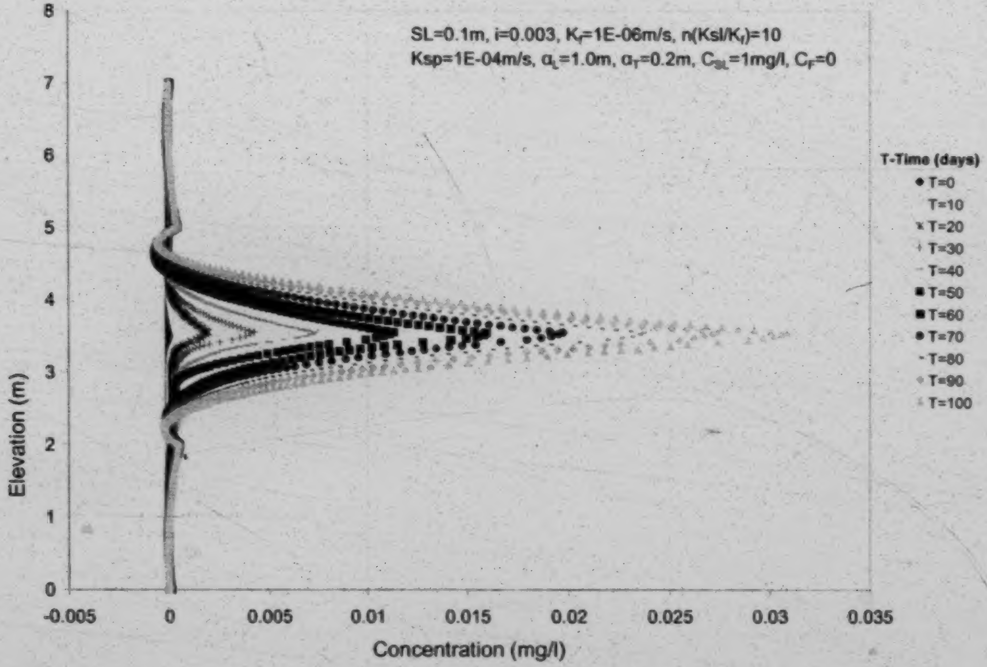

Figure B2.28 Case II-Hn10-CHA (α_L = 1.0m, α_T = 0.2m, V_{sl} = 2.37m/y, V_f = 0.287m/y)

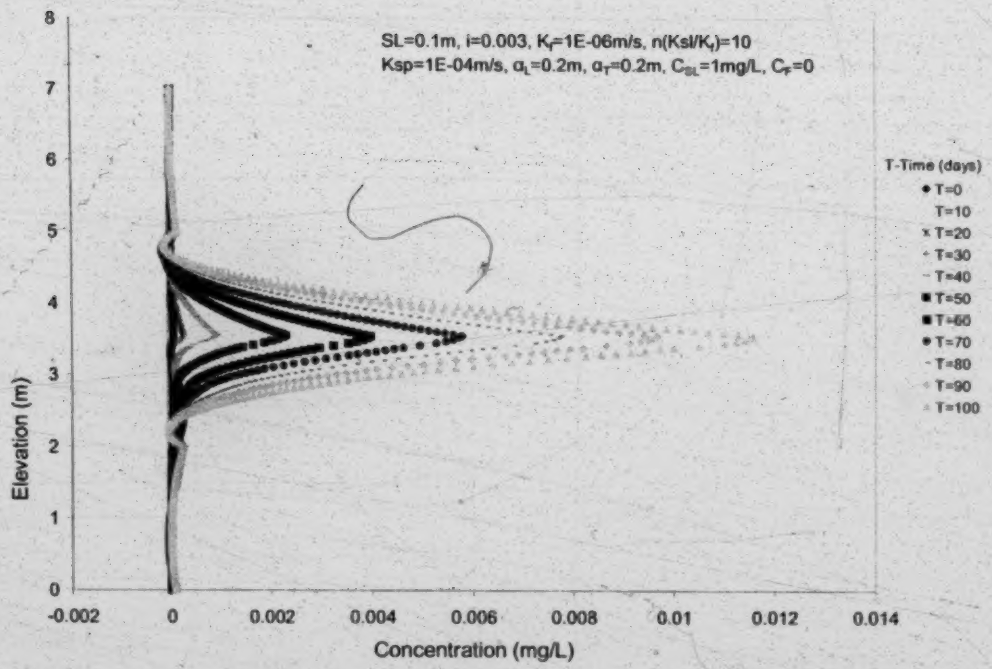

Figure B2.29 Case II-Hn10-CHA (α_L = 0.2m, α_T = 0.2m, V_{sl} = 2.37m/y, V_f = 0.287m/y)

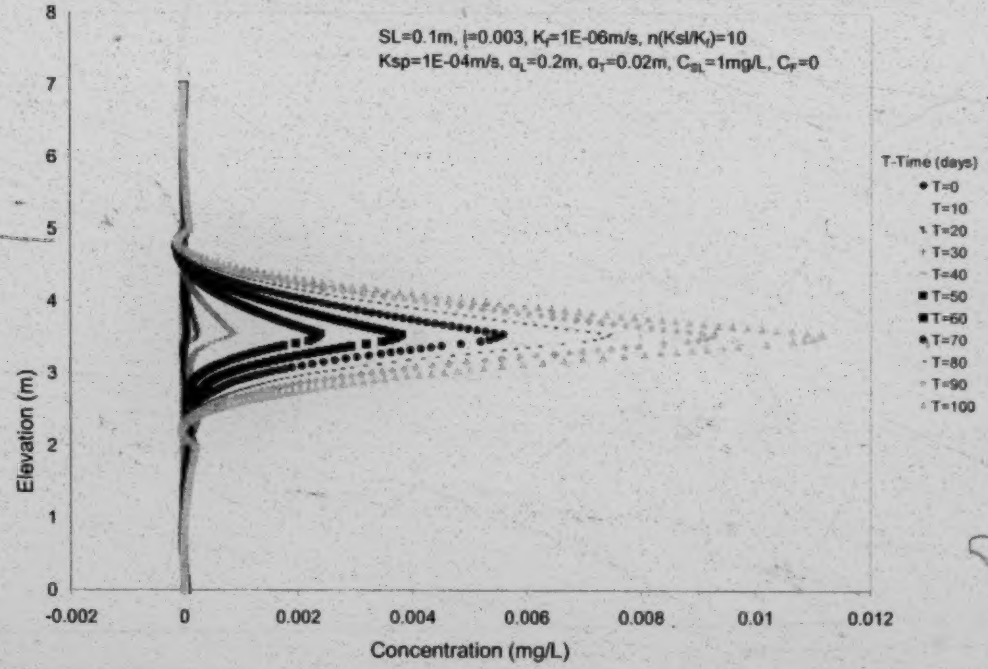

Figure B2.30 Case II-Hn10-CHA (α_L = 0.2m, α_T = 0.02m, V_{sl} = 2.37m/y, V_f = 0.287m/y)

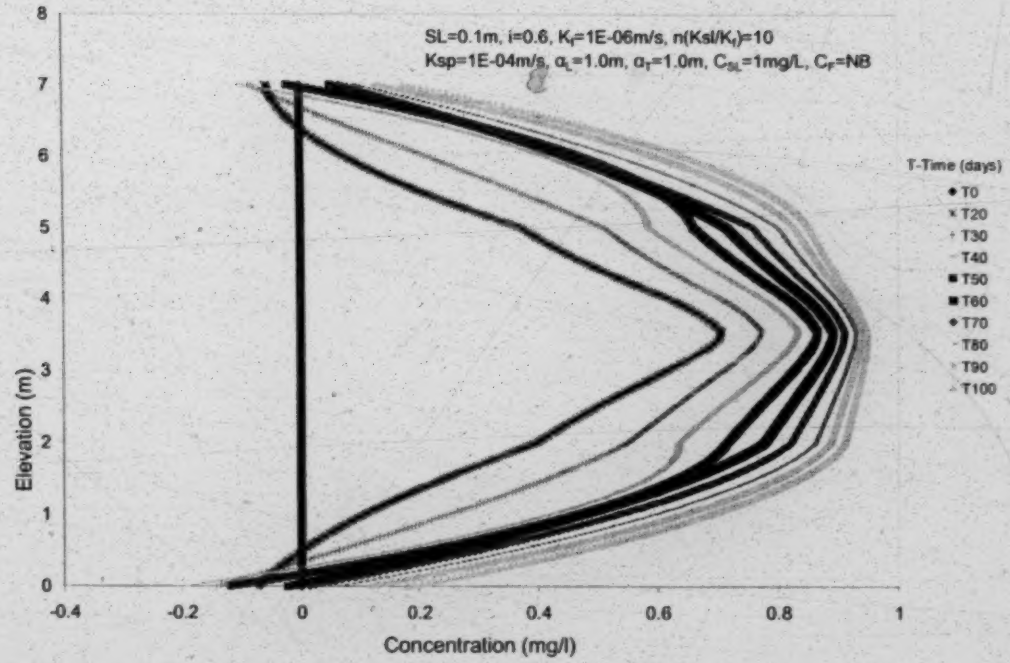

Figure B2.31 Case II-Hn10-CHA (α_L = 1.0m, α_T = 1.0m, V_{sl} = 473m/y, V_f = 57.3m/y)

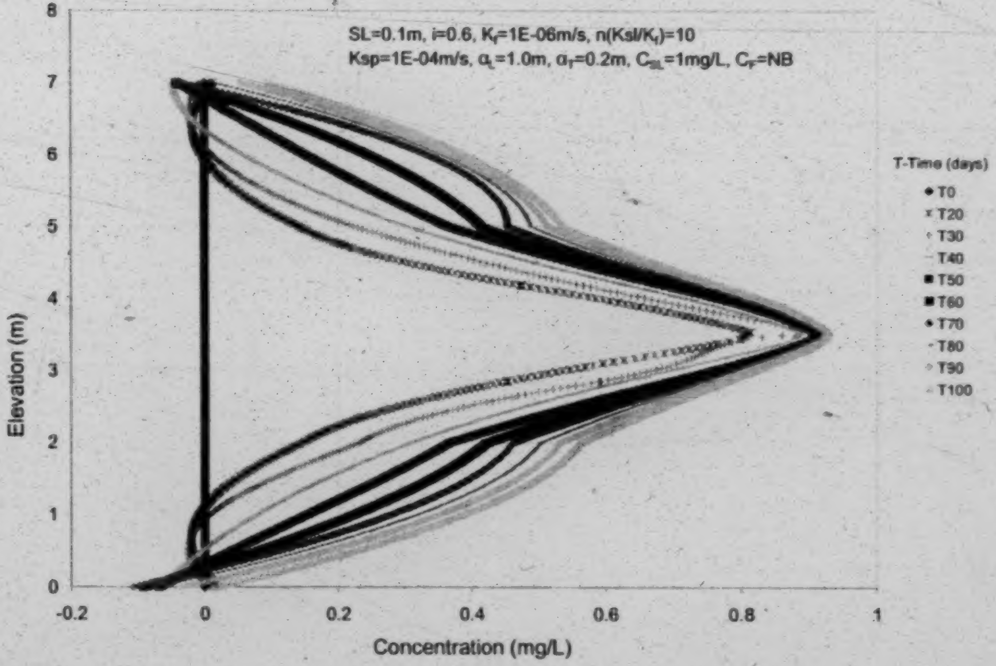

Figure B2.32 Case II-Hn10-CHA (α_L = 1.0m, α_T = 0.2m, V_{sl} = 473m/y, V_f = 57.3m/y)

APPENDIX B.3 Concentration profiles within the well

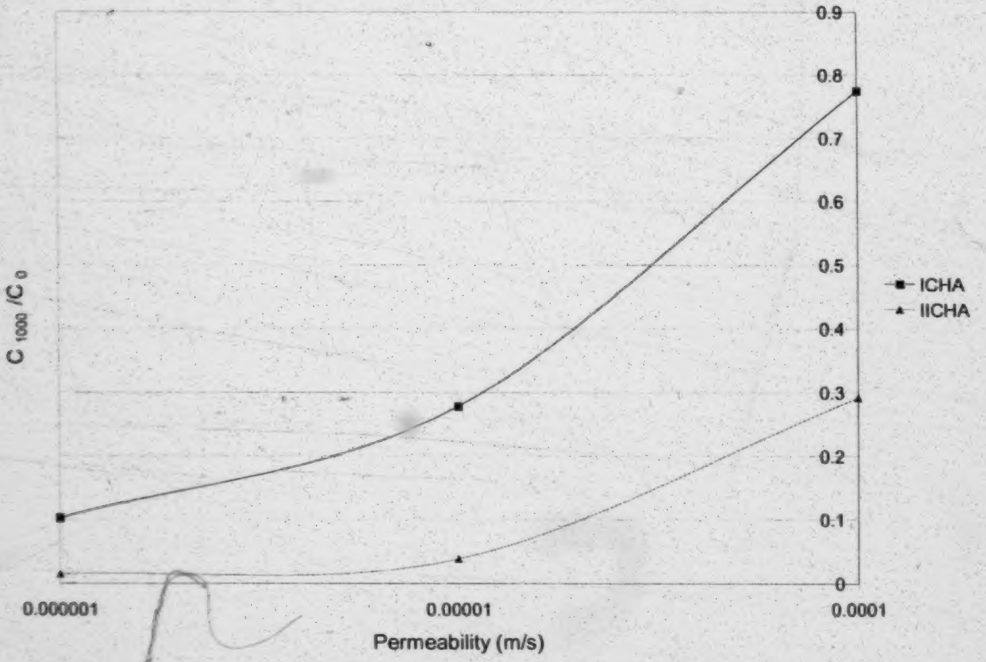

Figure B3.1 Concentration ratio at the well centre after 1000days

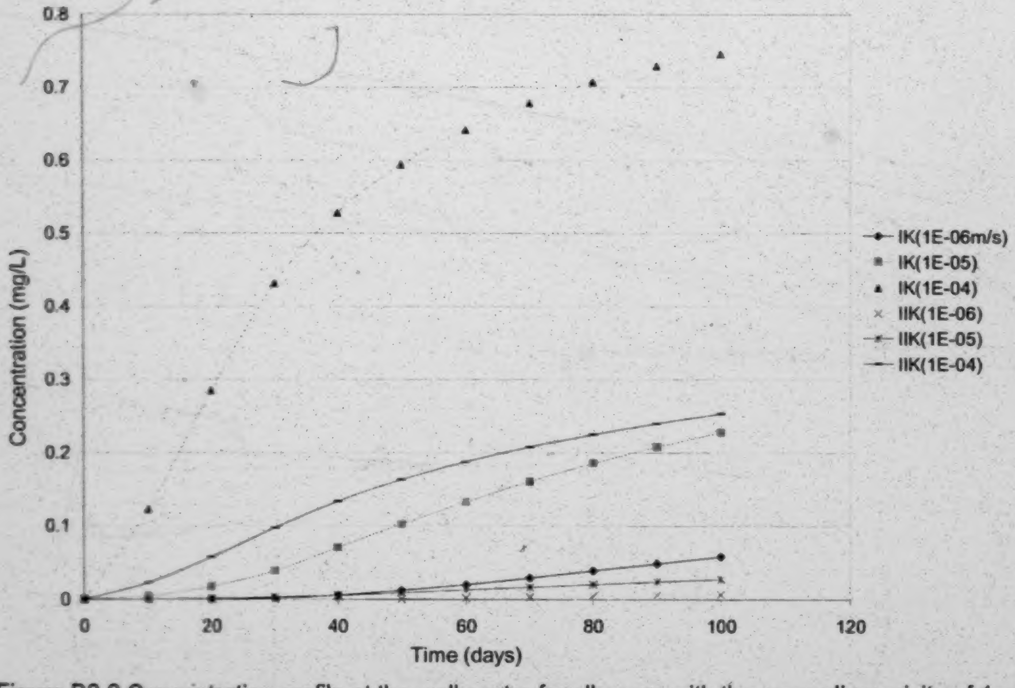

Figure B3.2 Concentration profile at the well centre for all cases with the same dispersivity of 1m

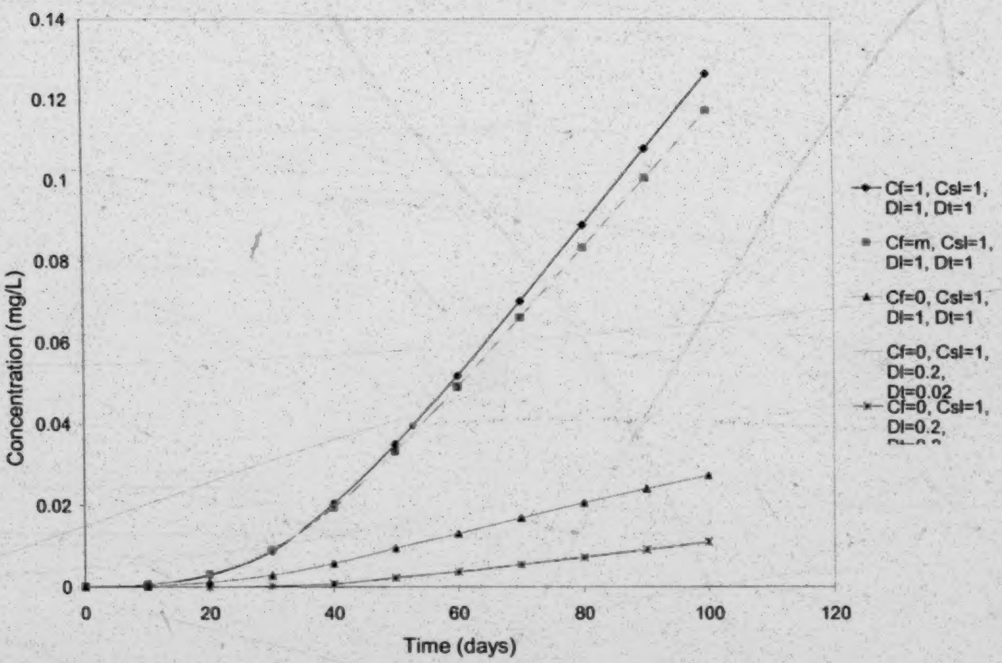

Figure B3.3 Concentration profile at the well centre for Case II (K=1E-05), for different values of dispersivity